



Julius-Maximilians-Universität Würzburg  
Fakultät für Biologie

**Identification and Characterisation of the Domains  
of RS1 (RSC1A1) Inhibiting the Monosaccharide  
Dependent Exocytotic Pathway of Na<sup>+</sup>-D-Glucose  
Cotransporter SGLT1 with High Affinity**

**Dissertation**

zur Erlangung des  
naturwissenschaftlichen Doktorgrades  
der Bayerischen Julius-Maximilians-Universität Würzburg

vorgelegt von

Alexandra Vernaleken

aus

Sankt-Petersburg

Würzburg 2007

**Eingereicht am:**

**Mitglieder der Promotionskommission:**

Vorsitzender: Prof. Dr. Dr. J. Müller

Gutachter: Prof. Dr. Hermann KOEPESELL

Gutachter: Prof. Dr. Roland BENZ

**Tag des Promotionskolloquiums: 09.01.2008**

**Doktorurkunde ausgehändigt am:**

*To my family*

# Table of Contents

Table of Contents.....	i
<b>1. Introduction .....</b>	<b>1</b>
1.1. Glucose absorption in small intestine and kidney .....	1
1.2. Regulation of the sodium-D-glucose co-transporter .....	4
1.3. The RS1 protein .....	6
1.4. Localization and function of the RS1 protein .....	8
1.5. Functions of the RS1 protein .....	9
1.6. Aim of the present study .....	11
<b>2. Materials .....</b>	<b>12</b>
2.1. Chemicals .....	12
2.2. Enzymes .....	14
2.3. Radioactive compounds.....	15
2.4. Antibodies .....	15
2.5. Kits .....	15
2.6. Equipment.....	16
2.7. Work materials .....	17
2.8. Employed vectors .....	18
2.9. Software.....	18
2.10. Animals.....	18
<b>3. Methods .....</b>	<b>19</b>
3.1. Molecular biological methods.....	19
3.1.1. Mutagenesis .....	19
3.1.2. Preparation of pRSSP vector and ligation with PCR fragments.....	20
3.1.3. Truncations at existing restriction sites.....	22
3.1.4. Purification of DNA by phenol extraction and ethanol precipitation.....	26
3.1.5. Precipitation of small amounts of DNA.....	26
3.1.6. Desalting of DNA.....	27
3.1.7. Isolation of plasmid DNA.....	27
3.1.8. cRNA synthesis .....	28
3.1.9. Agarose gel electrophoresis.....	29
3.1.10. Determination of the protein concentration.....	30
3.1.11. SDS-PAGE and Western-blotting .....	30
3.2. Cell Biological Methods .....	32
3.2.1. Transformation of competent <i>E.coli</i> cells .....	32
3.2.2. Isolation and purification of plasmids from <i>E.coli</i> .....	32
3.2.3. Preparation of <i>Xenopus laevis</i> oocytes and injection of cRNA.....	33
3.2.4. Injection of peptides and biochemicals into oocytes.....	34
3.2.5. Incubation of oocytes with membrane-permeant biochemicals.....	35
3.2.6. Tracer-flux experiments .....	35

3.2.7.	Capacitance measurements .....	36
3.2.8.	Isolation of the plasma membrane from <i>Xenopus</i> oocytes.....	37
3.3.	Calculation and statistical analysis.....	39
3.3.1.	Calculation of uptake.....	39
3.3.2.	Calculation of inhibition rate.....	40
3.3.3.	Statistical analysis .....	40
<b>4.</b>	<b>Results .....</b>	<b>45</b>
4.1.	Different fragments of hRS1 down-regulate the hSGLT1-mediated uptake of AMG in <i>Xenopus</i> oocytes.....	45
4.2.	hRS1 derived peptides inhibit hSGLT1-mediated AMG uptake .....	46
4.3.	QCP inhibits hSGLT1 mediated AMG uptake with high affinity .....	48
4.4.	Effect of different tripeptides, derived from QCP, on hSGLT1-mediated uptake of AMG.....	50
4.5.	QSP down-regulates hSGLT1-mediated uptake of AMG with high affinity.....	51
4.6.	QCP reduces the amount of hSGLT1 in the plasma membrane .....	53
4.7.	QCP blocks the exocytotic pathway of hSGLT1 .....	56
4.8.	Down-regulation of hSGLT1 by QCP and QSP is monosaccharide-dependent.....	58
4.9.	QCP exhibits glucose-dependent down-regulation of the organic cation transporter hOCT2.....	62
4.10.	Down-regulation of hSGLT1 by QCP is independent of Protein Kinase C (PKC) .....	63
4.11.	Extracellular QCP has no effect on the hSGLT1-mediated uptake of AMG in <i>Xenopus</i> oocytes.....	65
4.12.	Extracellular application of QCP decreases hPEPT1-mediated transport of glycyl-sarcosine in <i>Xenopus</i> oocytes.....	66
4.13.	QCP, transported via hPEPT1 transporter, down-regulates hSGLT1 in <i>Xenopus</i> oocytes .....	67
4.14.	Intracellular QCP does not influence activity of the hPEPT1 transporter in <i>Xenopus</i> oocytes.....	69
<b>5.</b>	<b>Discussion .....</b>	<b>70</b>
5.1.	Tripeptides, derived from hRS1, block the exocytotic pathway of hSGLT1 with high affinity .....	70
5.2.	QCP and QSP are substrates of the peptide transporter PEPT1 .....	72
5.3.	Down-regulation of hSGLT1 by QCP and QSP is monosaccharide dependent.....	76
5.4.	Specificity of QCP .....	79
5.5.	Biomedical implications .....	80
<b>6.</b>	<b>Summary.....</b>	<b>85</b>
<b>7.</b>	<b>List of publications .....</b>	<b>87</b>

<b>8.</b>	<b>References.....</b>	<b>88</b>
<b>9.</b>	<b>Appendix .....</b>	<b>100</b>
9.1.	N-terminal fragment of hRS1 down-regulates the hSGLT1 mediated uptake of AMG in <i>Xenopus</i> oocytes.....	100
9.2.	Peptides derived from the N-terminus of hRS1 inhibit hSGLT1-mediated AMG uptake.....	101
<b>10.</b>	<b>List of abbreviations.....</b>	<b>106</b>
	<b>Curriculum Vitae .....</b>	<b>108</b>
	<b>Acknowledgements.....</b>	<b>109</b>

### 1. Introduction

#### 1.1. Glucose absorption in small intestine and kidney

The monosaccharide glucose is the major source of energy in mammals. It is mainly ingested in form of polysaccharides, e.g. starch. The digestion of those polysaccharides begins in the mouth where salivary amylases hydrolyze polysaccharides into smaller units like the disaccharide maltose. In the intestine, further digestion occurs by the action of pancreatic amylases and disaccharidases. Small intestinal glucose absorption, the reabsorption of glucose from the glomerular filtrate, brain uptake across the blood-brain barrier, and the uptake and release of glucose from all cells in the body are mediated by the transporters of two families. These are the facilitated glucose transporters, GLUT or SLC2 gene family (Uldry and Thores, 2004), and sodium-coupled glucose co-transporters, the SGLT or SLC5 gene family (Hediger and Rhoads, 1994; Wright and Turk, 2004). The main function of GLUTs is the downhill, passive transport of glucose across cell membranes; for example, GLUTs speed up or facilitate the equilibration of the sugar across a membrane. Prime examples include ubiquitously expressed GLUT1 (Mueckler et al., 1985), responsible for the basic supply of cells with glucose and involved in the transport of glucose across the endothelial cells of the blood-brain barrier, GLUT2 (Fukumoto et al., 1988), a low-affinity glucose transporter with predominant expression in pancreatic  $\beta$ -cells, liver, kidney, and small intestine (basolateral membrane), and GLUT4 (Fukumoto et al., 1989), a high-affinity glucose transporter expressed in insulin-sensitive tissues such as heart, skeletal muscle, and adipose tissue (Wright et al., 2007). Active absorption of D-glucose across epithelial cells of the small intestine and the kidney proximal tubule is provided by sodium-D-glucose co-transporters (SGLT1) in the brush-border membranes. The SGLT family comprises Na<sup>+</sup>-dependent glucose co-transporters SGLT1 and SGLT2 (Hediger et

## 1. Introduction

al., 1987; Kanai et al., 1994), the glucose sensor SGLT3 (Diez-Sampedro et al., 2003), the widely distributed inositol (Berry et al., 1995) and multivitamin transporters SGLT4 and SGLT6 (Balamurugan et al., 2003), and the thyroid iodide transporter SGLT5 (Smanik et al., 1996).

Figure 1.1 illustrates how the dual expression of SGLT1 and GLUT2 in enterocytes accounts for the complete absorption of glucose from food in the small intestine (Wright et al., 2007). SGLT1 is a 73 kDa protein consisting of 664 amino acids and supposedly of 14 transmembrane helices (Turk et al., 1996). SGLT1 is a high-affinity, low-capacity sodium-glucose symporter with  $K_m$  for D-glucose is 0.3 mM in rabbits and 0.8 mM in humans (Hediger and Rhoads, 1994), expressed in the brush border membrane of the enterocytes. It couples the transport of two  $\text{Na}^+$  ions and one glucose molecule across the brush border membrane.

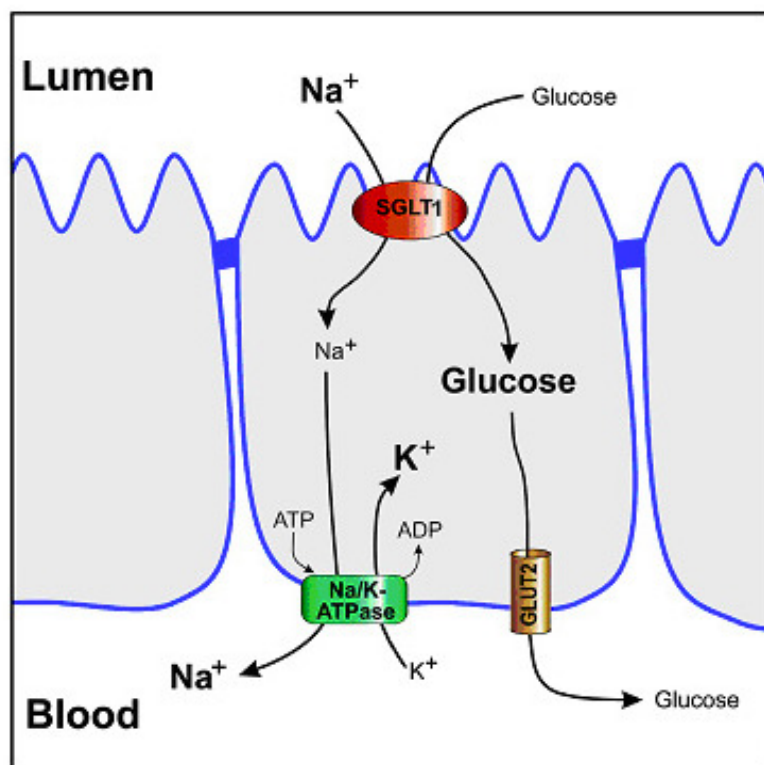


**Figure 1.1. A model for glucose (and galactose) absorption across the small intestine.** Shown is a cartoon of a mature enterocyte on the upper villus of the small intestine. Glucose (and galactose) is transported across the brush border membrane by Na-cotransport (SGLT1), and the Na is then transported out across the basolateral membrane by the Na/K-pump. Glucose (and galactose) accumulates within the cell and then diffuses out into blood across the basolateral membrane through GLUT2. Some glucose is phosphorylated within the cell and accumulated in endosomes before dephosphorylation and exocytosis into blood. Modified from Wright et al., 2004.



## 1. Introduction

---

The energy to drive glucose accumulation in the enterocyte against its concentration gradient is provided by the energy stored in the sodium electrochemical potential gradient across the brush border membrane. Sodium that enters the cell along with glucose is then transported out into blood by the Na/K-pump in the basolateral membrane, thereby maintaining the driving force for glucose transport. Since the sugar is accumulated within the enterocytes, it sets up a driving force for the glucose transport out of the cells into the blood via GLUT2 expressed in basolateral membranes.

A fraction of the intracellular glucose appears to be taken up into endosomes, as glucose-6-phosphate, and delivered to the blood by exocytosis through the basolateral membrane (Uldry and Thores, 2004). The net result is that across the enterocyte from gut lumen into blood one mole of glucose and two moles of sodium are transported, and this is followed by two moles of anions to ensure electroneutrality, and water. The energy for the overall process comes from the ATP consumed by the basolateral Na<sup>+</sup>/K<sup>+</sup>-pump.

Glucose absorption in the small intestine plays a pivotal role for the maintenance of blood glucose concentration (O'Donovan et al., 2004) and glucose and fat metabolism in the liver (Foufelle et al. 1996). In addition, small intestinal glucose uptake triggers glucose-dependent mechanisms, mediated by the glucose sensing neurons in the intestinal wall, such as regulation of intestinal motility (Rayner et al., 2001; Raybould and Zittel, 1995; Diez-Sampedro et al., 2003; Liu et al., 1999). Glucose reabsorption in the kidney is accomplished by a combination of the isoform SGLT2, which is, in contrast to SGLT1, a low-affinity, high-capacity sodium-glucose symporter with a sodium-to-glucose coupling ratio 1:1 (Scheepers et al., 2004), and the high-affinity isoform SGLT1. SGLT2 protein shows the high expression level in the kidney, where it mediates the absorption of the bulk of the filtered glucose in proximal convoluted tubule (Wright, 2001).

### 1.2. Regulation of the sodium-D-glucose co-transporter

The regulation of SGLT1-mediated D-glucose absorption was investigated in numerous studies. The regulatory mechanisms include the long-term regulation of SGLT1 expression at both transcriptional and post-transcriptional levels. An increase in dietary carbohydrates of ruminant animals, for example, caused an up-regulation of the activity and the expression of SGLT1 (Shirazi-Beechey et al., 1991). The mRNA levels of the SGLT1 gene were shown to be up-regulated after differentiation of the porcine renal cell line LLC-PK<sub>1</sub> (Shioda et al., 1994). Phosphorylation events may play an important role in transcriptional regulation of SGLT1, since both PKC and PKA affected the mRNA levels of the SGLT1 gene (Shioda et al., 1994).

The small intestinal absorption of glucose undergoes dramatical changes during development (Shirazi-Beechey et al., 1991). It is regulated in response to diet and during the food intake via changes of expression, location and activity of SGLT1 and/or GLUT2 (Ferraris and Diamond, 1989; Shirazi-Beechey et al., 1991; Kellett 2001). Expression of SGLT1 has been shown to be influenced by  $\beta$ -adrenergic innervation (Ishikawa et al., 1997), insulin (Stümpel et al., 1996), glucagon-37 (Stümpel et al., 1997), glucagon-like peptide 2 (Cheeseman 1997), and cholecystokinin (Hirsh and Cheeseman, 1998). Numerous studies report that cyclic AMP, protein kinase A, protein kinase C (PKC) and phosphoinositol 3-kinase are also involved in the short-term regulation of the glucose absorption pathways (Ishikawa et al., 1997; Stümpel et al., 1997; Cheeseman 1997; Hirsch et al., 1996). It has been shown that SGLT1 can be regulated by changes in transcription (Martin et al., 2000; Vayro et al., 2001), mRNA stability (Loflin and Lever, 2001), intracellular trafficking (Hirsch et al., 1998; Cheeseman 1997; Veyhl et al. 2006), and transporter activity (Vayro and Silverman, 1999). However, the individual regulatory pathways, their cross-talk, and their physiological importance are not understood.

## 1. Introduction

Eukaryotic cells are compartmentalized into the distinct membrane-bound organelles. Each of these has a specific composition of different proteins and lipids. Numerous pathways to transport the different molecules to their defined location exist in the cell (Fig. 1.2). Newly synthesized proteins move along the secretory pathway to their destined position within the cell (Rothman and Orci, 1992). The secretory pathway leads from the endoplasmic reticulum, where the correct folding of the protein is scrutinized and where proteins undergo initial glycosylation (Wei and Hendershot, 1996; Stevens and Argon, 1999), to the Golgi apparatus. In the Golgi, proteins are moved to the *trans*-Golgi network (TGN), where they are sorted according to their final destination, namely the plasma membrane, early endosomes or recycling endosomes. Transport vesicles shuttle the proteins between different organelles.

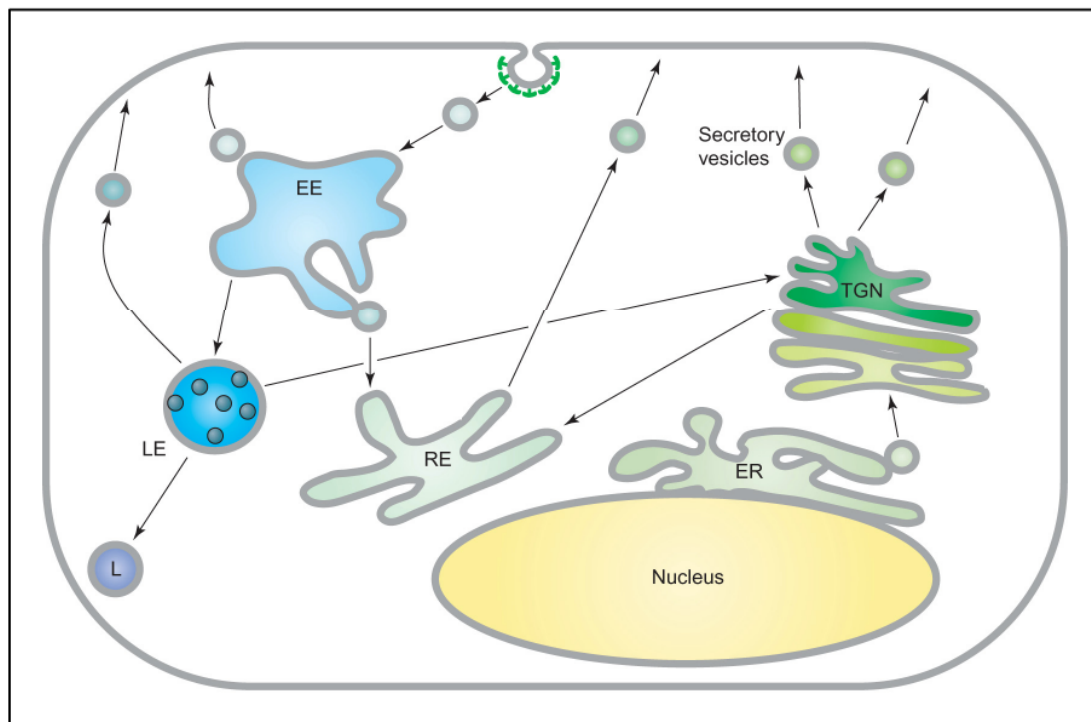


**Figure 1.2: Intracellular membrane trafficking.** Explanations see text. Modified from (Gaborik and Hunyady, 2004). (EE = early endosomes, ER = endoplasmic reticulum, LE = late endosomes, RE = recycling endosomes, TGN = *trans*-Golgi network).

The TGN is the site where the secretory pathway and the endocytic pathways converge. The first step of the endocytic pathways is either a clathrin-

dependent (Rappoport et al., 2004) or clathrin-independent (Nichols and Lippincott-Schwartz, 2001) internalization of membrane vesicles from the plasma membrane. The internalized membrane vesicles fuse then with the early endosomes (Bishop, 2003). In the early endosomes, the internalized cargo is further sorted to different destinations within the cell. Proteins bound for degradation in lysosomes are transported through the late endosomes, fuse with lysosomes and are subsequently enzymatically digested (Pillay et al., 2002).

From the early endosomes proteins are also cycling back to the plasma membrane (Gruenberg, 2001). Apparently, at least two routes of recycling exist. A rapid recycling pathway leads from the early endosomes directly to the plasma membrane. Alternatively, proteins are recycled back to the membrane via recycling endosomes along the slow recycling pathway (Deneka and van der Sluijs, 2002). In many cell types recycling endosomes are located in the perinuclear space (Gruenberg and Kreis, 1995). In addition to the described pathways, several retrograde tracks exist, resulting in a complex network of membrane trafficking (Fig. 1.2). Commonly, in all regulatory pathways the transporters are regulated in their plasma membrane abundance by shifting transporters between intracellular sites and the plasma membrane.

### 1.3. The RS1 protein

Previously, the intracellular protein RS1 (human gene *RSC1A1*) was identified as membrane associated polypeptide, which altered rate and apparent glucose dependence of Na<sup>+</sup>-D-glucose co-transporter SGLT1 and proposed to be a regulatory subunit of SGLT1 (Veyhl et al., 1993; Lambotte et al., 1996). *RSC1A1* is an intronless single copy gene that was only detected in mammals (in human, gene *RSC1A1* is localised in the chromosome 1p36.1) and codes for 67-68 kDa RS1 proteins. RS1s, cloned from pig (Veyhl et al., 1993), rabbit (Reinhardt et al., 1999), mouse (Osswald et al., 2005), and human (Lambotte et al., 1996), exhibit about 70% identity on the amino acid level through all four species (Fig. 1.3).

## 1. Introduction

---

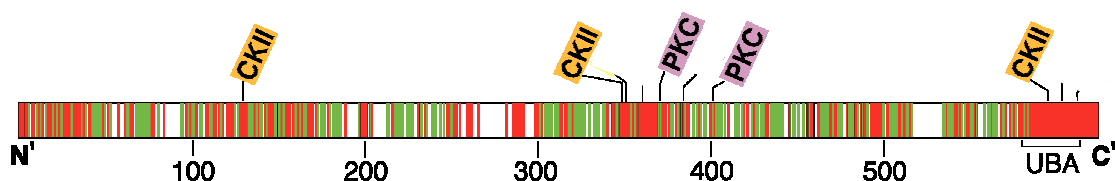


**Figure 1.3. Comparison of the homologous regions of RS1 protein cloned from pig, human, mouse, and rabbit.** Red – identical amino acid residues, green – similar amino acid residues. Above are shown predicted phosphorylation sites for casein kinase 2 (CKII), protein kinase C (PKC), and ubiquitin-associated domain (UBA).

The RS1 protein contains two conserved consensus sequences for the phosphorylation by protein kinase C (PKC), three conserved consensus sequences for the phosphorylation by casein kinase 2 (CKII), two consensus sequences for potential binding to the 14-3-3 proteins, localised in the N-terminus, and a ubiquitin associated domain (UBA, 42 amino acids), localised in the C-terminal part of the protein. Finding of RS1-homologous mRNAs in renal outer cortex including S1, S2, and S3 segments of renal proximal tubules, in outer medulla, small intestinal epithelial and subepithelial cells, hepatocytes, liver, and neurons (Veyhl et al., 1993; Poppe et al., 1997; Reinhardt et al., 1999), suggested that RS1 has a broad tissue distribution; however, RS1 was not found in the skeletal muscle, heart muscle, Madin-Darby canine kidney (MDCK) cells, colon, stomach, and renal inner medulla. Little amounts of RS1 were also found in the lung and spleen.

### 1.4. Localization and function of the RS1 protein

In the LLC-PK<sub>1</sub> cells, the renal epithelial cell line originally derived from the porcine kidneys, RS1 was located at the intracellular side of the plasma membrane, at the TGN and within the nucleus (Kroiss et al., 2006). Remarkably, amount and distribution of RS1 were dependent on the state of confluence. Whereas subconfluent LLC-PK<sub>1</sub> cells contained the large amounts of RS1 protein and exhibited the evident nuclear location of RS1, the amount of RS1 was decreased in the confluent LLC-PK<sub>1</sub> cells and RS1 did not distribute into nuclei (Kroiss et al., 2006). The observed changes in distribution correlate with functional data showing that RS1 down-regulates the transcription of SGLT1 in subconfluent LLC-PK<sub>1</sub> cells (Korn et al., 2001).

In the human embryonic kidney cells HEK-293 and in LLC-PK1 cells, RS1 was shown to be located at the intracellular side of the plasma membrane, at vesicles below the plasma membrane, at the TGN, and within the nucleus (Kroiss et al., 2006). Comparison of the subcellular distribution of the endogenously expressed SGLT1 and RS1 in two cell lines, LLC-PK<sub>1</sub> and HEK-293, in both subconfluent and confluent states, revealed considerable differences. Both proteins were found colocalized with the dynamin at the TGN; however, colocalization of RS1 and SGLT1 at the plasma membrane could not be demonstrated by immunofluorescence microscopy (Kroiss et al., 2006). Intracellularly, most of SGLT1 was associated with tubulovesicular compartments, previously identified as endosomes in Caco-2 cells (Kipp et al., 2003), that were lined up along the microtubules. RS1 protein was found at smaller vesicles but mostly at tubulovesicular structures of the TGN. The observed colocalization of RS1, SGLT1, and dynamin at the TGN is consistent with the hypothesis that RS1 blocks the release of SGLT1 from the TGN.

In *Xenopus* oocytes, most of the over-expressed RS1 protein was found in as soluble protein in cytosol; however, a small fraction of RS1 was associated with the plasma membrane.

### 1.5. Functions of the RS1 protein

Investigations in LLC-PK<sub>1</sub> cells provided evidence that RS1 is involved in the transcriptional down-regulation of SGLT1 in the subconfluent state (Shioda et al., 1994; Korn et al., 2001). Transcriptional up-regulation of SGLT1 in the confluent cells was associated with a post-transcriptional decrease of the amount of RS1 protein.

Studies aimed to understand the mechanisms underlying the post-transcriptional down-regulation of SGLT1 were performed using the co-expression of the cRNAs of different plasma membrane transporters along with cRNA of RS1. These investigations revealed that RS1 participates in the post-transcriptional regulation not only of SGLT1 (Veyhl et al., 1993; Lambotte et al., 1996; Reinhardt et al., 1999; Korn et al., 2001; Veyhl et al., 2003; Osswald et al., 2005; Veyhl et al., 2006, Kroiss et al., 2006), but also of some other plasma membrane transporters (Veyhl et al., 2003) such as sodium-*myo*inositol co-transporter SMIT, the organic cation transporters OCT1 and OCT2, the organic anion transporter OAT1, and the Na<sup>+</sup>-co-transporter for serotonin SERT. On the contrary, RS1 has had no inhibitory effect on the H<sup>+</sup>-peptide co-transporter PEPT1 and sodium-independent facilitated glucose transporter GLUT1 (Veyhl et al., 1993; Lambotte et al., 1996; Reinhardt et al., 1999, Veyhl et al., 2003, Jiang et al., 2005). The inhibition of hSGLT1-mediated uptake of the non-metabolised substrate methyl- $\alpha$ -D-glucopyranoside (AMG) by hRS1 was abolished when a dominant-negative dynamin mutant was co-expressed; however, it was not possible to distinguish whether the observed effects of RS1 were due to stimulation of the dynamin-dependent endocytosis or due to inhibition of cycling from an intracellular compartment.

The experiments with co-injection of the purified RS1 protein into the hSGLT1 expressing oocytes indicated that short-term post-transcriptional down-regulation of SGLT1 by RS1 occurs within 30 min and is due to blockage of the release of hSGLT1 containing vesicles from TGN (Kroiss et al., 2006; Veyhl et al.,

## 1. Introduction

---

2006). This post-transcriptional down-regulation of SGLT1 by RS1 was increased by PKC and modulated by intracellular AMG (Veyhl et al., 2006).

It has also been shown that the short-term inhibition of hSGLT1-mediated AMG uptake and hOCT2-mediated tetraethyl-ammonium (TEA) by hRS1 protein were modulated by the intracellular AMG concentration (Veyhl et al., 2006). Particularly, the inhibition levels of hSGLT1 and hOCT2 by hRS1 were decreased at an enhanced intracellular AMG concentration.

Recently, a 28 kDa ischemia/reperfusion inducible protein, called IRIP, was found associated with RS1. This interaction was identified using the yeast two-hybrid system screening and proved by co-immunoprecipitation analysis (Jiang et al., 2005). IRIP protein is up-regulated in kidney after ischemia and reperfusion, is expressed at the relatively high level in the testis, bronchial epithelia, thyroid, ovary, colon, kidney, and brain. At the low level, the expression of IRIP was identified in the spleen, muscle, heart and small intestine. Interestingly, IRIP protein could negatively modulate activity of different plasma membrane transporters such as GAT, SERT, SGLT1, OCT2, OCT3, and OAT1, but not GLUT1 or PEPT1. No additive or synergic interaction between effects of IRIP and RS1 on OCT2 was observed, and the effect of RS1 was abolished when the dominant negative mutant of IRIP was co-expressed. Similar effects of IRIP were observed with OCT3 and OAT1 transporters (Jiang et al., 2005).

The selectivity of RS1 is not yet understood. Nonetheless, the physiological and potential biomedical importance of RS1 was demonstrated by targeting disruption of the *Rsc1A1* gene in mice. Removal of *RSC1A1* gene coding for RS1 protein in mice caused the up-regulation of SGLT1 and of glucose absorption in the small intestine, and the animals developed an obese phenotype (Osswald et al., 2005).



### **1.6. Aim of the present study**

The present study was devoted to the identification and characterisation of the domain(s) of human RS1 protein (hRS1) responsible for the short-term post-transcriptional down-regulation of hSGLT1. Therefore, a series of truncated mutants of the hRS1 protein was generated and investigated on their effects on hSGLT1 using *Xenopus laevis* oocytes as an expression system. For a detailed characterisation of the short-term effects of the inhibitory domain of hRS1, the synthetic peptides derived from this domain were examined for effects on solute carrier transporters expressed in *Xenopus* oocytes.

## 2. Materials

### 2.1. Chemicals

Chemical substance	Manufacturer
1,4 Dithio-DL-threitol (DTT)	Fluka (Neu-Ulm, Germany)
2-deoxyglucose	Sigma-Aldrich (Seelze, Germany)
Acrylamide	Roth (Karlsruhe, Germany)
Agar	Difco (Hamburg, Germany)
Agarose	Serva (Heidelberg, Germany)
Ammonium persulfate (APS)	Sigma-Aldrich (Seelze, Germany)
Ampicillin	Sigma-Aldrich (Seelze, Germany)
Bacto-tryptone	Difco (Hamburg, Germany)
Botulinum toxin B (BtxB)	Sigma-Aldrich (Seelze, Germany)
Bovine serum albumin (BSA)	AppliChem (Darmstadt, Germany)
Bradford reagent	Biorad (Hercules, CA, USA)
Brefeldin A (BFA)	Sigma-Aldrich (Seelze, Germany)
Bromophenol blue	Serva (Heidelberg, Germany)
CaCl <sub>2</sub>	Sigma-Aldrich (Seelze, Germany)
CH <sub>3</sub> COONa (Sodium acetate)	Sigma-Aldrich (Seelze, Germany)
CH <sub>3</sub> COONH <sub>4</sub> (Ammonium acetate)	Sigma-Aldrich (Seelze, Germany)
Chloroform	Roth (Karlsruhe, Germany)
Colloidal silica	Sigma-Aldrich (Seelze, Germany)
D-fructose	Sigma-Aldrich (Seelze, Germany)
D-glucose	Sigma-Aldrich (Seelze, Germany)
Dimethylsulphoxide (DMSO)	Sigma-Aldrich (Seelze, Germany)
DNA molecular weight standard markers GeneRuler 100 bp DNA Ladder, GeneRuler 1 kb DNA Ladder	MBI Fermentas (St. Leon-Rot, Germany)
ECL reagent	Amersham Bioscience (Freiburg, Germany)

## 2. Materials

<b>Chemical substance</b>	<b>Manufacturer</b>
Ethanol	J. T. Backer (Deventer, Holland)
Ethidium bromide	AppliChem (Darmstadt, Germany)
Ethylenediaminetetraacetic acid (EDTA)	Merck (Darmstadt, Germany)
Gentamycin sulphate	Fluka (Neu-Ulm, Germany)
Glycerine	AppliChem (Darmstadt, Germany)
Glycine	AppliChem (Darmstadt, Germany)
Glyoxal	Sigma-Aldrich (Seelze, Germany)
HEPES	AppliChem (Darmstadt, Germany)
Isoamyl alcohol	Sigma-Aldrich (Seelze, Germany)
Isopropanol	AppliChem (Darmstadt, Germany)
KCl	AppliChem (Darmstadt, Germany)
KH <sub>2</sub> PO <sub>4</sub>	Merck (Darmstadt, Germany)
Mannitol	Sigma-Aldrich (Seelze, Germany)
MES	Sigma-Aldrich (Seelze, Germany)
Methanol	AppliChem (Darmstadt, Germany)
Methyl- $\alpha$ -D-glucopyranoside	Fluka (Neu-Ulm, Germany)
MgCl <sub>2</sub>	Fluka (Neu-Ulm, Germany)
MgSO <sub>4</sub>	AppliChem (Darmstadt, Germany)
NaCl	Sigma-Aldrich (Seelze, Germany)
NaHCO <sub>3</sub>	Sigma-Aldrich (Seelze, Germany)
Name	Manufacturer
NaOH	Merck (Darmstadt, Germany)
Oligonucleotides	MWG Biotech (Ebersberg, Germany) Biomers.net GmbH (Ulm, Germany)
Phenol-Chloroform	Life Technologies (Eggenstein, Germany)
Phlorizin	Sigma-Aldrich (Seelze, Germany)
PMA	Sigma-Aldrich (Seelze, Germany)
Polyacrylic acid	Sigma-Aldrich (Seelze, Germany)
Prestained Protein Molecular Weight Marker	MBI Fermentas, (St. Leon-Rot, Germany)

## 2. Materials

<b>Chemical substance</b>	<b>Manufacturer</b>
Protease Inhibitor Cocktail (PI)	Sigma-Aldrich (Seelze, Germany)
Quinine	Sigma-Aldrich (Seelze, Germany)
RNA Ladder 0.24-9.5 kb	Invitrogen Corporation (Carlsbad, CA, USA)
Sn-1,2-dioctanoylglycerol (DOG)	Sigma-Aldrich (Seelze, Germany)
Sodium dodecyl sulphate (SDS)	Roth (Karlsruhe, Germany)
Sorbitol	Sigma-Aldrich (Seelze, Germany)
Tetraethyl-ethylenediamine (TEMED)	Fluka (Neu-Ulm, Germany)
Tricaine	Sigma-Aldrich (Seelze, Germany)
Tris(hydroxymethyl)aminomethane (Tris)	Fluka (Neu-Ulm, Germany)
Tris-base	Fluka (Neu-Ulm, Germany)

### 2.2. Enzymes

<b>Name</b>	<b>Manufacturer</b>
Pfu DNA polymerase	MBI Fermentas (St. Leon-Rot, Germany)
Klenow fragment	MBI Fermentas (St. Leon-Rot, Germany)
T4 DNA ligase	GIBCO BRL (Eggenstein, Germany)
Eco147I	MBI Fermentas (St. Leon-Rot, Germany)
Eco81I	MBI Fermentas (St. Leon-Rot, Germany)
MluI	MBI Fermentas (St. Leon-Rot, Germany)
EcoRI	MBI Fermentas (St. Leon-Rot, Germany)
NotI	MBI Fermentas (St. Leon-Rot, Germany)
Clal	New England Biolabs (Frankfurt am Main, Germany)
XhoI	New England Biolabs (Frankfurt am Main, Germany)
ApaI	New England Biolabs (Frankfurt am Main, Germany)
Collagenase I	Sigma-Aldrich (Seelze, Germany)

### 2.3. Radioactive compounds

Name	Manufacturer
[ <sup>14</sup> C]-methyl- $\alpha$ -D-glucopyranoside ([ <sup>14</sup> C]AMG)	Amersham Biosciences (Freiburg, Germany)
[ <sup>14</sup> C]-tetraethyl-ammonium ([ <sup>14</sup> C]-TEA)	Biotrend (Cologne, Germany)
[ <sup>3</sup> H]-glycylsarcosine ([ <sup>3</sup> H]-GlySarc)	American Radiolabeled Chemicals, Inc. (St. Louis, USA)

### 2.4. Antibodies

Name	Manufacturer
Polyclonal rabbit antibody against human SGLT1	Self production
Protein G – Horseradish Peroxidase Conjugate	Bio-Rad Laboratories (Hercules, CA, USA)

### 2.5. Kits

Name	Manufacturer
HiSpeed Midi Kit	Quiagen GmbH (Hilden, Germany)
mMESSAGE mMACHINE™ SP6 Kit	Ambion (Texas, USA)
mMESSAGE mMACHINE™ T3 Kit	Ambion (Texas, USA)
mMESSAGE mMACHINE™ T7 Kit	Ambion (Texas, USA)
DNA purification kit EasyPure	BioZym (Hess. Oldendorf, Germany)

## 2.6. Equipment

Appliance	Model	Manufacturer
Capillaries puller	P30	Sutter (Novato, CA, USA)
Centrifuges and rotors	5415C Biofuge 28 RS Rotor HFA 22.1 JS21 Rotor JA14 Rotor JA20 Rotor J-21C RC2-B Rotor GSA Rotor SS-34 Rotor SLA-1500	Eppendorf (Hamburg, Germany) Heraeus Sepatech GmbH (Osterode, Germany) Beckmann (Munich, Germany)  Sorvall Superspeed (Bad Homburg, Germany)
Dissection microscope	Stemi 1000	Zeiss (Jena, Germany)
Electroporator	Biojet MI	Biomed (Theres, Germany)
Gel chamber		Hartenstein (Würzburg, Germany)
Hose pump		LKB (Bromma, Sweden)
Incubator Shaker	G25	New Brunswick Scientific Inc. (Edison, New Jersey, USA)
Microwave	Jet900W	Philips (Sweden)
Nanoliter injector		World Precision Instruments (Sarasota, FL, USA)
PCR amplifcator	Hybaid OmniGene	MWG Biotech (Ebersberg, Germany)
Photo camera		Polaroid (Offenbach, Germany)
pH meter	S20 SevenEasy pH	Mettler-Toledo GmbH (Schwerzenbach, Switzerland)
Scintillation counter	1500 Tri-Carb  2100 TR	Packard Instrument Co (Meridon, CT, USA) Packard Instrument Co (Meridon, CT, USA)
SDS-Gel chamber		Hartenstein (Würzburg, Germany)

## 2. Materials

<b>Appliance</b>	<b>Model</b>	<b>Manufacturer</b>
Semi-dry Blotter		Hartenstein (Würzburg, Germany)
Spectrophotometer	Ultraspec3	Pharmacia (Freiburg, Germany)
Thermostat	IPP-400	Memmert GmbH (Schwabach, Germany)
UV Transilluminator		Herolab (St. Leon-Rot, Germany)
Vortexer	MS1	IKA (Staufen, Germany)
Feedback amplifier	TEC-05	NPI Electronic (Tamm, Germany)
Analog-to-digital converter	ITC-16	Instrutech (Port Washington, NY, USA)

### 2.7. Work materials

<b>Material</b>	<b>Manufacturer</b>
Developer	Kodak (Stuttgart, Germany)
Filter paper, Whatman	Hartenstein (Würzburg, Germany)
Fixer	Kodak (Stuttgart, Germany)
Glass capillaries	World Precision Instruments (Sarasota, FL, USA)
Operation set (ovariectomy)	Hartenstein (Würzburg, Germany)
Operation Silk	Roeko (Langenau, Germany)
Polyvinylidene fluoride transfer membrane (PVDF) Immobilon-P, pore size 0.45um	Millipore Corporation (Bedford, MA, USA)
Roentgen film Kodak Biomax MR	Kodak (Stuttgart, Germany)
Scintillation counter tubes	Sarstedt (Nimbrecht, Germany)
Scintillation cocktail Lumasafe Plus	Lumac LSC (Groningen, Netherlands)
Single-use plastic test-tubes	Eppendorf (Hamburg, Germany) Greiner (Frickenhäusen, Germany) Nunc Seromed (Berlin, Germany) Sarstedt (Nimbrecht, Germany)

### 2.8. Employed vectors

The expression vectors used for the protein translation from cRNA injected into oocytes are listed in the table. The pRSSP (Busch, 1996) and pOG2 (Arndt et al., 2001) vectors contain non-translating regions of the *Xenopus*  $\beta$ -globin gene providing high expression in oocytes.

Plasmid	Enzyme	RNA Polymerase	Resistance
pBluescriptIISK	NotI	T7	Ampicillin
pBS	EcoRI	T3	Ampicillin
pOG2	NotI	T7	Ampicillin
pRSSP	MluI	SP6	Ampicillin

### 2.9. Software

Program	Reference
EndNote X	Thomson ResearchSoft (San Francisco, CA, USA)
GraphPad Prism 4.0	GraphPad Software Inc. (San Diego, CA, USA)
Image J	National Institute of Health (USA)
Microsoft Excel	Microsoft Corporation (Redmond, WA, USA)
Origin 6.0 Professional	Microcal Software Inc. (Northampton, MA, USA)
Vector NTI 10.0	Invitrogen Corporation (Carlsbad, CA, USA)
PULSE	Heka (Lambrecht, Germany)
X-CHART	Heka (Lambrecht, Germany)

### 2.10. Animals

*Xenopus laevis* toads were obtained from H. Kähler (Hamburg, Germany). Animals were housed and handled in compliance with institutional guidelines and German laws.



### 3. Methods

#### 3.1. Molecular biological methods

##### 3.1.1. Mutagenesis

Preparation of truncated mutants of the hRS1 was performed using a polymerase chain reaction (PCR). The primer sequences were perfectly complementary to the template DNA and contained the start- or stop- codon and introduced ApaI or XhoI restriction sites. The primers used for the PCR-based preparation of the mutants, are listed in the table 3.1.1. pRSSP-forward and pRSSP-reverse primers represent the pRSSP-plasmid specific primers.

The cycling reaction mix consisted of 5  $\mu$ l of 10xPCR reaction buffer, 10 ng of template plasmid, 8  $\mu$ l of dNTPs mix, 0.5  $\mu$ l of each oligonucleotide primer, 1  $\mu$ l of Pfu DNA-polymerase, and ddH<sub>2</sub>O was added to a final volume of 50  $\mu$ l. The polymerase chain reaction was performed under the following conditions:

Denaturation	94°C, 1 min	1 cycle
Denaturation Annealing Elongation	94°C, 30 sec 50°C, 1 min 72°C, 2 min	25 cycles
Elongation	72°C, 5 min	1 cycle

The efficiency of the polymerase chain reaction was verified by conventional agarose gel electrophoresis.

Subsequently, the resulting DNA fragment was purified and precipitated as described in 3.1.4, diluted in 20  $\mu$ l of nuclease-free water and digested with flanking restrictases ApaI and XhoI. The restriction mix consisted of 20  $\mu$ l of DNA after PCR, 3  $\mu$ l of 10xNEB4 buffer, and 1.5  $\mu$ l of ApaI (10 u/ $\mu$ l). Digestion with ApaI was performed at +25°C for two hours and then 1.5  $\mu$ l of XhoI (20 u/ $\mu$ l) was added. Digestion with XhoI was performed at +37°C for two hours.

The resulting DNA fragment was purified from the preparative 1% agarose gel and ligated with pRSSP vector digested with the same restrictases. Plasmid DNA was isolated and sequenced to verify the presence of desired mutation.

#### **3.1.2. Preparation of pRSSP vector and ligation with PCR fragments**

The hRS1wild type (hRS1wt) DNA in pRSSP vector was digested at ApaI and XhoI restriction sites. The restriction mix consisted of 2 µg of DNA hRS1wt in pRSSP vector, 3 µl of 10xNEB4 buffer, 1.5 µl of ApaI, and nuclease-free water was added to a final volume of 29 µl. Digestion was performed for two hours at +25°C. Then 1.5 µl of XhoI (20 u/µl) was added to the restriction mixture and digestion was performed for two hours at +37°C. The efficiency of digestion was verified by conventional agarose-gel electrophoresis as described in 3.1.9. Then the restriction mix was supplemented with 6 µl of 6xloading dye and loaded into preparative agarose gel. The agarose gel electrophoresis was performed as described in 3.1.9. The linear DNA fragment of interest was cut out of agarose gel and eluted from the agarose using the DNA purification kit EasyPure following the manufacturer's protocol. The concentrations of eluted DNA fragments were determined by analytical agarose gel electrophoresis using the GeneRuler DNA 1 kb Ladder as a control.

For the ligation reaction, 10 ng of pRSSP vector and insert DNA at 5:1 molar excess over vector were supplemented with 2 µl of 10xligase buffer, 0.5 µl of T4 DNA ligase (10 u/µl), and nuclease-free water was added to a final volume of 20 µl. The ligation mix was incubated overnight at +14°C and desalting procedure was performed as described in 3.1.6.

### 3. Methods

<b>Reagents used:</b>	
Template DNA	10 ng/μl
Forward primer	100 μM
Reverse primer	100 μM
10xPCR buffer with MgSO <sub>4</sub>	200 mM Tris-HCl, pH 8.8, 100 mM (NH <sub>4</sub> ) <sub>2</sub> SO <sub>4</sub> , 100 mM KCl, 1% Triton X-100, 1 mg/ml BSA, 20 mM MgSO <sub>4</sub>
dNTPs mix	Σ1,25 mM
DNA polymerase	Pfu DNA polymerase, 10 u/μl
10xLigase buffer	400 mM Tris-HCl, 100 mM MgCl <sub>2</sub> , 100 mM DTT, 5 mM ATP, pH 7.8 at +25°C
10xNEB2 buffer	500 mM NaCl, 100 mM Tris-HCl, 100 mM MgCl <sub>2</sub> , 10 mM DTT, pH 7.9 at +25°C
10xNEB4 buffer	500 mM potassium acetate, 200 mM Tris-acetate, 10 mM magnesium acetate, pH 7.9 at +25°C
10xREact® 1 buffer	500 mM Tris-HCl, 100 mM MgCl <sub>2</sub> , pH 8.0 at +25°C
10x G <sup>+</sup> buffer	100 mM Tris-HCl, 100 mM MgCl <sub>2</sub> , 500 mM NaCl, 1 mg/ml BSA, pH 7.5 at +37°C
10x B <sup>+</sup> buffer	100 mM Tris-HCl, 100 mM MgCl <sub>2</sub> , 1 mg/ml BSA, pH 7.5 at +37°C

**Table 3.1.1. Oligonucleotides for the preparation of the mutants:**

<b>Mutant</b>	<b>Primers: ApaI-start-(5'-3') forward/reverse-stop-XhoI</b>
535-617	GCAGGGCCCATGGACAGGCCTGAAACCAGA/pRSSP-reverse
1-250	pRSSP-forward/CGCTCGAGTCAGATTTCCATAAATGTTTCTG
326-617	GCAGGGCCCATGTATGGCCATTACTCCTCTCC/ pRSSP-reverse
407-617	GCAGGGCCCATGCAGAATGAACAGTGTCCA/ pRSSP-reverse

### 3. Methods

Mutant	Primers: <b>ApaI</b> -start-(5'-3') forward/reverse-stop- <b>XhoI</b>
350-425	GCAGGGCCCATGCCGTCTATAACGGCAGC/ CGCTCGAGTCACTCCACTGATACAGATATG
396-425	GCAGGGCCCATGTCTGAAAGATGGACCCAAAATG/ CGCTCGAGTCACTCCACTGATACAGATATG
407-415	CATGCAGAATGAACAGTGTCCACAAGTCTCATGAC/ TCGAGTCATGAGACTTGTGGACACTGTTCATTCTGCATGGGCC
1-183	pRSSP-forward /CGCTCGAGTCATGAAGCTTTTTGTTGTGCAAC
1-111	pRSSP-forward /CGCTCGAGTCACTCCAGATTACCTGCAACAG
1-120	pRSSP-forward /CGCTCGAGTCAGCCCTGGGTGCTTCTTTC
50-183	GCAGGGCCCATGCCTAAAGCTGTGAAGGC/ CGCTCGAGTCATGAAGCTTTTTGTTGTGCAAC
20-50	GCAGGGCCCATGAGTCCTGATGTTGGTAATC/ CGCTCGAGTCAAGGTTCAATGCGATCTGCG
20-40	GCAGGGCCCATGAGTCCTGATGTTGGTAATC/ CGCTCGAGTCAGATAGGGCAGACTGAAGC
40-50	GCAAGCTTATGATCAAGCCCAGTGAAGTCAAG/ CGCTCGAGTCAAGGTTCAATGCGATCTGCG

#### 3.1.3. Truncations at existing restriction sites

##### **hRS1(1-535) fragment**

The hRS1wt DNA in pRSSP vector was digested with Eco147I for two hours at +37°C. The reaction mix consisted of 1.5 µg of hRS1wt DNA in pRSSP vector, 1 µl Eco147I (10 u/µl), 2 µl of 10xB<sup>+</sup> reaction buffer, and nuclease-free water was added to a final volume of 20 µl. The efficiency of digestion was verified by conventional agarose-gel electrophoresis as described in 3.1.9. Then 1 µl of dNTPs (Σ1.25 mM) and 0.5 µl of Klenow Fragment (10 u/µl) were added to 18 µl of the restriction mix in order to fill in cohesive ends and digest away

protruding 3'-overhangs of linearised DNA. The reaction mix was incubated at +37°C for 30 min and subsequently heated at +70°C for inactivation of Klenow Fragment. The resulting DNA was precipitated as described in 3.1.5. Dried DNA was dissolved in 8 µl of 100 µM spe2 adaptors, supplemented with 1 µl of 10xligase buffer and 1 µl of T4 DNA ligase (10 u/µl), and incubated overnight at +14°C. For subsequent ligase inactivation, the ligation mix was heated at +70°C for 10 min. To remove excess of spe2 adaptors, DNA was digested with SpeI at 37°C for four hours. The restriction mix consisted of 20 µl of ligation mixture, 4 µl of 10xNEB2 buffer, 3 µl of SpeI, and nuclease-free water was added to a final volume of 40 µl. Then the restriction mix was supplemented with 6 µl of 6xloading dye and loaded into preparative agarose gel. The agarose gel electrophoresis was performed as described in 3.1.9. The linear DNA fragment of interest was cut out of the agarose gel and eluted from the agarose using the DNA purification kit EasyPure following the manufacturer's protocol. The concentration of the eluted DNA fragment was determined by analytical agarose gel electrophoresis using GeneRuler DNA 1 kb Ladder as a control. For the self-ligation reaction, 50 ng of the eluted DNA fragment was mixed with 5 µl of 10xT4 DNA ligase buffer, 0.5 µl of T4 DNA ligase, and nuclease-free water was added to a final volume of 50 µl. The ligation mix was incubated overnight at +14°C, and the desalting procedure was performed as described in 3.1.6.

#### **hRS1(251-617) fragment**

The hRS1wt DNA in pRSSP vector was digested with ApaI at +25°C for two hours. The restriction mix consisted of 1.5 µg of hRS1wt DNA in pRSSP vector, 2 µl of 10xNEB4 buffer, 1 µl of ApaI (10 u/µl), and nuclease-free water was added to a final volume of 20 µl. The efficiency of digestion was verified by conventional agarose gel electrophoresis as described in 3.1.9. The restriction mix was then heated at +70°C for 10 min for inactivation of ApaI. Linearised DNA was precipitated as described in 3.1.5, dissolved in 7 µl of nuclease-free water, supplemented with 1 µl of ApaI/ClaI adaptors (6 µg/µl), 1 µl of T4 DNA ligase buffer, and 1 µl of T4 DNA ligase. The ligation reaction was incubated overnight

### 3. Methods

---

at +14°C and subsequently heated at +70°C for 10 min for ligase inactivation. To remove excess of ApaI/ClaI adaptors and concurrently digest hRS1 DNA at the ClaI site, the resulting DNA was digested with ClaI for four hours at +37°C. The restriction mix consisted of 10 µl of ligation mixture, 3 µl of REact® 1 buffer, 3 µl of ClaI (10 u/µl), and nuclease-free water was added to a final volume of 40 µl. To isolate the fragment of interest, the restriction mix was supplemented with 6µl of 6xloading dye and applied into preparative agarose gel. Agarose gel electrophoresis was performed as described in 3.1.9. The linear DNA fragment of interest was cut out of agarose gel and eluted from the agarose using the DNA purification kit EasyPure following the manufacturer's protocol. The concentration of the eluted DNA fragment was determined by analytical agarose gel electrophoresis using the GeneRuler DNA 1 kb Ladder as a control. For the self-ligation reaction, 50 ng of the eluted DNA fragment was mixed with 5 µl of 10xT4 DNA ligase buffer, 0.5 µl of T4 DNA ligase, and nuclease-free water was added to a final volume of 50 µl. The ligation mix was incubated overnight at +14°C, and the desalting procedure was performed as described in 3.1.6.

#### **hRS1(251-487) fragment**

The hRS1(251-617) DNA in pRSSP vector was digested with XhoI and Eco81I at +37°C for two hours. The restriction mix consisted of 1.5 µg of hRS1(251-617) DNA in pRSSP vector, 2 µl of 10xG<sup>+</sup>buffer, 0.5 µl of XhoI (20 u/µl), 1 µl of Eco81I (10 u/µl), and nuclease-free water was added to a final volume of 20 µl. The efficiency of digestion was verified by conventional agarose gel electrophoresis as described in 3.1.9. Then 1 µl of dNTPs (Σ1.25 mM) and 0.5 µl of Klenow Fragment (10 u/µl) were added to 18 µl of restriction mix in order to fill in cohesive 5'-ends and digest away protruding 3'-overhands of linearised DNA. The reaction mix was incubated at +37°C for 30 min and subsequently heated at +70°C for inactivation of Klenow Fragment. The resulting DNA was precipitated as described in 2.2. Dried DNA was dissolved in 8 µl of 100 µM spe2 adaptors, supplemented with 1 µl of 10xligase buffer and 1 µl of T4 DNA ligase (10 u/µl), and incubated overnight at +14°C. For subsequent ligase inactivation, the

### 3. Methods

---

ligation mix was heated at +70°C for 10 min. To remove excess of spe2 adaptors, the DNA was digested with SpeI at 37°C for four hours. The restriction mix consisted of 20 µl of ligation mixture, 4 µl of 10xNEB2 buffer, 3 µl of SpeI, and nuclease-free water was added to a final volume of 40 µl. Then the restriction mix was supplemented with 6 µl of 6xloading dye and loaded into preparative agarose gel. Agarose gel electrophoresis was performed as described in 3.1.9. The linear DNA fragment of interest was cut out of the agarose gel and eluted from the agarose using the DNA purification kit EasyPure following the manufacturer's protocol. The concentration of the eluted DNA fragment was determined by analytical agarose gel electrophoresis using the GeneRuler DNA 1 kb Ladder as a control. For the self-ligation reaction, 50 ng of eluted DNA fragment was mixed with 5 µl of 10xT4 DNA ligase buffer, 0.5 µl of T4 DNA ligase, and nuclease-free water was added to a final volume of 50 µl. The ligation mix was incubated overnight at +14°C, and the desalting procedure was performed as described in 3.1.6.

#### Adaptors:

ApaI/ClaI	5'-CACCATGAT-3' 3'- <u>CCGGTGGTACTAGC</u> -5' ApaI                      ClaI
spe1	SpeI 5'-CTG <u>ACTAGTC</u> AG-3' 3'-CAGTGATCAGTC-5'
spe2	SpeI 5'-TG <u>ACTAGTCA</u> -3' 3'-ACTGATCAGT-5'

#### **3.1.4. Purification of DNA by phenol extraction and ethanol precipitation**

To purify DNA, an equal volume of phenolchloroform was added to a DNA containing reaction mixture and mixed gently. The aqueous phase containing DNA was separated from the organic phase in the microfuge at 10000 rpm for 5 min. Subsequently, the aqueous phase was carefully removed into a fresh microfuge tube. An equal amount of 24:1 (v/v) chloroform-isoamyl alcohol was added, mixed gently, and the aqueous phase was separated by centrifugation at 10000 rpm for 10 min (Wallace, 1987). To precipitate DNA, a 0.1 volume of 3 M sodium acetate, pH 5.2, and 2.5 volumes of absolute ethanol were added to the aqueous phase, and following incubation for 2 hours at -20°C DNA was recovered by centrifugation in the microfuge at 14000 rpm for 30 min. Washing with 70% ethanol (v/v) was performed to remove excess of the salt from the pellet. The dried DNA was resuspended in nuclease-free water.

#### **3.1.5. Precipitation of small amounts of DNA**

To purify small amounts of DNA (up to 1.5 µg), the phenol extraction was performed as described above. For precipitation of DNA, a 0.25 volume of ammonium acetate and 2 volumes of absolute ethanol were added to the aqueous phase and the mixture was incubated at room temperature for 30 min. The DNA was then recovered by centrifugation in the microfuge at 14000 rpm for 15 min and subsequently washed with 70% ethanol (v/v). The dried DNA was dissolved in nuclease free water if not specified otherwise.



#### **3.1.6. Desalting of DNA**

For electroporation, it is required to desalt DNA samples (Dower, 1988). The phenol extraction of DNA after ligation reaction was performed as described above. To precipitate DNA, a linear polyacrylamide was used as a carrier. A 0.1 volume of 3 M sodium acetate, pH 5.2, 6  $\mu$ l of linear polyacrylamide (2.5  $\mu$ g/ $\mu$ l), and 2 volumes of absolute ethanol were added to an aqueous phase and the DNA was recovered by centrifugation in a microfuge at 13000 rpm for 30 min at room temperature. The precipitate was then washed with 1 ml of 70% ethanol (v/v). In order to remove excess salt from the pellet, precipitated DNA was incubated with 500  $\mu$ l of 70% ethanol (v/v) for 30 min at room temperature. Following centrifugation (5 min, 13000 rpm, room temperature), DNA was air-dried and dissolved in 10 $\mu$ l of nuclease-free water.

#### **3.1.7. Isolation of plasmid DNA**

The colonies of E.coli transformed with the plasmid of interest were cultured overnight in LB medium supplemented with ampicillin to a final concentration of 50  $\mu$ g/ml. Cells from 150 ml of culture were harvested by centrifugation at 6000g for 10 min at +4°C. The plasmid DNA was isolated by the principle of SDS/alkaline lysis, according to the manufacturer's instructions (HiSpeed Midi Kit, Quiagen). The purified DNA was then concentrated by the ethanol precipitation and diluted in suitable volume of nuclease-free water.

---

LB medium: 5 g/l NaCl, 10 g/l Bacto-tryptone, 5 g/l yeast extract, pH 7.5 adjusted with NaOH, medium sterilized by autoclaving.

---

### 3.1.8. cRNA synthesis

For oocyte microinjections, m<sup>7</sup>G(5')ppp(5')G-capped cRNAs were synthesized by means of T3 mMESSAGE mMACHINE kit (for hSGLT1 in pBS vector), T7 mMESSAGE mMACHINE kit (for hOCT2 in pOG2, hPEPT1 in pBluescriptIISK) or SP6 mMESSAGE mMACHINE kit (for hRS1). These kits enable the synthesis of large amounts of capped RNA from a linearised cDNA template by incorporation of a cap analog (m<sup>7</sup>G(5')ppp(5')G) during the polymerase reaction.

#### Reagents used:

10xEnzyme Mix	A combination of bacteriophage T3, T7 or SP6 RNA polymerase, ribonuclease inhibitor and other unlisted components
10xTranscription Buffer	T3, T7 or SP6 reaction buffer, composition not provided by manufacturer
2xRibonucleotide Mix (dNTP/Cap Mix)	T3: 15 mM dATP, 15 mM dCTP, 15 mM dUTP, 3 mM dGTP and 12 mM Cap Analog T7: 15 mM dATP, 15 mM dCTP, 15 mM dUTP, 3 mM dGTP and 12 mM Cap Analog SP6: 10 mM dATP, 10 mM dCTP, 10 mM dUTP, 2 mM dGTP and 8 mM Cap Analog
DNaseI	RNase free (2 u/μl) supplied in 50% glycerol buffer

The plasmids were first linearised with MluI, EcoRI, or NotI. The cRNA transcription reaction was assembled at room temperature. The reaction mix consisted of 2 μl of 10xReaction Buffer, 10 μl of dNTP/Cap Mix, 1 μg of linear template DNA, 2 μl of the enzyme mix, and nuclease-free water to a final volume of 20 μl. The reaction mix was incubated for 2 hours at 37°C. Thereafter, the template DNA was removed by the addition of 1 μl RNase-free DNaseI and incubation at 37°C for 15 min. Following synthesis, cRNAs were purified with

Phenol/Chloroform, Chloroform/Isoamyl alcohol and precipitated with NaAc in ice-cold 75% ethanol. Purified cRNAs were then diluted in RNase-free water. The verification of cRNA products and an estimation of their concentrations were performed using agarose gel electrophoresis.

#### **3.1.9. Agarose gel electrophoresis**

Conventional agarose gel electrophoresis was used for visualization and/or isolation of DNA after PCR amplification or restriction digestion (Sambrock et al., 1989) and for visualization and estimation of cRNA concentration (Gründemann and Koepsell, 1994) after *in vitro* synthesis. To prepare the gel, 1% agarose was dissolved in buffer (TAE for DNA gels, BES for cRNA gels) by heating in a microwave for 3 min at 350 W. After cooling to 60-70°C, 10 mg/ml of ethidium bromide solution was added to a final concentration of 0.3 mg/ml to a DNA-gel, or iodine acetate was added to a final concentration of 1 µg/ml to a cRNA-gel, mixed thoroughly, and the solution was immediately poured onto a plastic tray surrounded by masking tape. Combs with 3 mm wells and 200 mm wells were used for analytical and preparative electrophoresis, respectively. The gel was completely set after 45-60 min at room temperature.

The samples of DNA were applied on the gel in a loading buffer and gel electrophoresis was performed at 100 V for one hour.

The samples of cRNA were first mixed with glyoxal/DMSO buffer and heated at 55°C for one hour. Then the loading buffer was added, samples were applied on the gel and gel electrophoresis was performed at 45 V for 90-120 min. To avoid the rise of the pH-gradient, the running buffer (BES) was circulating from anode to cathode by a hose pump.

The results of electrophoresis were visualized with a Dual Intensity Ultraviolet Transilluminator and photo-documented.

**Solutions:**

---

TAE buffer:	40 mM Tris-Acetate, 1 mM EDTA, pH 8.0
BES buffer:	10 mM BES, 0.1 mM EDTA, pH 6.7
Loading buffer:	30% (v/v) Glycerine, 0.25% (w/v) Bromophenol blue
Glyoxal/DMSO:	50 µg/ml ethidium bromide (added fresh), 50% DMSO, 1 M Glyoxal in BES buffer

---

#### **3.1.10. Determination of the protein concentration**

The concentration of the proteins was determined according to Bradford using bovine serum albumin as a standard (Bradford, 1976). 1 µl of the protein solution was diluted in 99 µl of H<sub>2</sub>O prior to addition of 900 µl of Bradford reagent. Following 5 min incubation at room temperature, the extinction of the sample was measured at 595 nm using a spectrophotometer and subsequently correlated to the extinction of the solvent.

#### **3.1.11. SDS-PAGE and Western-blotting**

For the application in SDS-PAGE (Laemmli et al., 1970), 2 µg of protein samples were pre-treated for 45 min at 37°C in sample buffer (SB), loaded on SDS-polyacrylamide gels, and electrophoresis was performed at 25 mA per gel for 1.5 hours. Then the proteins were electrophoretically transferred to a PVDF membrane by semi-dry blotting at 120 mA per membrane for 2 hours (Gershoni and George, 1983).

The PVDF membranes were blocked for 2 hours at room temperature in blocking buffer. For antibody reaction, the blots were incubated for 2 hours at room temperature with affinity-purified polyclonal rabbit antibodies against

### 3. Methods

human SGLT1 diluted 1:1000 in blocking buffer. After washing of the blots with blocking buffer, they were incubated for 2 hours at room temperature with peroxidase-conjugated goat anti-rabbit IgG antiserum diluted 1:5000 in blocking buffer. Then the blots were washed twice with blocking buffer, and the bound label was visualized by enhanced chemiluminescence (ECL system). The obtained pictures were scanned and densitometric analysis was performed using program Image J.

#### Composition of the gels and solutions:

Stacking gel 5%:	0.125 M TrisHCl, pH 6.8, 5% (w/v) acrylamide, 0.1% (w/v) SDS, 0.4% (w/v) ammonium persulfate, 1.2 µl/ml Temed
Resolving gel 10%:	0.375 M TrisHCl, pH 8.8, 10% (w/v) acrylamide, 0.1% (w/v) SDS, 0.1% (w/v) ammonium persulfate, 0.7 µl/ml Temed
Running buffer:	25 mM Tris base, pH 8.3, 192 mM glycine, 0.1% (w/v) SDS
Sample buffer (SB):	60 mM TrisHCl, pH 6.8, 100 mM DTT, 2% (w/v) SDS, 7% (v/v) glycerol, 0.1% (w/v) Bromophenol blue
Blotting buffer:	25 mM Tris base, pH 8.3, 150 mM glycine, 10% (v/v) methanol
Blocking buffer:	2.7 mM KCl, 4.3 mM Na <sub>2</sub> HPO <sub>4</sub> , 1.8 mM KH <sub>2</sub> PO <sub>4</sub> , 137 mM NaCl, pH 7.4, 0.1% (v/v) Tween 20, 2% (w/v) bovine serum albumin
Washing buffer:	2.7 mM KCl, 4.3 mM Na <sub>2</sub> HPO <sub>4</sub> , 1.8 mM KH <sub>2</sub> PO <sub>4</sub> , 137 mM NaCl, pH 7.4, 0.1% (v/v) Tween 20

## 3.2. Cell Biological Methods

### 3.2.1. Transformation of competent *E.coli* cells

Electrocompetent *E.coli* cells DH10B (GibcoBRL) were prepared according to the manufacturer's protocol and stored at  $-80^{\circ}\text{C}$ . 20  $\mu\text{l}$  of the cells was defrosted and mixed with 1  $\mu\text{l}$  of plasmid DNA. The mix was loaded into a pre-chilled 2 mm cuvette and electroporation was performed by triggering a 1600V pulse (Dower, 1988). Then 1 ml of SOC medium was added and gently mixed with the cells. The suspension was incubated for 1 hour at  $37^{\circ}\text{C}$  and 50-250  $\mu\text{l}$  thereof were plated on LB-agar plates containing 50  $\mu\text{g}/\text{ml}$  ampicillin.

---

SOC medium:	10 g/l yeast extract, 20 g/l Bacto-tryptone, 10 mM NaCl, 2.5 mM KCl, 10 mM $\text{MgCl}_2$ , 10 mM $\text{MgSO}_4$ , 20 mM D-glucose, pH 7.0
LB agar:	5 g/l yeast extract, 10 g/l Bacto-tryptone, 5 g/l NaCl, 1.5% agar, pH 7.5

---

### 3.2.2. Isolation and purification of plasmids from *E.coli*

Plasmid DNA was isolated and purified from *E. coli* overnight culture grown in LB medium using the HiSpeed Plasmid Midi Kit from QIAGEN according to the manufacturer's protocol. DNA concentration was determined by UV-photospectrometry at 260 nm with the Ultraspec3 spectrophotometer.

### 3.2.3. Preparation of *Xenopus laevis* oocytes and injection of cRNA

Mature female *Xenopus laevis* were anaesthetized by immersion in fresh water containing 1 mg/ml of Tricaine supplemented with 1 mg/ml of NaHCO<sub>3</sub>. Oocytes at the stages V and VI were obtained by partial ovariectomy, dissected out and treated overnight with collagenase I (10 mg/ml in ORi). The oocytes were then washed twice with Ca<sup>2+</sup>-free ORi and kept at 16°C in sterile modified Barth's solution. Selected oocytes were injected with 25 nl of water containing cRNA-solutions (see table 3.2.3.1 of cRNAs for injection) using a nanoliter microinjector with glass capillaries. For protein expression, injected oocytes were kept for 3 days at 16°C in modified Barth's solution. Non-injected oocytes served as a control.

cRNAs injected	Amount injected, ng/oocyte
hSGLT1	2.5
hSGLT1	2.5
hRS1wt, mutans	7.5
hPEPT1	10.0
hSGLT1	2.5
hPEPT1	10.0
hOCT2	2.5
hOCT2	2.5
hRS1wt	7.5

Table 3.2.3.1. Amounts of cRNAs injected into the *Xenopus* oocytes.

### 3. Methods

---

#### Solutions:

---

Barth's modified solution:	15 mM HEPES pH 7.6, 88 mM NaCl, 1 mM KCl, 0.3 mM Ca(NO <sub>3</sub> ) <sub>2</sub> , 0.41 mM CaCl <sub>2</sub> , 0.82 mM MgSO <sub>4</sub> , 12.5 µg/ml gentamycin
ORi buffer (oocytes Ringer solution):	5 mM HEPES pH 7.6, 100 mM NaCl, 3 mM KCl, 2 mM CaCl <sub>2</sub> , 1 mM MgCl <sub>2</sub>
Ca <sup>2+</sup> -free ORi buffer:	5 mM HEPES pH 7.6, 100 mM NaCl, 3 mM KCl, 1 mM MgCl <sub>2</sub>
K-ORi buffer:	5 mM HEPES pH 7.6, 100 mM KCl, 3 mM NaCl, 2 mM CaCl <sub>2</sub> , 1 mM MgCl <sub>2</sub>

---

#### 3.2.4. Injection of peptides and biochemicals into oocytes

75 pmol of the peptides derived from hRS1 (QNEQCPQVS, QNEQCP, QCPQVS, QCP, IKPSDSDRIEP, IKPSDSDR, SDSLRIEP and control peptides SVQPCQENQ, PCQ, and PEIRDSDSPKI), 0.5 pmol sn-1,2-dioctanoylglycerol (DOG; activator of PKC), 2 ng of Botulinum Toxin B (BtxB; inhibitor of exocytosis) or 0.5 pmol of Brefeldin A (BFA; inhibitor of vesicle release from *trans*-Golgi network) were injected into oocytes with 25 nl of K-ORi buffer on the third day of the protein expression. After injection of peptides and/or biochemicals, oocytes were incubated at 21°C in ORi buffer one hour prior to tracer-flux measurements. For affinity studies with QCP and the PCQ-control peptide, different amounts of these peptides (as detailed in the results) were injected into hSGLT1-expressing oocytes. One hour later, hSGLT1-mediated uptake of [<sup>14</sup>C]-methyl- $\alpha$ -D-glucopyranoside (AMG) was measured as described below.

To investigate the influence of intracellular sugars on QCP-dependent down-regulation of hSGLT1, different concentrations of methyl- $\alpha$ -D-



glucopyranoside, D-glucose, D-fructose, 2-deoxyglucose and the sugar alcohols mannitol and sorbitol were injected with 25 nl of K-ORi into the hSGLT1 expressing oocytes with or without 75 pmol QCP one hour before tracer-flux measurements.

#### **3.2.5. Incubation of oocytes with membrane-permeant biochemicals**

For protein kinase C (PKC) stimulation, the hSGLT1 expressing oocytes, on the third day after cRNA injection, were incubated with 1  $\mu$ M phorbol-12-myristate-13-acetate (PMA) for 2 min and washed twice with ORi buffer. Another group of hSGLT1-expressing oocytes were first injected with 25 nl containing 75 pmol QCP in K-ORi buffer, incubated for one hour at 21°C in ORi buffer and then treated with PMA as described above. Then, tracer-flux measurements were performed as described in 3.2.6.

#### **3.2.6. Tracer-flux experiments**

For tracer-flux measurements, oocytes that express transporters, non-injected control oocytes, oocytes injected with peptides or biochemicals, or oocytes incubated with membrane-permeant biochemicals were divided into groups of 8-11 oocytes and transferred into 1 ml vials with 200  $\mu$ l ORi uptake medium, containing the radioactively labelled substrate with or without specific inhibitor (Veyhl et al., 1993, Veyhl et al., 2003).

Oocytes expressing hSGLT1 and non-injected control oocytes were incubated for 15 min at room temperature in ORi buffer containing 50  $\mu$ M or the indicated concentrations of methyl- $\alpha$ -D-[<sup>14</sup>C]-glucopyranoside ([<sup>14</sup>C]-AMG) in the presence or absence of 200  $\mu$ M phlorizin.

### 3. Methods

---

Oocytes expressing hOCT2 and non-injected control oocytes were incubated for 15 min at room temperature in ORi buffer with 10  $\mu\text{M}$  of [ $^{14}\text{C}$ ]-tetraethylammonium ([ $^{14}\text{C}$ ]-TEA) in the absence or presence of 100  $\mu\text{M}$  quinine.

Oocytes expressing hPEPT1 and non-injected control oocytes were incubated at room temperature in ORi buffer pH 6.5 with 200  $\mu\text{M}$  of [ $^3\text{H}$ ]-glycylsarcosine in the presence or absence of 150  $\mu\text{M}$  QCP for 15 min and then transferred in ORi buffer, pH 7.6.

Oocytes co-expressing hPEPT1 and hSGLT1 transporters were incubated with QCP in ORi buffer pH 6.5 for 1 hour at room temperature, transferred into ORi buffer pH 7.4 and the uptake of [ $^{14}\text{C}$ ]-AMG was performed as described above.

After 15 min of incubation with substrates and inhibitors, where applicable, uptake was terminated by aspiration of the incubation medium and oocytes were washed 3 times with ice-cold ORi. Individual oocytes were then transferred into 5 ml scintillation vials and solubilized in 250  $\mu\text{l}$  of 5% SDS. Thereafter 2.5 ml of LumaSafe scintillation cocktail was added, and the radioactivity was analysed by scintillation counting.

#### **3.2.7. Capacitance measurements**

The transmembrane conductance and membrane current were recorded using conventional two-electrode voltage-clamp techniques (Schmitt and Koepsell, 2002). To perform the two-electrode voltage-clamp (TEVC), the feedback amplifier TEC-05 controlled by PULSE and X-CHART software was used. The amplifier and personal computer were connected via an analog-to-digital converter ITC-16. The signals were low-pass filtered at 20 kHz for measurements of steady-state currents and at 20 kHz with a four-pole Bessel filter for measurements of membrane capacitance.

### 3. Methods

---

The *Xenopus laevis* oocytes were placed in a custom-built Teflon chamber and clamped with two microelectrodes filled with 3 M KCl. The electrodes had a final resistance of 0.5-2 M $\Omega$  and 1-3 M $\Omega$  for the current and the potential electrode, respectively. The changes of the plasma membrane surface area were recorded by continuous membrane capacitance measurements under voltage-clamp conditions. Oocytes were clamped to a potential of -40 mV and the holding current was recorded. The PULSE and X-CHART software was programmed to carry out stimulation, data acquisition, signal averaging, calculation of membrane capacitance (C<sub>m</sub>), and the display of raw traces and calculated C<sub>m</sub> values.

To compare phlorizin-induced capacitance changes, measurements on oocytes expressing hSGLT1 coinjected with 75 pmol QCP one hour prior to measurements and a control group of hSGLT1 expressing oocytes were carried out. The clamped oocytes were constantly superfused with ORi buffer via a gravity-fed system. To induce an inward current, 5 mM AMG was applied over a time period of 90 sec, and the changes of current and membrane capacitance were recorded. The oocytes were then washed with ORi buffer for 5 min. To induce the membrane capacitance change, 100  $\mu$ M phlorizin was applied by direct pipetting into the chamber for 90 sec and then washed out for 5-10 min. The phlorizin-induced capacitance changes in hSGLT1 expressing oocytes coinjected and non-coinjected with QCP were recorded and subsequently analysed using a t-test.

#### **3.2.8. Isolation of the plasma membrane from *Xenopus* oocytes**

For the isolation of the plasma membranes (Kamstead and Deen, 2001), on the third day after cRNA injection, hSGLT1 expressing oocytes and non-injected oocytes, free from follicle membrane and without even small damages, were

### 3. Methods

---

selected. The group of hSGLT1 expressing oocytes was injected with 23 nl of QCP diluted in K-ORi buffer and kept for one hour at 21°C in Barth's modified solution. Thereafter oocytes were incubated for 15 min at room temperature in ORi buffer containing 50 µM AMG, and washed twice with ORi buffer. After that oocytes were placed into Eppendorf-tubes filled completely with 1% positively charged colloidal silica in fresh MES-buffered saline, and rotated for 30 min at +4°C. Then oocytes were washed twice with MBSS and rotated another 30 min at +4°C with 0.1% polyacrylic acid. After two washing steps with Barth's modified solution, oocytes were homogenized with 200 µl (yellow tip) pipette in a final volume of 1.5 ml HB/PI, and centrifuged at 10 g for 30 sec at +4°C. Then ~85% of the volume (1300 µl) was discarded from the top. The pellet was washed 3 times with 1 ml HB/PI by short (30 sec) centrifugation steps: 10 g, 20 g, and 40 g, and then centrifuged for 30 min at 16000 g. All centrifugation steps were performed at +4°C. The resulting pellet was resuspended in suitable volume of 1% SDS (4 µl/oocyte) and subsequently analysed by Western-blotting.

#### **Solutions:**

---

MBSS (MES buffered saline)	20 mM MES pH=6.0, 80 mM NaCl
HB (Homogenization buffer)	20 mM Tris pH=7.4, 5 mM MgCl <sub>2</sub> , 5 mM NaH <sub>2</sub> PO <sub>4</sub> , 1 mM EDTA, 80 mM sucrose
Protease Inhibitors Cocktail (PI)	1/200

---

### 3.3. Calculation and statistical analysis

#### 3.3.1. Calculation of uptake

The uptake rates represent the normalized means  $\pm$  SE from 8-10 oocytes expressing hSGLT1, hOCT2 or hPEPT1 that were corrected to the uptake rates measured in non-injected control oocytes. In control oocytes without expression of transporters, uptake of [<sup>14</sup>C]-AMG, [<sup>14</sup>C]-TEA and [<sup>3</sup>H]-glycylsarcosine was less than 1% of those in oocytes expressing transporters. In the presence of 200  $\mu$ M phlorizin and 100  $\mu$ M quinine, the uptake of [<sup>14</sup>C]-AMG and [<sup>14</sup>C]-TEA was inhibited by >95%.

An uptake value for every single oocyte ( $J_i$ , pmol/15 min) was calculated using the formula:

$$J_i = \frac{D_i}{\bar{S}} \times V \times C;$$

where  $D_i$  [dpm] is a count of a single oocyte in 15 min,  $\bar{S}$  [dpm] is an average of counts in standards (calculated out of two standards for each group of oocytes),  $V$  [ $\mu$ l] is the final volume of uptake medium used for each group of oocytes, and  $C$  [ $\mu$ M] is the concentration of substrate.

A mean value of the total uptake for each group of oocytes ( $\bar{J}$ , pmol/15 min) was calculated using the formula:

$$\bar{J} = \frac{\sum J_i}{N};$$

where  $J_i$  is an uptake value for a single oocyte in 15 min,  $N$  is a number of oocytes in a group.

### 3. Methods

---

The hSGLT1 specific uptake ( $J_{sp}$ , pmol/15 min) was calculated using the formula:

$$J_{sp} = \bar{J} - \bar{J}_{phlo};$$

where  $\bar{J}$  is a total uptake for non inhibited group of oocytes in 15 min,  $\bar{J}_{phlo}$  - a total uptake for phlorizin inhibited group of oocytes in 15 min.

To normalize data, a value for every single oocyte ( $J_{in}$ ) was calculated using the formula:

$$J_{in} = \frac{J_i}{\bar{X}};$$

where  $J_i$  is an uptake value for a single oocyte and  $\bar{X}$  is a mean uptake value for control group of oocytes.

#### 3.3.2. Calculation of inhibition rate

The inhibition rates ( $I$ ) shown in the figures were obtained using a formal:

$$I = 1 - J_{in};$$

where  $J_{in}$  is a normalized uptake value for a single oocyte.

#### 3.3.3. Statistical analysis

The test for significance of differences between mean values was performed using one-way ANOVA test with a post hoc Tukey comparison for at least three experiments performed with different batches of oocytes.

## 4. Results

### 4.1. Different fragments of hRS1 down-regulate the hSGLT1-mediated uptake of AMG in *Xenopus* oocytes

Previously it has been shown that [<sup>14</sup>C]-AMG uptake in *Xenopus laevis* oocytes co-expressing hSGLT1 and hRS1 was decreased by about 50% in comparison to the oocytes expressing only hSGLT1 (Lambotte et al., 1996; Veyhl et al., 2003; Veyhl et al., 2006). In the present study, co-expression of different truncated mutants of hRS1 together with hSGLT1 was performed to identify the domain(s) of hRS1 responsible for the down-regulation of hSGLT1. For this purpose, *X. laevis* oocytes were injected with cRNA encoding hRS1wt or hRS1-truncated mutants together with cRNA coding for hSGLT1 as described in 3.2.3. After three days of incubation of the oocytes, uptake of 50 μM [<sup>14</sup>C]-AMG was measured over a time period of 15 min as described in 3.2.6. As shown in figure 4.1, the uptake of 50 μM [<sup>14</sup>C]-AMG mediated by hSGLT1 was inhibited by about 50% when hRS1wt was co-expressed. The inhibition of the hSGLT1-mediated AMG uptake was also observed when various fragments of hRS1 were co-expressed together with hSGLT1. Particularly, co-expression of the fragments encoding amino acids 1-251 and 251-617 with hSGLT1 led to the inhibition of AMG uptake by 40-50%, suggesting that both the N- and C-terminal domains of hRS1 can mediate the down-regulation of hSGLT1, and that effects of both domains are not additive. Deletion of the amino acids 535-617 containing ubiquitin-associated domain (UBA-domain, aa 571-611, for review see Hurley et al., 2006) of the protein did not significantly alter the down-regulation of hSGLT1. This suggests that UBA-domain of hRS1 is not directly involved into the post-transcriptional down-regulation of hSGLT1. Interestingly, co-expression of the fragment containing the UBA-domain (aa 535-617) led to some small albeit still significant inhibition of the hSGLT1-mediated AMG uptake, which may be due to various ubiquitin-related effects. Focussing on the middle part of the protein (aa 251-

535), additional truncations were performed, and the inhibitory effect was attributed to a cRNA fragment coding for aa 407-415 (Fig.4.1).

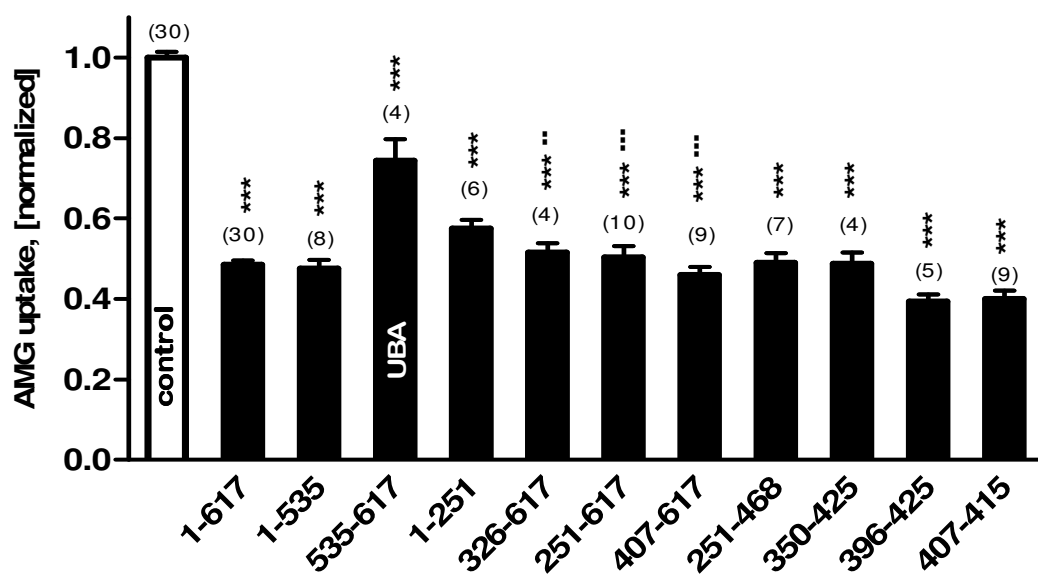


**Figure 4.1. Identification of the hRS1 fragments, that inhibit hSGLT1-mediated uptake of [<sup>14</sup>C]-AMG.** 2.5 ng of hSGLT1 cRNA were injected in *X. laevis* oocytes either alone (control) or together with 7.5 ng cRNA coding for hRS1wt (aa 1-617) or the indicated hRS1 fragments. Oocytes were incubated for three days and uptake of 50  $\mu$ M [<sup>14</sup>C]-AMG was measured. Uptake rates were normalized to parallel measurements in control oocytes from the same batch. Mean values  $\pm$  SE are indicated. The number of independent experiments is given in parentheses \*\*,  $P < 0.01$  and \*\*\*,  $P < 0.001$  for difference to control; ..,  $P < 0.01$  and ..,  $P < 0.001$  for difference to co-expression of hSGLT1 and the small hRS1 fragment containing the UBA domain of hRS1 (UBA), determined according to the ANOVA with post hoc Tukey's test.

## 4.2. hRS1 derived peptides inhibit hSGLT1-mediated AMG uptake

Previous observation indicated that hRS1 protein purified from *Xenopus* oocytes and from Sf9 cells, and injected into hSGLT1 expressing oocytes inhibits hSGLT1-mediated uptake of [<sup>14</sup>C]-AMG within 30 min (Veyhl et al., 2006). Since the co-expression experiments described above do not differentiate between the post-transcriptional short-term effects of hRS1 on hSGLT1, and long-term effects that may involve endogenous oocyte proteins which participate in the regulation of the hSGLT1, the experiments with co-injection of the synthetic peptides, derived from hRS1, into hSGLT1 expressing oocytes were performed. 75 pmol of



## 4. Results

the acetylated synthetic peptide comprising the nine amino acids domain (QNEQCPQVS), identified in the co-expression experiments (aa 407-415), was injected into hSGLT1 expressing oocytes. The reversal nine amino acids peptide SVQPCQENQ served as a control. Assuming that oocytes contain an internal aqueous volume of about 0.4  $\mu\text{l}$  (Zeuthen et al., 2002), the intracellular concentrations of injected peptides were about 0.2 mM. After injection of the peptides, oocytes were incubated at room temperature for one hour and then uptake of [ $^{14}\text{C}$ ]-AMG was measured over a time period of 15 min as described in 3.2.6. Figure 4.2 shows that after co-injection of nonapeptide QNEQCPQVSac the hSGLT1-mediated uptake of [ $^{14}\text{C}$ ]-AMG was inhibited by about 50%, similar to the down-regulation observed in experiments with coexpression of cRNAs (Fig.4.1).

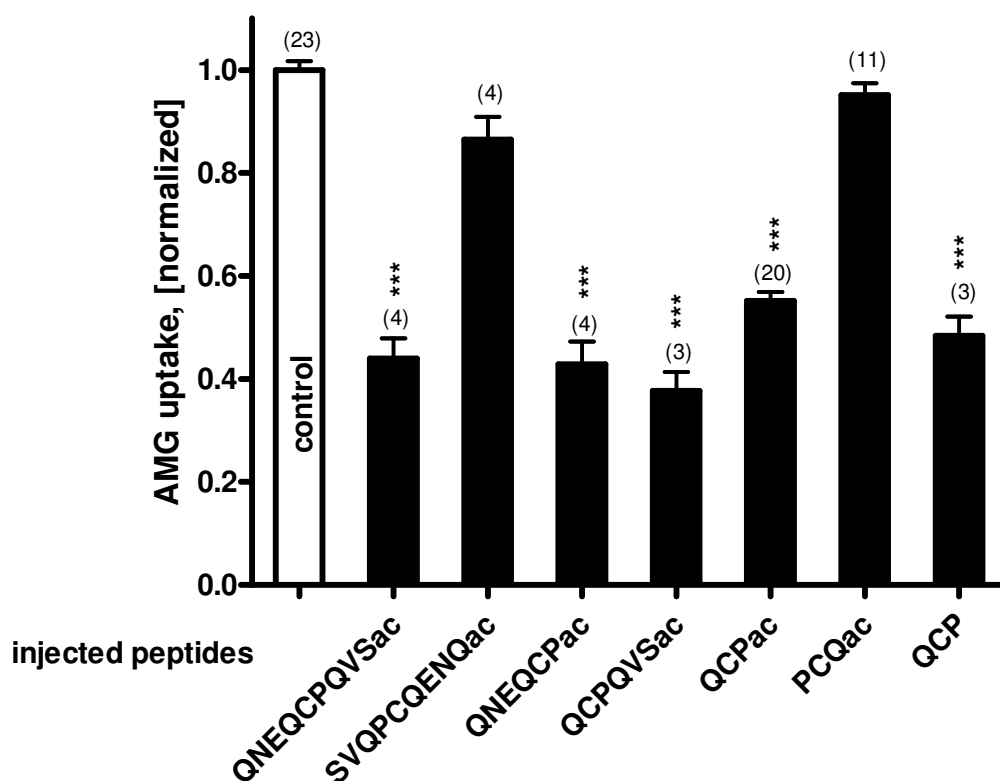


**Figure 4.2. Short-term effects of peptides derived from hRS1 on AMG uptake expressed by hRS1.** 2.5 ng of hSGLT1 cRNA were injected in *X. laevis* oocytes, the oocytes were incubated for three days, and 25 nl K-ORi buffer (control) or 25 nl K-ORi buffer containing 75 pmol of the indicated peptides were injected. Acetylated (ac) and nonacetylated peptides were injected. One hour later uptake of 50  $\mu\text{M}$  [ $^{14}\text{C}$ ]-AMG was measured. Uptake measurements were normalized to parallel performed measurements in the control. Mean values  $\pm$  SE are indicated. The number of independent experiments is given in parentheses. \*\*\*,  $P < 0.001$  for difference to control, determined according to the ANOVA with post hoc Tukey's test.

No significant down-regulation of hSGLT1-mediated uptake of [<sup>14</sup>C]-AMG was observed when the reversal control peptide SVQPCQENQac was co-injected to a final concentration of 0.2 mM. To identify whether the whole nine amino acids sequence QNEQCPQVS is prerequisite for the down-regulation of hSGLT1 expressed in *Xenopus* oocytes, two hexapeptides derived by the deletion of three amino acids from amino- or carboxy-termini (QNEQSPac and QCPQVSac, respectively) were co-injected into hSGLT1 expressing oocytes, and after one hour of incubation the uptake of [<sup>14</sup>C]-AMG was measured. Both hexapeptides QNEQCPac and QCPQVSac revealed the same level of down-regulation of hSGLT1 mediated [<sup>14</sup>C]-AMG uptake as the nonapeptide, and contained an overlapping region QCP. This suggests that QCP might be the active domain involved in the regulatory processes described above. To investigate whether only the QCP sequence is responsible for the down-regulation of hSGLT1, the QCP tripeptide was co-injected into hSGLT1 expressing oocytes to a final concentration of 0.2 mM and after one hour of incubation hSGLT1-mediated uptake of [<sup>14</sup>C]-AMG was determined. hSGLT1 expressing oocytes, injected with reversal tripeptide PCQac one hour prior to uptake measurements, served as a control. In the presence of QCPac, the uptake of [<sup>14</sup>C]-AMG was down-regulated by about 50%, as well as in presence of nonapeptide QNEQCPQVSac, whereas no down-regulation of [<sup>14</sup>C]-AMG uptake after co-injection of reversal control tripeptide PCQac was observed. Similar degrees of inhibition were obtained for both acetylated and nonacetylated QCP tripeptides (Fig. 4.2).

### **4.3. QCP inhibits hSGLT1 mediated AMG uptake with high affinity**

To identify the affinity for the inhibition of hSGLT1-mediated AMG uptake by acetylated and nonacetylated QCP, different amounts of these tripeptides were co-injected into hSGLT1 expressing oocytes one hour prior to uptake measurements, and then the uptake of 50 $\mu$ M [<sup>14</sup>C]-AMG was measured

## 4. Results

as described in 3.2.6 (Fig. 4.3a, b). hSGLT1 expressing oocytes served as a control. Assuming a distribution volume of 0.4  $\mu\text{l}$  per oocyte (Zeuthen et al., 2002),  $\text{IC}_{50}$  values of  $2.01 \pm 0.08$  nM for QCPac (n=5) and  $2.08 \pm 0.3$  nM for non acetylated QCP (n=2) were obtained. The data indicate high affinity down-regulation of hSGLT1-mediated uptake of [ $^{14}\text{C}$ ]-AMG by QCP. The affinity of the tripeptides is not changed by the N-terminal acetylation.

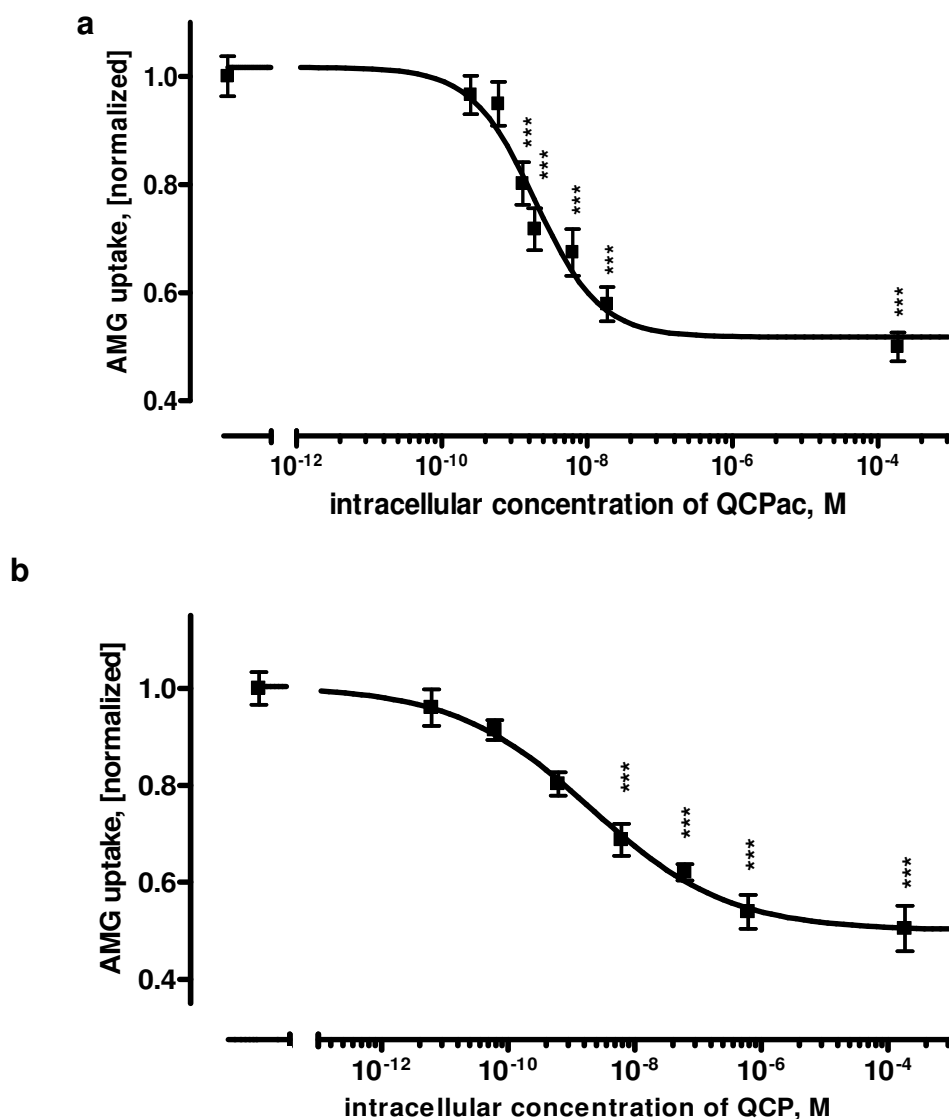


**Figure 4.3. Concentration dependence for inhibition of hSGLT1 by intracellular QCP and QCPac.** hSGLT1 expressing oocytes were injected with 25 nl K-ORi containing various amounts of QCPac (a) or QCP(b). After 1 h incubation at room temperature, uptake of 50  $\mu\text{M}$  [ $^{14}\text{C}$ ]AMG was measured. The indicated curves were obtained by fitting the Hill equation to data obtained from 2 to 5 experiments with the different tripeptides. \*\*\* indicate significantly lower AMG uptake compared to AMG uptake in oocytes without injected tripeptides ( $P < 0.001$ ), determined according to the ANOVA with post hoc Tukey's test.

### **4.4. Effect of different tripeptides, derived from QCP, on hSGLT1-mediated uptake of AMG**

The tripeptide QCP derived from the middle part of hRS1 might be active due to presence of the cysteine in the middle position, which can lead both to the formation of unspecific disulfate bounds to an intracellular protein and/or to the dimerization of the tripeptides. To investigate whether the cysteine in the middle position of QCP is crucial for its function, a screening of different QCP-like tripeptides, in which the middle cysteine residue was substituted by other amino acids (Fig. 4.4) was performed. First of all, the tripeptides QSP and QPP were selected for the screening. These tripeptides are present in the sequence of the human, mouse and rabbit RS1 protein, and the tripeptide QTP, present in the porcine RS1. Since the middle amino acid residues in the tripeptides listed above had different biochemical properties (serine and treonine are hydrophilic neutral; proline and cysteine are hydrophobic), amino acids with different biochemical features were chosen for the next mutations and introduced into the tripeptides: glutamate as hydrophilically charged, asparagine as hydrophilically neutral, and glycine and leucine as hydrophobic amino acids. 75 pmol of the tripeptides were injected into the hSGLT1 expressing oocytes. After one hour incubation at room temperature the uptake of [<sup>14</sup>C]-AMG was measured as described in 3.2.6. Of all tested mutations, under the employed experimental conditions only the tripeptide QNPac had no inhibitory effect on the hSGLT1-mediated AMG uptake. Down-regulation by the tripeptides QEP, QPPac, QTPac, QGPac, and QLPac was not as strong as by QCP, QCPac, QSP and QSPac, but still significant. This suggests that cysteine in the middle position of QCP is not essential for the function; however, the substitution of the cysteine may change the affinity of the tripeptide for the down-regulation of hSGLT1 (Fig. 4.4).

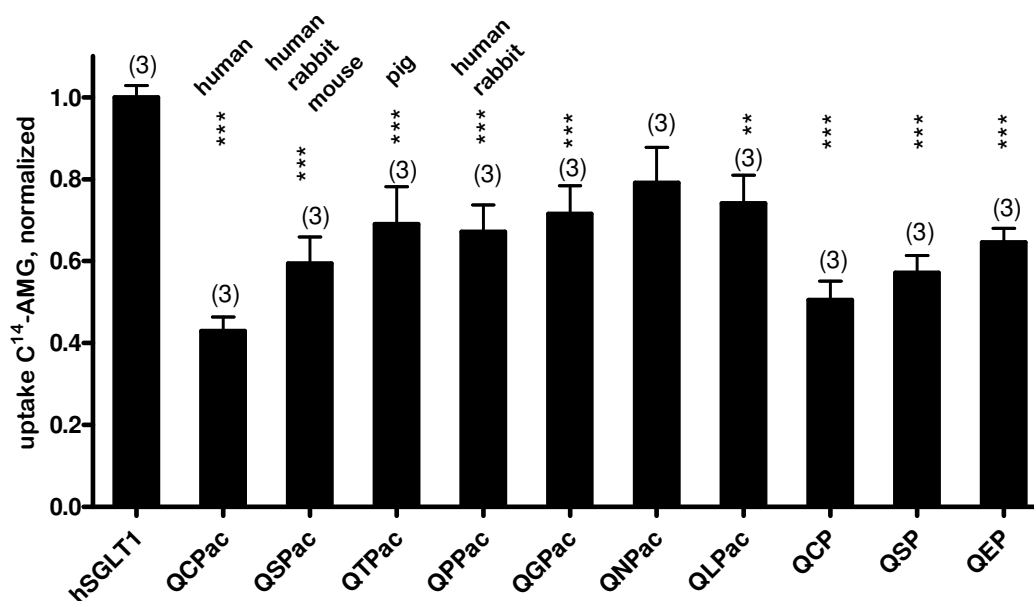


**Figure 4.4. Short-term effects of peptides derived from hRS1 on AMG uptake expressed by hRS1.** 2.5 ng of hSGLT1 cRNA were injected in *X. laevis* oocytes, the oocytes were incubated for three days, and 25 nl K-ORi buffer (control, hSGLT1) or 25 nl K-ORi buffer containing 75 pmol of the indicated peptides were injected. Acetylated (ac) and nonacetylated peptides were injected. One hour later uptake of 50  $\mu$ M [ $^{14}$ C]-AMG was measured. Uptake measurements were normalized to parallel performed measurements in the control. \*\*,  $P < 0.01$  and \*\*\*,  $P < 0.001$  for difference to control, determined according to the ANOVA with post hoc Tukey's test.

#### 4.5. QSP down-regulates hSGLT1-mediated uptake of AMG with high affinity

Inasmuch as the sequence of the hRS1 contains two QSP tripeptides in the N-terminal part (aa 19-21 and aa 91-93), the identification of the affinity of QSPac and QSP for the down-regulation of the hSGLT1-mediated uptake of [ $^{14}$ C]-AMG was performed. Different amounts of the QSP and QSPac tripeptides were injected with 25 nl of K-ORi buffer into the hSGLT1 expressing oocytes and following one hour of incubation at room temperature the uptake of 50  $\mu$ M [ $^{14}$ C]-AMG was determined as described in 3.2.6. (Fig. 4.5). Oocytes expressing hSGLT1 served as a control. Assuming a distribution volume of 0.4  $\mu$ l per oocyte (Zeuthen et al., 2002),  $IC_{50}$  values of  $0.17 \pm 0.03$  nM for QSPac (n=2) and  $0.16 \pm 0.003$  nM for QSP (n=3) were obtained. Data indicates high affinity down-regulation of SGLT1-mediated uptake of [ $^{14}$ C]-AMG by QSP.

## 4. Results

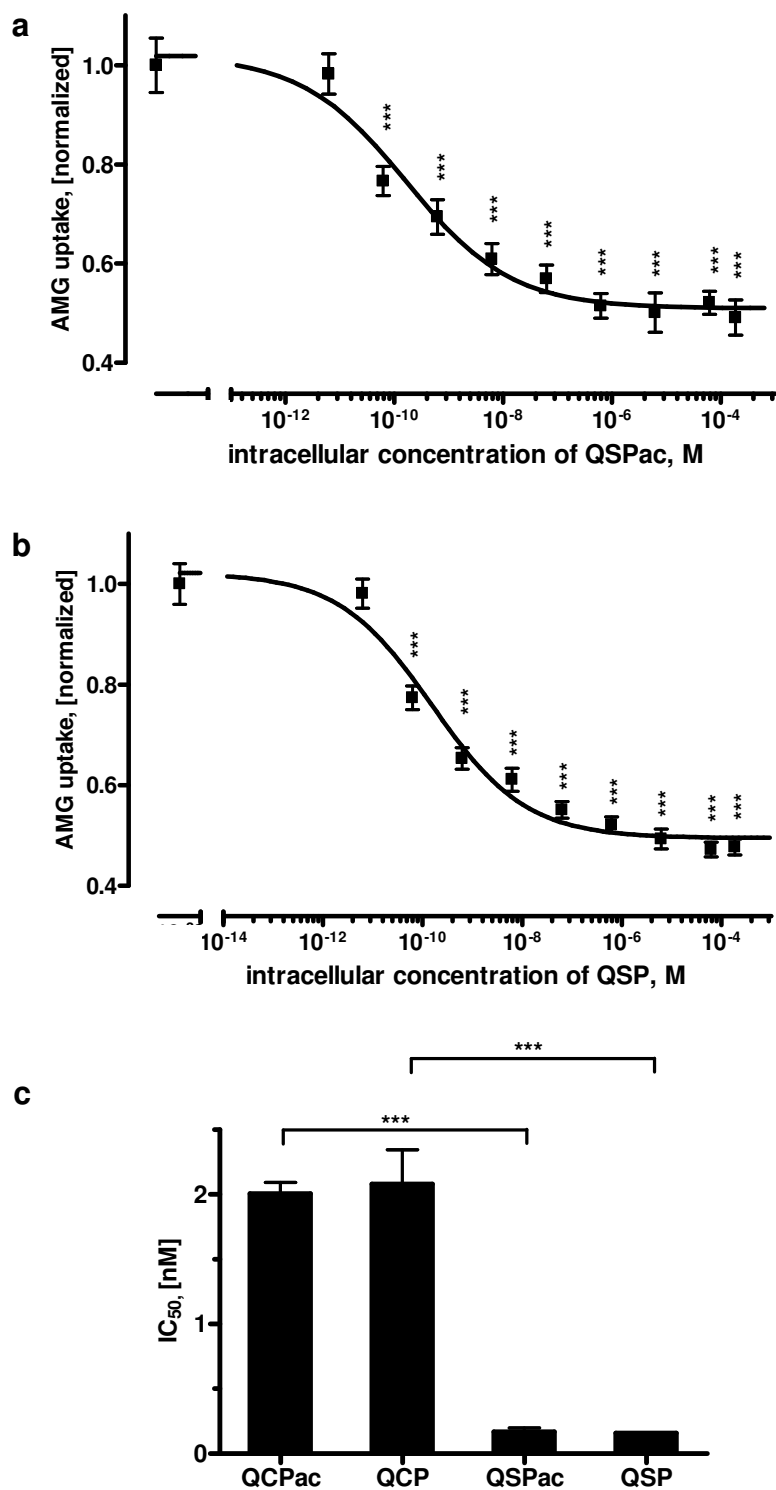


Figure 4.5. Concentration dependence for inhibition of hSGLT1 by intracellular QSP and QSPac. hSGLT1 expressing oocytes were injected with 25 nl K-ORi containing various amounts of QSPac (a) or QSP(b). After 1 h incubation at room temperature, uptake of 50  $\mu$ M [<sup>14</sup>C]AMG was measured. The indicated curves were obtained by fitting the Hill equation to data obtained from 2 to 5 experiments with the different tripeptides. \*\*\* indicate significantly lower AMG uptake compared to AMG uptake in oocytes without injected tripeptides ( $P < 0.001$ ), determined according to the ANOVA with post hoc Tukey's test. (c) Comparison of the mean IC<sub>50</sub> values determined by fitting the Hill equation to individual concentration inhibition curves. \*\*\*,  $P < 0.001$  for difference, determined according to the ANOVA with post hoc Tukey's test.

The affinity of the tripeptides is not changed by the N-terminal acetylation. Compared to the IC<sub>50</sub> values obtained for the inhibition of hSGLT1 by QCP (4.3), both acetylated and non acetylated QSP inhibit hSGLT1-mediated AMG uptake about ten-fold more effectively (Fig. 4.5c).

### **4.6. QCP reduces the amount of hSGLT1 in the plasma membrane**

In earlier studies, hRS1wt has been proposed to decrease the hSGLT1-mediated uptake of AMG by reduction of the amount of hSGLT1 in the plasma membrane via inhibition of SGLT1 release from TGN (Veyhl et al., 2003; Kroiss et al., 2006). To investigate whether down-regulation of hSGLT1 by QCP undergoes the same mechanism, the isolation of the plasma membrane of non-injected control oocytes, hSGLT1-expressing oocytes, and hSGLT1-expressing oocytes coinjected with 75 pmol of QCP was performed. The group of hSGLT1-expressing oocytes was coinjected with 25 nl of K-ORi containing 75 pmol QCP and incubated for one hour at room temperature. Then both control, hSGLT1 expressing oocytes, and QCP-injected hSGLT1 expressing oocytes were incubated with 50 µM AMG for 15 min at room temperature, washed three times with ice-cold ORi buffer. Subsequently, an isolation of the plasma membranes was performed. The total protein content in the samples from five experiments (two samples per experimental condition) was determined according to Bradford and normalized to the control in each experiment.

To evaluate the content of hSGLT1 protein in the isolated plasma membrane fractions of hSGLT1 expressing oocytes, injected with QCP and non-injected, the densitometric analysis of the immunoblots was performed. For each experiment, the density of SGLT1 corresponding band of plasma membrane fraction of hSGLT1 expressing control oocytes were taken as 100%, and the density of the hSGLT1-corresponding band in other samples was normalized as a percentage of the control (Fig. 4.7b). The obtained data showed decrease of the

## 4. Results

content of the hSGLT1 protein in the plasma membrane by about 50% when QCPac was coinjected.

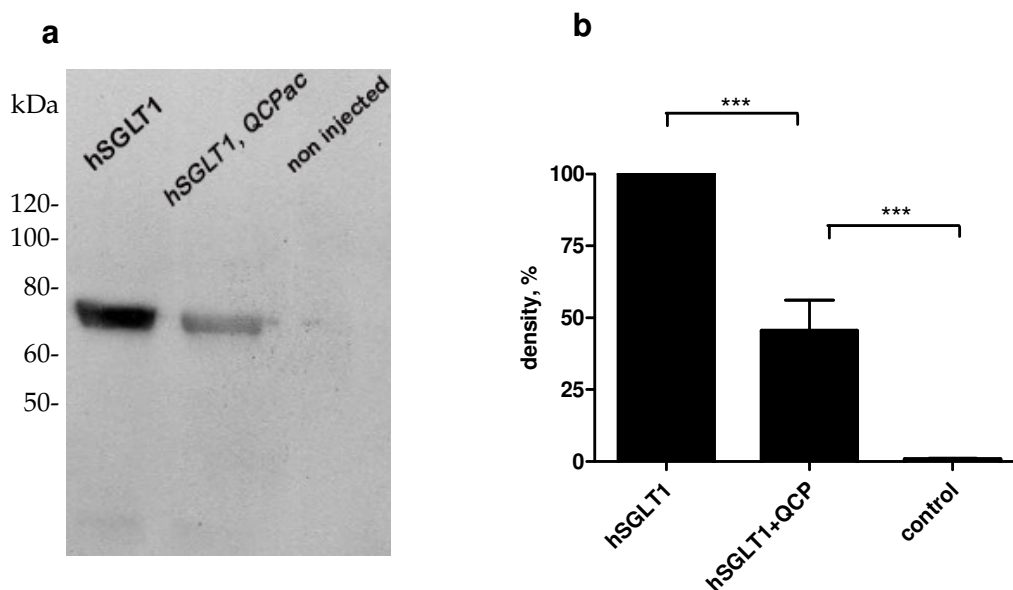


**Figure 4.7. Quantification of hSGLT1 protein in the plasma membrane.** Plasma membranes were isolated from non-injected, oocytes expressing hSGLT1, and oocytes expressing hSGLT1 that were injected with 75 pmol QCPac, incubated for 1 hour and then, for another 15 min, in ORi buffer containing 50  $\mu$ M AMG. (a) The left panel shows a Western blot from a typical experiment that was stained with affinity purified antibody against hSGLT1. Per lane, 2  $\mu$ g of protein was applied. (b) A densitometric quantification of five independent experiments. \*\*\*,  $P < 0.001$ , determined according to the ANOVA with post hoc Tukey's test.

Phlorizin-induced change of plasma membrane capacitance of *Xenopus* oocytes expressing hSGLT1 has been previously shown to be due to an alteration of amount of the hSGLT1 protein in the plasma membrane (Parent et al., 1992). The superfusion of the oocytes with AMG alters the cytoplasmic concentration of AMG, and thereafter modulates the effect of QCP on hSGLT1 (see below). Phlorizin itself does not induce current because it is not transported; however, it decreases the membrane capacitance by the blockage of the potential-dependent charge movements within hSGLT1. To investigate whether QCP can influence the number of functionally active hSGLT1 molecules within the plasma membrane, the capacitance measurements were performed. Oocytes expressing hSGLT1 were injected with 25 nl of  $K^+$ -ORi buffer with or without 75 pmol QCP and incubated at room temperature for one hour. Then capacitance measurements under two-electrode voltage clamp conditions were performed.



## 4. Results

Oocytes were clamped to a holding potential  $-40$  mV and the inward current and capacitance change were induced by application of  $5$  mM AMG for  $90$  sec. To wash out the AMG, the oocytes were superfused with ORi buffer until the current and membrane capacitance means reversed to the initial levels. Application of  $100$   $\mu$ M phlorizin for  $90$  sec led to the change of the membrane capacitance, whereas no inward current was observed (Fig. 4.8a). When the oocytes were subsequently washed with ORi buffer, the membrane capacitance reversed to the initial level.

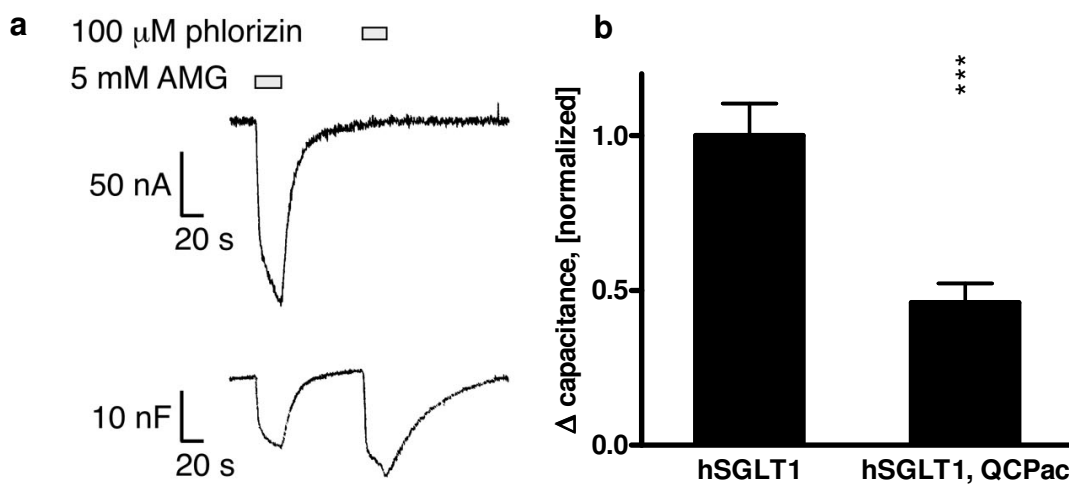


**Figure 4.8. QCP decreases the amount of hSGLT1 protein and phlorizin binding sites in the plasma membrane.** (a) Effect of QCP on phlorizin induced capacitance changes in oocytes expressing hSGLT1. Oocytes expressing hSGLT1 were superfused with ORi buffer and clamped to  $-50$  mV. Inward currents and capacitance were measured when oocytes were superfused with ORi buffer containing  $5$  mM AMG or  $100$   $\mu$ M phlorizin (left panel). (b) Phlorizin induced capacitance decrease in hSGLT1 expressing oocytes injected with K-ORi buffer (hSGLT1) or K-ORi buffer containing  $75$  pmol per oocyte of QCP is compared on the right. Mean values  $\pm$  SE of  $9$  oocytes from three independent experiments are compared. \*\*\*,  $P < 0.001$ , determined according to the ANOVA with post hoc Tukey's test.

The obtained results indicate a decrease of phlorizin-induced capacitance change by about  $50\%$  in the hSGLT1-expressing oocytes, coinjected with QCP, compared with control oocytes (Fig. 4.8b). These results support the hypothesis that the short-term down-regulation of hSGLT1-mediated uptake of AMG by QCP is due to a decrease of the amount of functional hSGLT1 transporters in the plasma membrane.

### 4.7. QCP blocks the exocytotic pathway of hSGLT1

It has been previously shown that the post-transcriptional down-regulation of hSGLT1 by hRS1 does not occur through the modulation of endocytosis (Veyhl et al., 2006). Moreover, no effect on hSGLT-mediated [<sup>14</sup>C]-AMG uptake was observed when either release of the vesicles from trans-Golgi network or fusion of vesicles with the plasma membrane was blocked (Veyhl et al., 2006), which suggests that hRS1 inhibits the exocytotic pathway of hSGLT1.

To investigate whether the post-transcriptional down-regulation of hSGLT1-mediated [<sup>14</sup>C]-AMG uptake by QCP undergoes a similar mechanism, experiments with the inhibitors of exocytosis, Botulinum toxin B and Brefeldin A, were performed.

Botulinum toxin B (BtxB) is a neurotoxic protein with the zinc-dependent endopeptidase activity, produced by the Bacterium *Clostridium Botulinum*. BtxB prevents the fusion of the exocytotic vesicles with the plasma membrane by cleavage of vesicle-associated membrane protein (VAMP or synaptobrevin). As a key step in the pathway to exocytosis, synaptobrevin, a SNARE protein, incorporated into the transport vesicles membranes, primarily mediates the fusion of the cellular transport vesicles and contributes to the specificity of membrane fusion (Sollner et al., 1993). The synaptobrevin had also been demonstrated to be expressed in the *Xenopus* oocytes (Aleu et al., 2002).

To block exocytosis, oocytes expressing hSGLT1 were injected with 2 ng/oocyte of BtxB and uptake of [<sup>14</sup>C]-AMG was measured after incubation of oocytes for 30 min at 21°C. An application of BtxB led to the inhibition of hSGLT1-mediated [<sup>14</sup>C]-AMG uptake by about 60% within 30 min (Fig. 4.9). This observation implies that VAMP/synaptobrevin-mediated exocytosis is the critical step for the rapid turnover of hSGLT1 in the plasma membrane. Injection of 75 pmol of QCP did not lead to an additional down-regulation of hSGLT1-mediated [<sup>14</sup>C]-AMG uptake (Fig. 4.9). These data suggest that QCP down-regulates either recycling or the exocytotic pathway of hSGLT1.

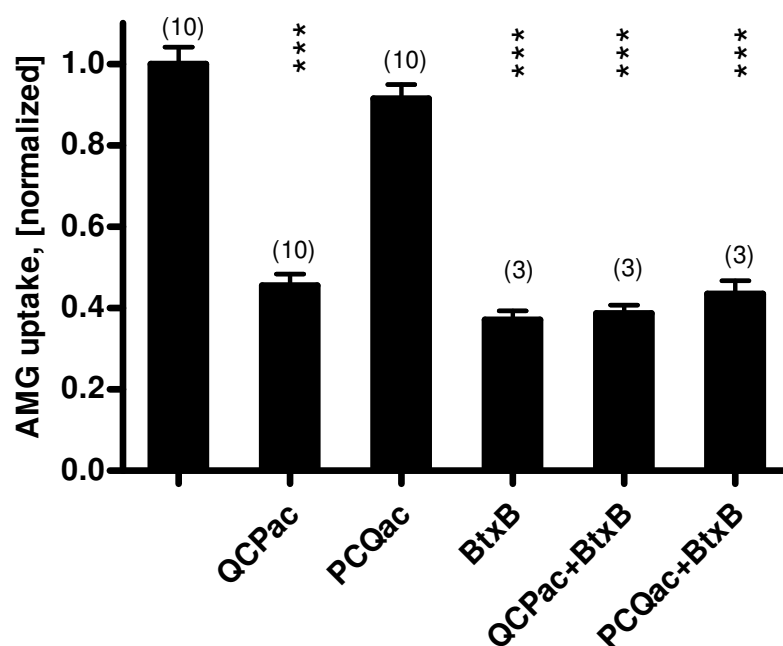
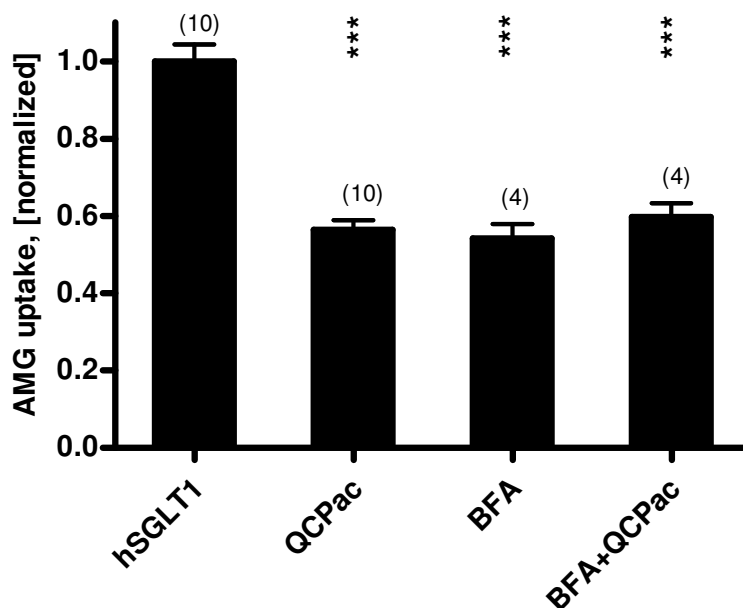


Figure 4.9. QCP does not inhibit hSGLT1-mediated AMG uptake when the fusion of the exocytotic vesicles with the plasma membrane is blocked. hSGLT1 expressing oocytes were injected with 25 nl K-ORi buffer or with 25 nl K-ORi buffer containing 75 pmol QCPac, 2 ng BtxB, QCPac plus BtxB, or PCQac plus BtxB. After 1 h incubation, uptake of 50  $\mu$ M [ $^{14}$ C]-AMG was measured. The number of independent experiments is given in parentheses. \*\*\*,  $P < 0.001$ , determined according to the ANOVA with post hoc Tukey's test.

Brefeldin A (BFA), a lactone antibiotic produced by fungal organisms such as *Eupenicillium brefeldimun*, inhibits the transport in the *trans*-Golgi network. The main targets of the BFA are the guanosine nucleotide exchange factors responsible for the activation of ADP-ribosylation factor that regulates the assembly of the coat complexes at *trans*-Golgi network and endosomes, involved in the protein sorting and release of the vesicles (Chardin and McCormick, 1999; Donaldson et al., 1992; Helms and Rothman, 1992). Co-injection of 0.5 pmol BFA into hSGLT1-expressing oocytes decreased the [ $^{14}$ C]-AMG uptake by about 50% within 30 min, similarly to the effect of QCP (Fig. 4.10).



**Figure 4.10. QCP does not inhibit hSGLT1-mediated AMG uptake when the exocytotic pathway is blocked by inhibition of transport in TGN.** hSGLT1 expressing oocytes were injected with 25 nl K-ORi buffer or with 25 nl K-ORi buffer containing 75 pmol QCPac, 0.5 pmol BFA, or QCPac plus BFA. After 1 h incubation uptake of 50  $\mu$ M [ $^{14}$ C]-AMG was measured. The number of independent experiments is given in parentheses. \*\*\*,  $P < 0.001$ , determined according to the ANOVA with post hoc Tukey's test.

Moreover, no further significant decrease in [ $^{14}$ C]-AMG uptake was observed when QCPac and BFA were co-injected. The data indicate that QCP blocks the exocytotic pathway of hSGLT1 most probably by inhibiting of the release of the hSGLT1-containing vesicles, derived from trans-Golgi network or endosomes and critically involved in the short-term regulation.

#### **4.8. Down-regulation of hSGLT1 by QCP and QSP is monosaccharide-dependent**

It has been reported earlier, that inhibition of hSGLT1-mediated AMG uptake in *Xenopus* oocytes injected with purified hRS1 protein was prevented when oocytes were preloaded with D-glucose (Veyhl et al., 2006). The present study investigated whether different monosaccharides have any protective

## 4. Results

---

effects on the inhibition of hSGLT1-mediated AMG uptake by QCP and QSP. The hSGLT1 expressing oocytes had been injected with 25 nl K-ORi buffer with or without 75 pmol QCP or QSP containing various amounts of mannitol, sorbitol, D-glucose, D-fructose, AMG, or 2-deoxyglucose. Oocytes were incubated for 1 h at room temperature in ORi buffer, pH 7.6, and uptake of 1.75  $\mu$ M [ $^{14}$ C]-AMG was measured. Fig. 4.11a illustrates the control experiments testing the potential effects of intracellular polyalcohols and monosaccharides on the hSGLT1-mediated uptake of AMG in the absence of inhibitory tripeptides. AMG uptake was not influenced by intracellular sorbitol, mannitol, D-glucose, 2-deoxyglucose, and AMG up to the concentration of about 60 mM and by intracellular concentrations of 0.025, 0.25, 2.5, and 62.5 mM D-fructose (Fig. 4.11a). At variance, AMG uptake was 30% increased by 25 mM intracellular D-fructose. Various intracellular concentrations of mannitol and sorbitol did not influence the inhibition of hSGLT1-mediated AMG uptake by QCPac (Fig. 4.11b), hence excluding potential osmotic effects. By contrast, the inhibition of AMG uptake by QCPac was significantly protected when the oocytes contained 0.25-62.5 mM of D-glucose or D-fructose. The monosaccharides AMG and 2-deoxyglucose exhibited biphasic effects on the inhibition of hSGLT1-mediated AMG uptake by QCPac and QSP. The inhibitory effect of the tripeptides was most strongly prevented by 0.25 mM AMG or 2-deoxyglucose. Higher concentrations of these monosaccharides were less effective (Fig. 4.11b). The observed high and low affinity effects of various hexoses suggest the existence of intracellular high and low affinity sugar binding sites.

## 4. Results

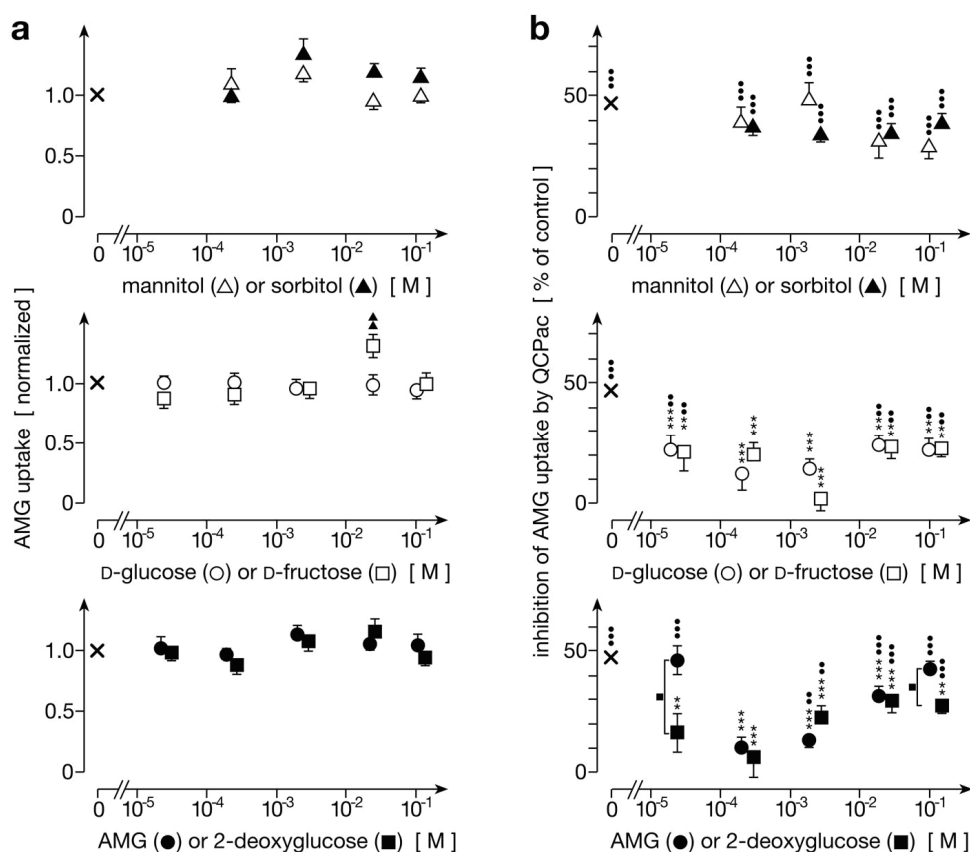


**Figure 4.11. Effects of intracellular monosaccharides on the inhibition of hSGLT1 expressed AMG uptake.** hSGLT1 expressing oocytes were injected with 25 nl K-ORi containing either indicated concentrations of polyalcohols and hexoses or 75 pmol of tripeptides plus polyalcohols or monosaccharides. After 1 h incubation at room temperature, uptake of 1.75  $\mu\text{M}$  [<sup>14</sup>C]AMG was measured. Each data point represents the mean value of 25-30 individual measurements from 3 independent experiments. (a) Effects of injected polyalcohols and monosaccharides on hSGLT1-mediated AMG uptake in the absence of tripeptides. (b) Effects of injected polyalcohols and monosaccharides on the inhibition of hSGLT1-mediated AMG uptake by QCPac. \*\*,  $P < 0.01$  and \*\*\*,  $P < 0.001$  for inhibitory effect of tripeptides. \*\*,  $P < 0.01$ , \*\*\*,  $P < 0.001$  for protective effects of monosaccharides. ▲▲ $P < 0.01$  for stimulation of hSGLT1-mediated AMG uptake by D-fructose; ■,  $P < 0.01$ . P values determined according to the ANOVA with post hoc Tukey's test.

To determine the half-maximal concentrations for the protective high affinity effects ( $PC_{50}$ ) of AMG and 2-deoxyglucose, hSGLT1 expressing oocytes had been injected with 25 nl K-ORi containing different amounts of AMG or 2-deoxyglucose with or without 75 pmol of QCPac or QSP, incubated at room temperature for 1 hour and uptake of 1.75  $\mu\text{M}$  [<sup>14</sup>C]-AMG was measured (Fig. 4.12). Significantly different  $PC_{50}$  values of  $11.9 \pm 0.7 \mu\text{M}$  and  $53.1 \pm 1.7 \mu\text{M}$  for 2-deoxyglucose and AMG, respectively, were obtained ( $n=3$  each,  $P < 0.001$ ). For the high affinity protective effect of D-glucose on the inhibition of hSGLT1 mediated AMG uptake by QSP, a  $PC_{50}$  value of  $30.2 \pm 6.2 \mu\text{M}$  ( $n=3$ ) was determined. The

## 4. Results

obtained data indicate an involvement of a high affinity monosaccharide binding site in the modulation of QCP/QSP-mediated post-transcriptional down-regulation of hSGLT1.

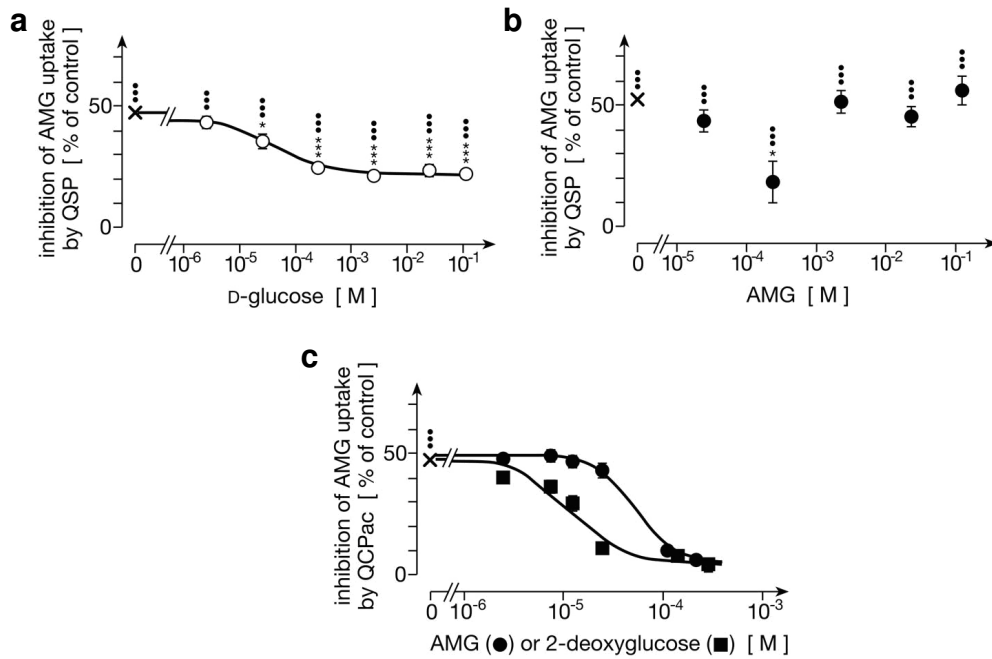


**Figure 4.12. Effects of intracellular monosaccharides on the inhibition of hSGLT1 expressed AMG uptake.** (a) Protective high affinity effect of D-glucose on the inhibition of AMG uptake by QSP. (b) Inhibition of AMG uptake by QSP in the presence of different intracellular concentrations of AMG. (c) Comparison of protective high affinity effects of AMG or 2-deoxyglucose on the inhibition of AMG uptake by QCPac. The lines in figures (a) and (c) were obtained by fitting the Hill equation to the data. \*\*,  $P < 0.01$  and \*\*\*,  $P < 0.001$  for inhibitory effect of tripeptides. \*\*,  $P < 0.01$ , \*\*\*,  $P < 0.001$  for protective effects of monosaccharides, determined according to the ANOVA with post hoc Tukey's test.

### **4.9. QCP exhibits glucose-dependent down-regulation of the organic cation transporter hOCT2**

Co-expression of hRS1wt with the human organic cation transporter hOCT2 had been previously shown to induce a significant decrease of the hOCT2-mediated uptake of [<sup>14</sup>C]-TEA (Veyhl et al., 2003). On the contrary, the hOCT2-mediated TEA uptake was not inhibited, when purified hRS1 protein was injected into hOCT2 expressing oocytes 1 hour prior to uptake measurements. Further investigations identified that intermediate intracellular concentrations of glucose are required for the down-regulation of hOCT2. The short-term inhibition of hOCT2 by hRS1 protein was only observed when the intracellular concentration of AMG in the oocytes raised by injecting AMG to an intracellular concentration of about 0.25 mM. To determine whether QCP also down-regulates hOCT2 in the presence of intracellular AMG, oocytes expressing hOCT2 had been injected with 25 nl of K-ORi buffer containing 75 pmol QCPac alone, 75 pmol QCPac with 0.1 nmol AMG, or 75 pmol QCPac with 1 nmol AMG. After injection, oocytes were incubated at room temperature for 1 hour in ORi buffer pH 7.6, and uptake of 10 μM [<sup>14</sup>C]-TEA was measured as described in 3.2.6. As shown in figure 4.13, no significant alteration in hOCT2-mediated TEA uptake was observed when QCPac alone was injected. By contrast, in presence of 0.25 mM and 2.5 mM of AMG intracellularly, [<sup>14</sup>C]-TEA uptake was decreased by 36±2.6% and 23±2.4%, respectively. The data suggest that QCP exhibits the same transporter specificity and monosaccharide dependence for the short-term down-regulation of hOCT2 as the total hRS1 protein.



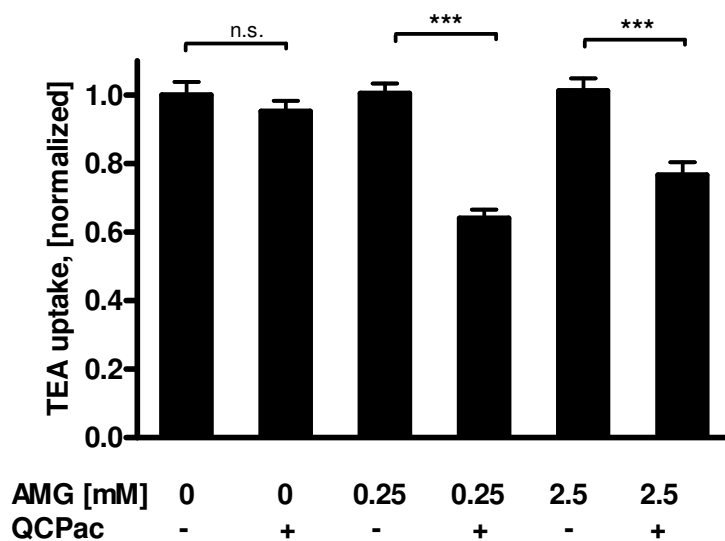


**Figure 4.13.** Effects of QCP in the absence and presence of intracellular AMG on hOCT2-mediated TEA uptake and hSGLT2-mediated AMG uptake. hOCT2 cRNA was injected into the oocytes and the oocytes were incubated for 3 days. Oocytes were injected with 25 nl K-ORi buffer without or with 75 pmol QCPac. In some experiments, the K-ORi buffer also contained 4 or 40 mM AMG leading to the indicated intracellular concentrations of 0.25 mM or 2.5 mM AMG, respectively. After 1 h incubation, uptake of 10  $\mu$ M [ $^{14}$ C]TEA was measured. \*\*,  $P < 0.01$ , \*\*\*,  $P < 0.001$  for the effects of monosaccharides, determined according to the ANOVA with post hoc Tukey's test.

#### 4.10. Down-regulation of hSGLT1 by QCP is independent of Protein Kinase C (PKC)

Earlier studies performed in our laboratory observed that in hSGLT1 expressing oocytes, the effect of the hRS1 protein was increased after stimulation of PKC (Veyhl et al., 2003). Therefore, the present study investigated whether PKC is also involved in the short-term down-regulation of hSGLT1-mediated AMG uptake by QCP (Fig. 4.14). For PKC stimulation, hSGLT1 expressing oocytes injected with 25 nl K-ORi buffer or K-ORi buffer containing 75 pmol QCPac were either co-injected with 0.5 pmol of DOG 1 hour prior to tracer uptake measurements, or incubated with 1  $\mu$ M PMA for 2 min, washed twice, and uptake of [ $^{14}$ C]-AMG was determined as described.

## 4. Results

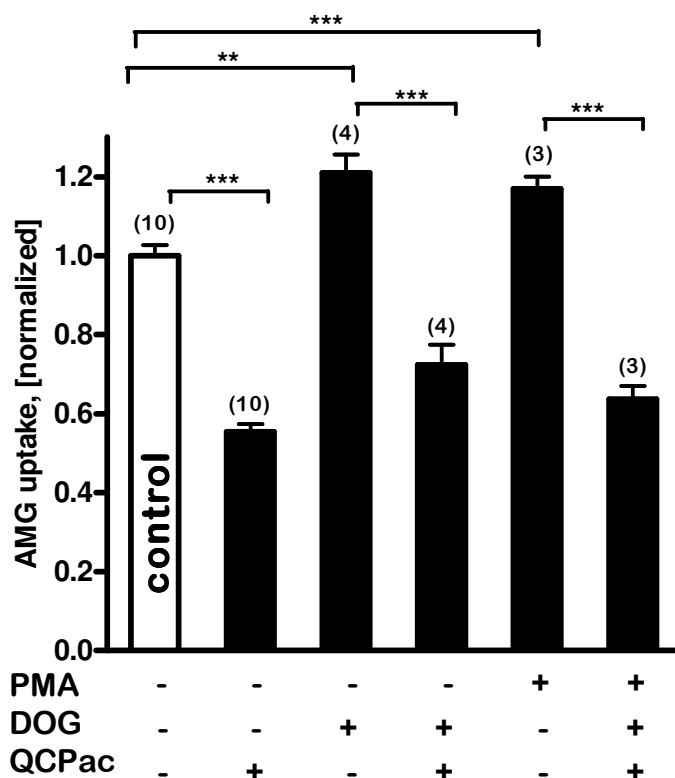


**Figure 4.14. Analysis of the effect of PKC stimulation on hSGLT1 expressed AMG uptake in the absence and presence of QCP.** hSGLT1 expressing oocytes were injected with 25 nl K-ORi without and with 75 pmol QCPac and/or 0.5 pmol DOG. After 1 h incubation at room temperature, uptake of 50  $\mu$ M [ $^{14}$ C]-AMG was measured. In some experiments the oocytes were incubated with 1  $\mu$ M PMA 2 min prior to uptake measurements. The number of independent experiments, in each of which 8-11 oocytes were analyzed, is given in parentheses. \*\*,  $P < 0.01$ , \*\*\*,  $P < 0.001$ , determined according to the ANOVA with post hoc Tukey's test.

The activation of PKC by both DOG and PMA in hSGLT1 expressing oocytes resulted in increase of hSGLT1-mediated AMG uptake. Whereas stimulation of PKC increased the short-term inhibition of AMG uptake by purified hRS1 protein (Veyhl et al., 2006), no alteration in the QCP-induced down-regulation of hSGLT1 was observed after PKC activation (Fig. 4.14). This indicates that the short-term down-regulation of hSGLT1 by hRS1 is mediated via QCP and/or QSP sites in hRS1 that are modulated by PKC-dependent phosphorylation of hRS1.

#### 4.11. Extracellular QCP has no effect on the hSGLT1-mediated uptake of AMG in *Xenopus* oocytes

To elucidate whether extracellular application of QCP may also effect the activity of the transporter, hSGLT1-expressing oocytes were incubated for 1 hour in ORi buffer pH 7.6 containing 1 mM QCPac, and the tracer uptake measurements were performed as described in 3.2.6. hSGLT1 expressing oocytes incubated in ORi buffer without addition of QCPac served as a control (Fig. 4.15).

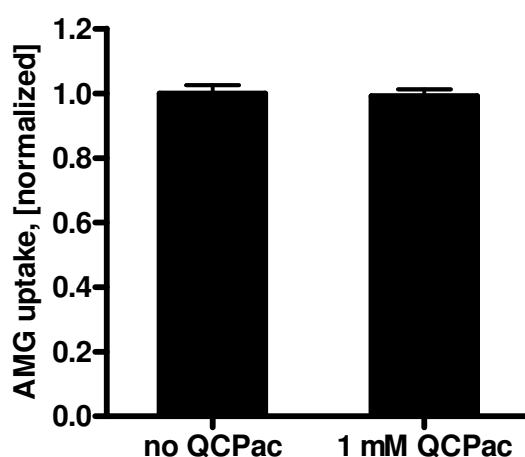


**Figure 4.15. Effect of extracellular QCP on hSGLT1.** hSGLT1 expressing oocytes were incubated in ORi buffer containing 1 mM QCPac for 1 hour, washed in ORi buffer, and uptake of [<sup>14</sup>C]-AMG was measured. Mean values ± SE of 3 independent experiments are presented.

As shown in the figure 4.15, in the oocytes incubated in ORi buffer containing QCPac uptake values were not significantly different compared to control oocytes. This data indicates that extracellular QCP has no effect on SGLT1.

#### 4.12. Extracellular application of QCP decreases hPEPT1-mediated transport of glycyl-sarcosine in *Xenopus* oocytes

Intestinal peptide transport plays a central role in the absorption of the protein digestion end-products as well as a number of peptide-like drugs. At the same time, the intestinal absorption of glucose, which allows its transfer from the lumen to the blood, occurs through enterocytes. Earlier studies indicated that the small intestine absorbs dietary protein predominantly in form of small peptides rather than single amino acids, and revealed the existence of specific peptide plasma membrane transport proteins (Ganapathy et al., 1994). While many ion-coupled solute transporters in mammalian cells are driven by an inwardly directed electrochemical Na<sup>+</sup>-gradient, oligopeptide transporters of intestinal brush-border membrane vesicles and Caco-2 cells are energized by the proton-motive force (Thwaites et al., 1993a,b). The four mammalian transporters are known to transport dipeptides, whereas the ability to transport tripeptides has been shown only for the PEPT1 and PEPT2 transporters. Beside their role in active absorption of the food-derived dipeptides and tripeptides, both transporters are known to transport a large number of bioactive, structurally related compounds such as various cephalosporins, angio-tensin converting enzyme inhibitors, and 5'-amino acid esters of the antiviral nucleosides, acyclovir and zidovudine (AZT) (Sadee and Anderle, 2006). To assess the possibility to transport QCP or QSP into the intestinal cells via human PEPT1 transporter (hPEPT1), *Xenopus* oocytes expressing hPEPT1 were incubated at room temperature for 15 min in ORi buffer, pH 6.0, either containing 200 μM [<sup>3</sup>H]-glycyl-sarcosine, the well-known substrate of hPEPT1, or 200 μM [<sup>3</sup>H]-glycyl-sarcosine together with 150 μM QCPac. Non-injected oocytes served as a control. As shown in the figure 4.16, in the presence of QCPac in the extracellular medium, hPEPT1-mediated uptake of [<sup>3</sup>H]-glycyl-sarcosine was decreased by about 50% suggesting interaction of QCP with the hPEPT1 transporter.

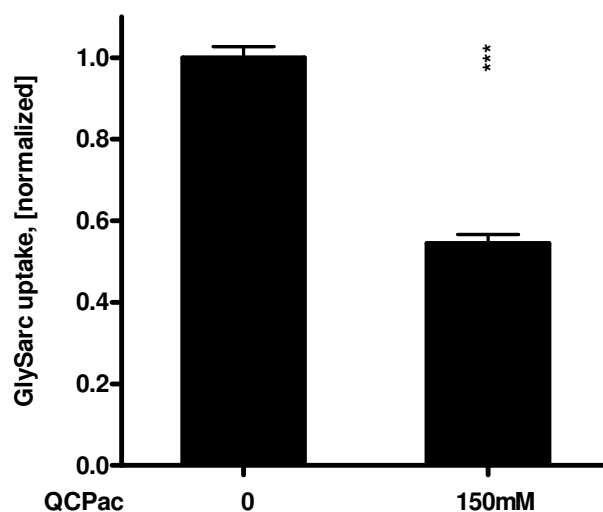


**Figure 4.16. QCPac interacts with hPEPT1 transporter.** Oocytes expressing hPEPT1 were incubated in ORi buffer, pH6.0, supplemented with 150  $\mu$ M QCPac, at room temperature for 1 hour, washed twice, and uptake of [ $^3$ H]-glycyl-sarcosine was measured. Mean values  $\pm$  SE of 3 independent experiments are presented. \*\*\*,  $P < 0.001$ , determined according to the unpaired Student's test.

The further electro-physiological investigations on hPEPT1-expressing *Xenopus* oocytes, carried out at the department of Food and Nutrition of the Technical University of Munich, proved that both QCPac and QSP are transported via hPEPT1 transporter with  $K_m$  values of  $21.4 \pm 6.6$  mM and  $4.2 \pm 0.2$  mM ( $n=6$  each), respectively (Vernaleken et al., 2007).

#### **4.13. QCP, transported via hPEPT1 transporter, down-regulates hSGLT1 in *Xenopus* oocytes**

To investigate whether QCPac, transported by the hPEPT1 transporter, can effectively down-regulate hSGLT1-mediated uptake of AMG, tracer flux measurements were performed using *Xenopus* oocytes co-expressing both hPEPT1 and hSGLT1 transporters. Oocytes were first incubated for 1 hour at room temperature in ORi buffer pH 6.0 with and without 1 mM QCPac, and then transferred into the ORi buffer pH 7.6, and uptake of [ $^{14}$ C]-AMG was measured

## 4. Results

over a time period of 15 min. The hPEPT1/hSGLT1 co-expressing oocytes incubated in ORi buffer pH 6.0 with PCQac (reversal control peptide) served as a control (Fig. 4.17).

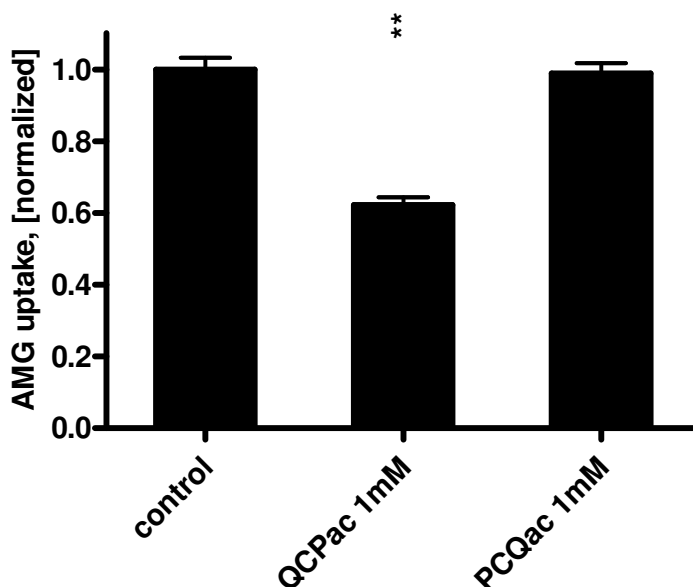


**Figure 4.17. Down-regulation of hSGLT1 in oocytes co-expressing hPEPT1 after incubation with QCPac.** Oocytes, co-expressing hSGLT1 and hPEPT1, were incubated for 1 hour at pH 6.0 in the absence of peptides (control), or in the presence of 1 mM QCPac or PCQac. The oocytes were washed twice and uptake of 50  $\mu$ M [ $^{14}$ C]-AMG was measured. Mean values  $\pm$  SE of 3 independent experiments are presented. \*\*,  $P < 0.01$ , determined according to the ANOVA with post hoc Tukey's test.

In the oocytes, pre-incubated with QCPac, hSGLT1-mediated uptake of [ $^{14}$ C]-AMG was significantly decreased, whereas incubation with reversal control peptide PCQac did not lead to the down-regulation of the [ $^{14}$ C]-AMG-uptake (Fig. 4.17). This suggests that QCP, transported into the cells via hPEPT1 transporter, can thereafter effectively down-regulate hSGLT1.

#### 4.14. Intracellular QCP does not influence activity of the hPEPT1 transporter in *Xenopus* oocytes

Previous studies showed that hRS1wt had no effect on the activity of the hPEPT1 transporter when both proteins were co-expressed in *Xenopus* oocytes (Veyhl et al., 2003). To explore whether intracellular QCP also does not modulate activity of the hPEPT1 transporter, the hPEPT1 expressing oocytes were injected with K-ORi buffer, pH 7.6, containing 75 pmol of QCPac or PCQac, one hour prior to the transport measurements. Intracellular application of QCPac as well as application of the control reversal tripeptide PCQac did not lead to any alterations in the activity of the hPEPT1 transporter (Fig. 4.18). This suggests that QCPac has the same transporter specificity as hRS1wt protein.

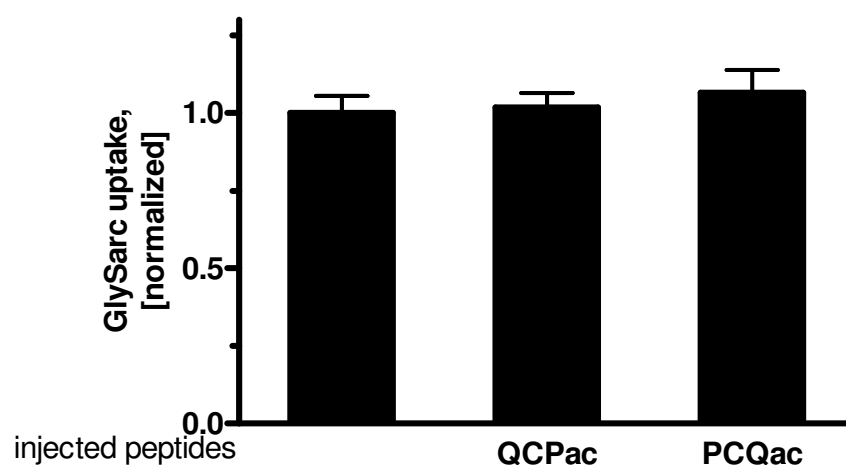


**Figure 4.18. Intracellular QCP does not effect activity of hPEPT1.** hPEPT1 expressing oocytes were injected with 25 nl K-ORi containing 75 pmol QCPac, incubated for 1 hour, and uptake of [<sup>3</sup>H]-glycyl-sarcosine was measured. Mean values  $\pm$  SE of 3 independent experiments are presented.

## 5. Discussion

### 5.1. Tripeptides, derived from hRS1, block the exocytotic pathway of hSGLT1 with high affinity

Studies of the SGLT1-mediated sodium-D-glucose reabsorption demonstrated that, besides transcriptional long-term regulation caused by changes in dietary carbohydrates, the short-term regulation occurs primarily at the translational and post-translational levels (Miyamoto et al., 1993; Hediger and Rhoads, 1994). In the present study, the previously described modulator of membrane transport, RS1, shown to participate in the short-term regulation of SGLT1 by inhibiting of the exocytotic pathway (Veyhl et al., 2003; Veyhl et al., 2006), was further investigated. The approach to measure the effects of hRS1 on the activity of hSGLT1 transporter expressed in *Xenopus laevis* oocytes allowed identifying the domains of hRS1 responsible for the post-transcriptional down-regulation of hSGLT1. The obtained data suggests that both N- and C-terminal domains of hRS1 are involved in mediation of the post-transcriptional down-regulation of hSGLT1 and effects of both domains are not additive. It has been also shown that the UBA-domain of hRS1 is not directly involved into the post-transcriptional down-regulation of hSGLT1. Screening of further truncations in the region aa 251-534 allowed attributing the inhibitory effect to the tripeptides QCP (aa 410-412) and QSP (aa 19-21, 91-93). Both tripeptides were shown to act as high affinity post-transcriptional inhibitors of hSGLT1. Extracellular application of QCP does not effect the hSGLT1-mediated uptake of AMG, suggesting that QCP and/or QSP are only able to efficiently down-regulate hSGLT1 from intracellular side.

The QCP- or QSP- dependent down-regulation of the hSGLT1 can occur due to several reasons. On the one hand, the tripeptides may bind to the hSGLT1 and thereafter inactivate it in the plasma membrane; on the other hand, the tripeptides can mediate the reduction of the amount of the functional hSGLT1 molecules within the plasma membrane. For the hRS1wt protein, a mechanism



by which the amount of hSGLT1 in the plasma membrane is decreased via inhibition of the hSGLT1 release from the *trans*-Golgi Network (TGN), has been proposed (Veyhl et al., 2003; Kroiss et al., 2006). In the present study, using capacitance measurements and Western-blot analysis of the isolated plasma membranes of hSGLT1-expressing oocytes, it has been shown that QCP decreases the number of functional active hSGLT1 within the plasma membrane. The reduction of the amount of the functional hSGLT1 molecules within the plasma membrane by QCP can occur either due to recruiting of the hSGLT1 molecules from the plasma membrane, or due to the blockage of the release of the hSGLT1 containing vesicles from the TGN. In the present study, implication of the inhibitors of exocytosis BtxB and BFA led to the inhibition of hSGLT1-mediated uptake of AMG within 30 min, indicating that the release of the hSGLT1 containing vesicles from TGN or endosomes participates in the short-term regulation. Since the addition of QCPac did not lead to the further increase of the inhibition of the hSGLT1-mediated uptake of AMG, the obtained data indicates that QCP is involved in the blockage of the hSGLT1 exocytotic pathway, which is critically involved in the short-term regulation of hSGLT1. Moreover, it has been recently shown that hRS1 is a coat protein of the TGN and dissociates from the TGN after application of BFA (Kroiss et al., 2006). This finding revealed the similarity between the observed post-transcriptional effects of hRS1 and tripeptides, and indicated that QCP and/or QSP are part of (a) post-transcriptionally active domain(s) of hRS1. The tripeptides are supposed to interact with a high affinity binding site of a protein that interacts with TGN. hRS1 contains two QSP motifs in the N-terminal part (aa 19-21 and 91-93) and one QCP motif in the middle part of the protein (aa 410-412). Since the effects of QCP and QSP were not additive (data not shown), the post-transcriptional active domain of hRS1 may be identical with the N-terminal sequence containing the two QSP sites; however, it is also possible that hRS1 has two active domains that act on the same regulatory pathway. Whether both QSP motives in the N-terminal domain of hRS1 are effective and whether the amino acids between these two sites that include two consensus sequences for the binding of protein

14-3-3 (aa 13-36 and aa 80-85) (12) and a consensus sequence for PKC-dependent phosphorylation (serine 45) have a functional role, must be clarified by future experiments. The inhibitory activity of small RS1 fragments, including tripeptides, suggests that the post-transcriptional down-regulation of hSGLT1 by hRS1 is mediated, at least partially, by hRS1 fragments. Indeed, the endogenous and over-expressed RS1 protein undergoes rapid degradation in HEK 293, Caco-2, and LLC-PK1 cells (Koepsell et al., unpublished data), and products of the degradation might possess inhibitory activity. It is important to mention that unlike the full-length hRS1 (Veyhl et al., 2006), the short-term QCP-mediated inhibition of SGLT1 was independent of PKC. This suggests that the short-term down-regulation of hSGLT1 by hRS1 is mediated via QCP and/or QSP sites in hRS1 that are modulated by PKC-dependent phosphorylation in hRS1.

### **5.2. QCP and QSP are substrates of the peptide transporter PEPT1**

Various dipeptides, tripeptides, as well as a number of peptide-like drugs are rapidly taken up into intestinal epithelial cells by a specific apical peptide transporter PEPT1. In the present study, the possibility to decrease small intestinal absorption of d-glucose by down-regulation of hSGLT1 via QCP or QSP, supplied with the food, and to down-regulate hSGLT1 and hSGLT2 in the renal proximal tubule by QCP or QSP in the blood, has been evaluated. The studies, aimed to determine whether hSGLT1 transporter can be down-regulated by extracellular application of QCP or QSP in cells, co-expressing hPEPT1 transporter, revealed that QCP, transported by the hPEPT1 transporter, is able to down-regulate hSGLT1-mediated uptake of AMG.

To characterise the hPEPT1-mediated transport of the hRS1-derived tripeptides, the electrophysiological experiments with *Xenopus* oocytes expressing hPEPT1 were performed by Dr. G. Kottra at the department of Food and Nutrition of the Technical University of Munich. The hPEPT1-expressing

oocytes, clamped to the various membrane potentials, were superfused with saturating concentrations (5 mM) of the control substrate glycyl-glutamin (GQ), QCPac, PCQac, or QSP. Significant inward currents were obtained with both acetylated and non acetylated tripeptides, indicating that QCPac, PCQac (data not shown) and QSP are substrates of hPEPT1 (Fig. 5.1). Measuring the hPEPT1-mediated inward currents at different concentrations of QCPac and QSP, the Michaelis-Menten type activation curves were obtained, and at -60 mV the  $K_m$  values of  $21.4 \pm 6.6$  mM and  $4.2 \pm 0.2$  mM ( $n=6$  each) were obtained for QCPac and QSP, respectively.

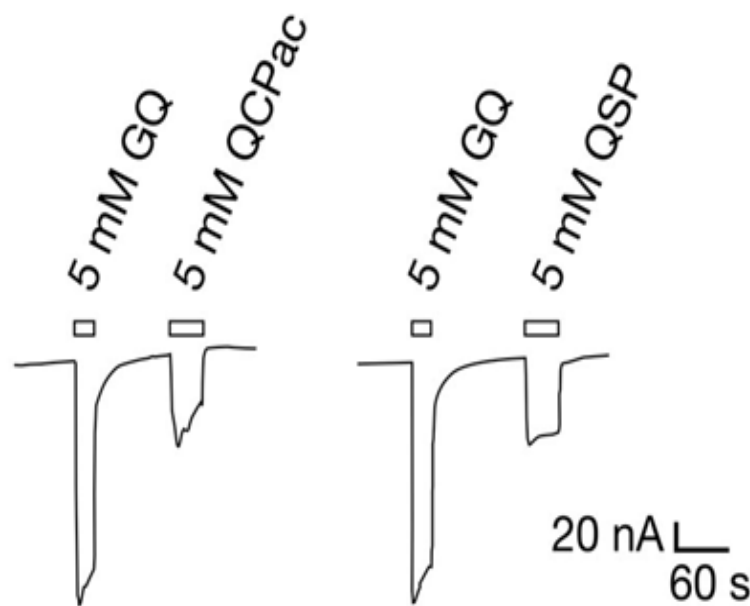


**Figure 5.1. Uptake of QCP and QSP by hPEPT1.** Oocytes injected with cRNA of hPEPT1 were incubated for three days for expression, superfused with modified Barth's solution, clamped to -60 mV and inward currents induced by 5mM glycyl-glutamin (GQ), QCPac, and QSP were measured.

An important issue was to explore whether the hRS1-derived tripeptides QCP and/or QSP, supplied with the food, are capable of down-regulating hSGLT1 in the human small intestine. Therefore, experiments, aimed to identify whether extracellular application of tripeptides QCP and QSP to confluent human colon carcinoma (Caco-2) cells inhibits AMG uptake by hSGLT1, were carried out by I. Schatz (AG Prof. H. Koepsell). At the late confluence, the Caco-2 cells exhibit similar morphological characteristics as the differentiated small intestinal enterocytes (Chantret et al., 1988). Caco-2 cells express hSGLT1 and

hPEPT1 and mediate phlorizin-inhibitable AMG and proton-dependent uptake of dipeptides (Kipp et al., 2003, Daniel and Kottra, 2004). The [ $^{14}\text{C}$ ]-AMG uptake was measured in the Caco-2 cells, cultivated for nine days after confluence. The cells were incubated for 1 hour without and with 1 mM QCPac or 1 mM QSP at pH 6.0, washed at pH 7.4, and uptake of 50  $\mu\text{M}$  [ $^{14}\text{C}$ ]-AMG was measured in the absence and presence of 0.5 mM phlorizin (Fig. 5.2). 30-50 % of [ $^{14}\text{C}$ ]-AMG uptake into Caco-2 cells was inhibited by phlorizin and was dependent on extracellular sodium (data not shown), representing the hSGLT1-mediated fraction of AMG uptake.

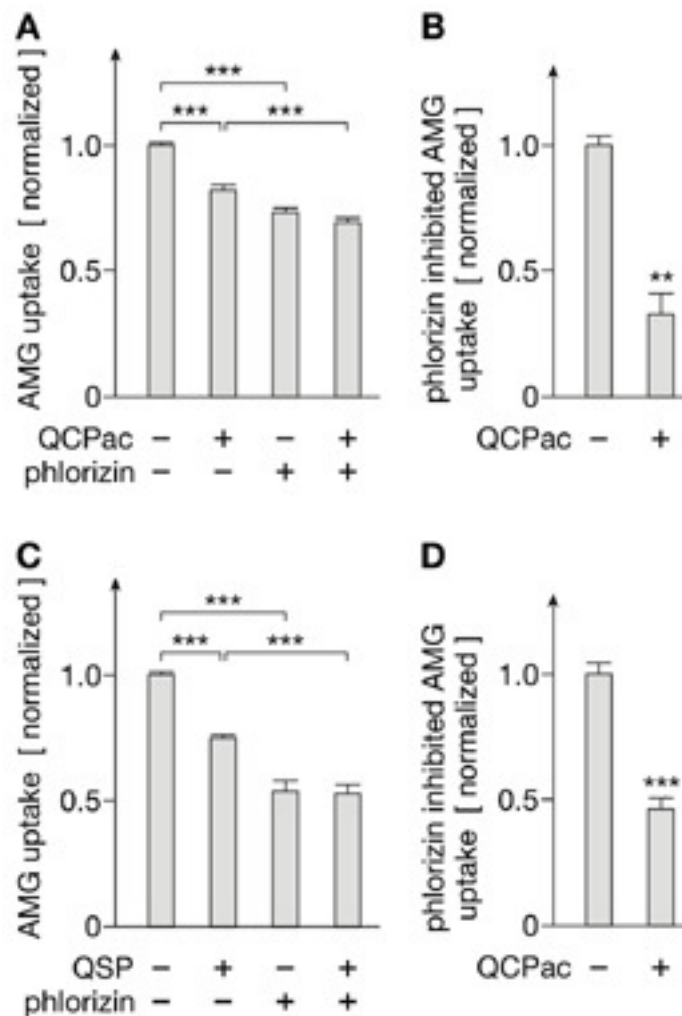


**Figure 5.2. Down-regulation of phlorizin inhibitable AMG uptake into Caco-2 cells after pre-incubation with QCP or QSP.** Caco-2 cells were grown for nine days after confluence, incubated for 1 h at pH 6.0 in the absence or presence of QCPac (a) or QSP (b), and uptake of 50  $\mu\text{M}$  [ $^{14}\text{C}$ ]-AMG was measured in the absence or presence of 0.5 mM phlorizin. Total AMG uptake (left panels) and phlorizin inhibited AMG uptake (right panels) are indicated. Mean values  $\pm$  SE of five independent experiments are presented. \*\*, P < 0.01, \*\*\*, P < 0.001, determined according to the ANOVA with post hoc Tukey's test.

The total [<sup>14</sup>C]-AMG uptake into the Caco-2 cells was significantly inhibited by 15-20% when cells had been pre-incubated with QCPac or QSP (Fig. 5.2). The phlorizin inhibited fraction of the AMG uptake was inhibited by 55-65% in the presence of QCPac or QSP. The data strongly suggest that QCP and QSP are taken up by human enterocytes and inhibit hSGLT1-mediated uptake of D-glucose and D-galactose.

To evaluate the effect of QSP on the small intestinal D-glucose absorption, experiments on intact small intestine isolated from rats were performed at the CardioMetabolic Research Department of Merck KGaA. A 25 cm-long small intestinal segments of male rat kidneys were perfused for 1 hour with the phosphate buffered saline (DPBS), pH 6.5, in the absence or presence of 15 mM QSP. Thereafter the segments were perfused for 20 min with DPBS, pH 7.4, containing 10 μM D-glucose, and for another 20 min with DPBS containing 50 μM D-glucose (Fig. 5.3).

During the perfusion with D-glucose, the absorption of D-glucose was determined by measuring the D-glucose concentration in the effluate (Wang et al., 1997). In control animals the concentration of D-glucose in the effluate was about 50% smaller compared to the infused solution. After pre-treatment with QSP, the concentration of D-glucose in the effluate was about 30% higher compared to the controls (Fig. 5.3). During perfusion with 50 μM D-glucose this effect of QSP was statistically significant ( $P < 0.05$ ). Assuming that the lower D-glucose concentration in the effluate, compared to the infused solution, was due to D-glucose absorption, the data indicated that QSP decreased small intestinal D-glucose absorption by more than 30% (Fig. 5.3).

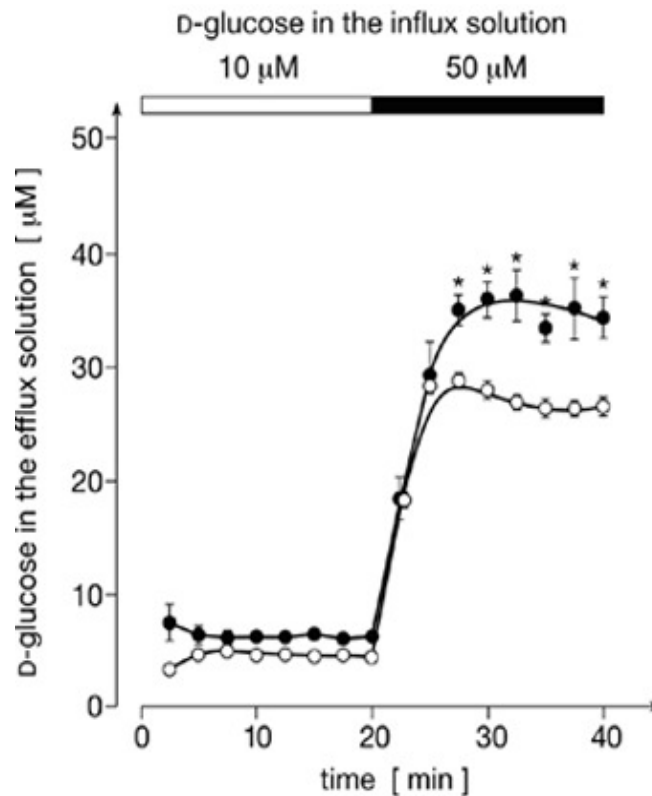


**Figure 5.3. Effect of QSP on the D-glucose absorption in rat small intestine.** Small intestinal segments of male rats were first perfused with DPBS adjusted to pH 6.5 in the absence (open circles) and presence of 15 mM QSP (closed circles). Thereafter the segments were washed and perfused with DPBS (pH 7.4) containing 10  $\mu$ M D -glucose and with DPBS containing 50  $\mu$ M. D -glucose. The glucose concentration in the effluat e was measured in 2.5 min intervals. Mean values  $\pm$  SE of three control animals and four animals treated with QSP are shown. \*,  $P < 0.005$ , determined according to the ANOVA with post hoc Tukey's test.

### 5.3. Down-regulation of hSGLT1 by QCP and QSP is monosaccharide dependent

The modulatory effect of D-glucose on the inhibition of the hSGLT1 by hRS1wt has been recently reported (Veyhl et al., 2006). In the present study, the effects of QCP and QSP on hSGLT1-mediated AMG uptake were assessed for the potential effects of the intracellular polyalcohols and the monosaccharide dependency. Similar effects of intracellular D-glucose, AMG, and 2-deoxyglucose on QCP- or QSP-mediated down-regulation of hSGLT1 had been observed. The resemblance between the observed post-transcriptional

monosaccharide-dependent effects of the hRS1 (Veyhl et al., 2006) and the tripeptides indicates that QCP and/or QSP are part of (a) post-transcriptionally active domain(s) of hRS1, and that a high affinity monosaccharide binding site is involved into the modulation of the QCP/QSP-mediated down-regulation of hSGLT1.

The observed effects of the metabolized monosaccharides (2-deoxyglucose, D-glucose and D-fructose) and of the non-metabolized monosaccharide AMG indicate the involvement of a hexokinase-independent pathway, triggered by a monosaccharide site with a  $K_d$  of about 30  $\mu\text{M}$  for D-glucose. For 2-deoxyglucose, a lower apparent  $K_d$  value was determined, however, it was not possible to distinguish whether this effect is due to the accumulation of 2-deoxyglucose-6-phosphate. The detected high affinity monosaccharide binding site cannot be located on hRS1 itself since the effects of hRS1-derived tripeptides, which are too small to form a monosaccharide binding site, were modulated by monosaccharides. The sugar specificity of this site should be different from the SGLT1-mediated monosaccharide transport as 2-deoxyglucose was effective whereas SGLT1 translocates neither 2-deoxyglucose nor 2-deoxyglucose-6-phosphate (Hediger and Rhoads, 1994). However, recent studies on rabbit SGLT1 showed that 2-deoxyglucose can bind to rSGLT1 and revealed that the substrate specificity of SGLT1 is determined by different recognition sites: one possibly located at the surface of the transporter and others located close to or within the translocation pathway (Puntheeranurak et al., 2007). Hence, it can not be excluded that the QCP/QSP-mediated post-transcriptional down-regulation of hSGLT1 can be attenuated by monosaccharides via binding of the monosaccharides to SGLT1. Nevertheless, this possibility is considered highly improbable since both hRS1 protein and QCP are also able to down-regulate hOCT2 in a monosaccharide dependent manner (Veyhl et al., 2006; M. Veyhl, A. Vernaleken, and H. Koepsell, unpublished data). The modulatory monosaccharide binding site in the RS1 regulation pathway is supposed to be localized on an intracellular protein different from SGLT1 that interacts with hRS1 at the TGN.

Several studies have previously described the post-transcriptional monosaccharide-dependent regulation of SGLT1. Sharp with co-workers showed that  $V_{max}$  of phlorizin-inhibitable D-glucose uptake in rat jejunum was increased after 30 min incubation with 25 mM D-glucose (Sharp et al., 1996). In this study, the authors did not distinguish whether amount of the SGLT1 protein in the plasma membrane or the turnover of SGLT1 was increased. Khoursandi and co-workers found that in Caco-2 cells, pre-incubated for 1 hour with 100 mM D-glucose, the phlorizin-inhibitable uptake of AMG was decreased by 45% (Khoursandi et al., 2004). Despite no significant changes in the intracellular distribution of SGLT1 were detected, the authors proposed that this down-regulation is due to increase of endocytosis.

The monosaccharide-dependent post-transcriptional regulation of several hexose transporters has been also described in yeasts (Boles and Hollenberg, 1997). Recently, the monosaccharide H<sup>+</sup>-cotransporter VvHT1 in grape has also been reported to be post-transcriptionally regulated by the non-metabolized monosaccharide 3-O-methyl-D-glucose (Conde et al., 2006). On the transcriptional level, the monosaccharide-dependent regulation of SGLT1 has been observed (Harris et al., 1986; Yasuda et al., 1990; Ohta et al., 1990; Korn et al., 2001); however, the involvement of the glucose metabolism could not be excluded (Shirazi-Beechey et al., 1991; Vayro et al., 2001).

A highly complex regulatory network, in which the small intestinal sugar absorption steers the regulation of gastric and intestinal mobility (Raybould and Zittel, 1995; Rayner et al., 2001; Freeman et al., 2006), liver metabolism (Foufelle et al., 1996; Bollen et al., 1998), and insulin secretion (Meier et al., 2002; Wideman and Kieffer, 2004), is developed in mammals. Both the glucose concentration in the small intestinal lumen and the activity of glucose uptake systems SGLT1 and GLUT2, determine the D-glucose concentration in the small intestinal submucosa and the portal blood. Glucose sensors in the small intestinal ganglia cells (Diez-Sampedro et al., 2003; Freeman et al., 2006), in the portal vein and/or liver (Jungermann and Stümpel, 1999; Turk et al., 1991, Valentin et al., 2000) transform the signal to the neuronal activity. Since SGLT1 in the brush border membrane of



the enterocytes mediates the first step in the glucose absorption, the monosaccharide-dependent regulation at this step may be most effective. Following the high glucose loading of the small intestine, GLUT2 re-distributes from the basolateral membrane of the enterocytes to the brush border membrane (Kellett, 2001). This re-distribution of GLUT2 is supposed to be triggered by the intracellular glucose and is consequently dependent on function of SGLT1. Along with the regulation of the intestinal glucose absorption by insulin (Stümpel et al., 1997), enterohormones (Cheeseman, 1997; Stümpel et al., 1997; Hirsh and Cheeseman, 1998; Meier et al., 2002) and the autonomous nervous system (Ishikawa et al., 1997), and considering the described functions of SGLT1, the physiological importance of the monosaccharide-dependent post-transcriptional regulations of SGLT1 for the short-term adaptations is obvious. In addition, the monosaccharide-dependent transcriptional regulation of SGLT1 expression is important for the long-term adaptation of the glucose absorption to diet.

### 5.4. Specificity of QCP

Referring to the earlier studies on the hRS1 (Veyhl et al., 2003), it has been observed that hRS1 exhibits the post-transcriptional selective inhibition of some, but not all, plasma membrane transporters, such as hOCT2, rbSGLT1, rOCT1, and rOCT2. Interestingly, this selectivity in the post-transcriptional inhibition does not correlate with the degree of overall structural similarity between transporters (Reinhardt et al., 1999); for example, uptake of TEA via hOCT2 was significantly inhibited when hRS1 was co-expressed with this transporter in *Xenopus* oocytes. Whereas the long-term down-regulation of hOCT2-mediated uptake of TEA by hRS1, observed in the co-expression experiments, was independent of the intracellular monosaccharides concentration (Veyhl et al., 2003), the short-term inhibition of hOCT2 by hRS1 in experiments with the purified hRS1 protein was only detected when the intracellular concentration of

monosaccharides in the hOCT2 expressing oocytes raised to about 0.25 mM. In the present study, the possibility to down-regulate hOCT2 by QCP or QSP and the potential monosaccharide dependency of the QCP/QSP effect on hOCT2 were evaluated. The obtained data revealed that, similar to the hRS1 purified protein (Veyhl et al., 2003), the short-term inhibition of the hOCT2 by QCP could only be observed when AMG was injected into the hOCT2 expressing oocytes. This indicates that QCP and the full-length hRS1 exhibit the same transporter specificity and monosaccharide dependency during the short-term down-regulation of transporters, whereas the regulation of various transporters, e.g. hSGLT1 and hOCT2, by hRS1 or the tripeptide is accomplished differently.

### 5.5. Biomedical implications

The identification of tripeptides that down-regulate the transport activity of SGLT1 and SGLT2, and are substrates of the H<sup>+</sup>-peptide co-transporter PEPT1 opens new possibilities for treatment of obesity and diabetes type 2. In humans, the small intestinal absorption of the glucose and peptides in enterocytes occurs via hSGLT1 and hPEPT1 transporters; the reabsorption of the glucose and peptides occurs across the brush-border membranes of the renal proximal tubular cells via low-affinity/high-capacity hSGLT2 and low-affinity hPEPT1 transporters in S1 segments, and via high-affinity/low-capacity hSGLT1 and high-affinity hPEPT2 transporters in S3 segments (Kanai et al., 1994; Takahashi et al., 1998; Shen et al., 1999; Daniel and Kottra, 2004).

In the present study, the intracellular concentration of QCP or QSP in the cells expressing PEPT1 transporter had been shown to be high enough to down-regulate SGLT1 when the tripeptides were added extracellularly. This was demonstrated in the *Xenopus* oocytes, in the polarized Caco-2 cells, widely used as a model for human enterocytes (Chantret et al., 1988), and in isolated and perfused rat small intestine. The experiments with the polarized Caco-2 cells and

the isolated rat small intestine showed that QCP or QSP, added to the food, may down-regulate small intestinal D-glucose and D-galactose absorption by 20-50%. This is beneficial for the prevention and treatment of diabetes since it alleviates postprandial glycaemic excursions as has been shown for the  $\alpha$ -glucosidase inhibitor acarbose (Casirola and Ferraris, 2006; Van De Laar et al., 2006). Glycaemic peaks during diabetes are responsible for the desensitisation of insulin receptors and cause vascular and renal complications. It has been shown that acarbose treatment of patients with impaired glucose tolerance was correlated with decreased incidence of diabetes type 2 (Van De Laar et al., 2006). QSP and related compounds are supposed to have a similar beneficial effect but two advantages compared to acarbose: less dosage and overdosage does not lead to the side effects caused by the sugar malabsorption.

QSP and related compounds may also be useful to decrease postprandial glucose peaks in the blood via inhibition of the glucose reabsorption in the S1 and S3 segments of the kidney proximal tubules. Several pharmaceutical companies focus on this strategy using analogues of the phlorizin that are selective for hSGLT2 in comparison to hSGLT1 (Asano et al., 2004; Dudash et al., 2004; Katsuno et al., 2007). SGLT2-specific inhibitors are preferred since the bulk of filtrated glucose is reabsorbed by the low affinity transporter hSGLT2, expressed in early proximal tubules, whereas the high affinity transporter hSGLT1 in the late proximal tubule mediates the fine adjustment of glucose reabsorption (Hediger and Rhoads, 1994). The dominant effect of hSGLT2 for the renal glucose reabsorption is indicated by symptoms in genetic diseases. Defect mutations of hSGLT1 cause the glucose-galactose malabsorption without decreasing in the renal glucose reabsorption (Turk et al., 1991), whereas defect mutations in hSGLT2 cause the renal glucosuria (Van den Heuvel et al., 2002). Recently reported prodrug of a novel selective SGLT2 inhibitor, Sergliflozin A, has been investigated *in vitro* and *in vivo* for its biological properties and potentials (Katsuno et al., 2007). In diabetic rats, Sergliflozin A, applied orally, exhibited glucose-lowering effects independently of insulin secretion and increased urinary glucose excretion by inhibiting renal glucose reabsorption.

However, application of Serliflozin A or similar compounds to human includes unpredictable risks due to the existence of the differences in expression and functional properties of SGLT subtypes between the distinct species. Thus, the porcine SGLT-subtype SGLT3, previously called SAAT1, is a Na<sup>+</sup>-D-glucose transporter, expressed in the epithelial cells (Kong et al., 1993; Mackenzie et al., 1994), whereas human SGLT3 is a D-glucose gated sodium channel and is expressed in the ganglia cells (Diez-Sampedro et al., 2003). Among all mammals, the high expression of SGLT1 in heart was only detected in human (Zhou et al., 2003). In addition, the inhibition of SGLT transporters in human brain (Pope et al., 1997) may have behavioural or intellectual consequences that are difficult to predict from the tests with animals. Using the non-hydrolysable QSP-related compounds it should be possible to down-regulate hSGLT1 and hSGLT2 in the kidney in addition to hSGLT1 in the small intestine. Such compounds may enter the blood by small intestinal absorption via PEPT1 in the brush-border membrane of the enterocytes and a second peptide transporter in the basolateral membrane (Irie et al., 2004; Groneberg et al., 2004). After filtration in the kidney, the compounds may be taken up into the proximal tubular epithelial cells by the H<sup>+</sup>-peptide co-transporters PEPT1 and PEPT2 that are co-localized with SGLT1 and SGLT2 in the brush border membrane (Daniel and Kottra, 2004). Since QSP-related compounds exhibit only the intracellular activity towards SGLT, the down-regulation of SGLT1 and/or SGLT2 will only occur in those cells, which also express a peptide transporter at the cell side of application. For this reason, orally or intravenously applied QSP-related compounds should not down-regulate SGLT1 in heart, brain, and lymphatic tissue and hence minimise the possible side effects.

## 6. Summary

The RS1 protein, a 67 kDa protein, encoded by an intronless single copy gene that was only detected in mammals, mediates transcriptional and post-transcriptional down-regulation of the sodium-D-glucose co-transporter SGLT1. The short-term post-transcriptional down-regulation of SGLT1 by RS1 has been shown to occur at the *trans*-Golgi network (TGN). In the present study, two tripeptides from the human RS1 protein (hRS1), GlnCysPro and GlnSerPro, that induce the post-transcriptional down-regulation of SGLT1 at the TGN, were identified. The application of the tripeptides led to 40-50% reduction of the amount of the SGLT1 protein in the plasma membrane, which correlated to the degree of decrease in SGLT1-mediated glucose transport. For the short-term down-regulation of SGLT1 by the tripeptides, the effective intracellular concentrations  $IC_{50}$  values of 2.0 nM (GlnCysPro, QCP) and 0.16 nM (GlnSerPro, QSP) were estimated. The observed down-regulation of SGLT1 by the tripeptides QCP and QSP, similar to hRS1 protein, was attenuated by different intracellular monosaccharides including nonmetabolized methyl- $\alpha$ -D-glucopyranoside and 2-deoxyglucose. On the contrary, the short-term inhibition of the hOCT2 by QCP could only be observed after rising of intracellular concentration of AMG. QCP and QSP are transported by H<sup>+</sup>-peptide cotransporter PEPT1 that is co-located with SGLT1 in the small intestinal enterocytes and thereafter effectively down-regulate hSGLT1-mediated transport of AMG. The data indicates that orally applied tripeptides QCP or QSP can be used to down-regulate D-glucose absorption in small intestine and used for treatment of obesity and diabetes mellitus.

## Zusammenfassung

Das RS1-Protein, das durch ein intronloses single-copy Gen kodiert wird, welches nur bei Säugetieren vorkommt, bewirkt eine posttranskriptionelle Herunterregulation des Natrium-D-Glukose-Cotransporters SGLT1. Es wurde gezeigt, dass eine kurzfristige posttranskriptionelle Hemmung von SGLT1 durch RS1 am *trans*-Golgi-Netzwerk (TGN) stattfindet. In der vorliegenden Arbeit wurden zwei Tripeptide des menschlichen RS1-Proteins (hRS1) identifiziert, GlnCysPro und GlnSerPro, welche die posttranskriptionelle Hemmung von SGLT1 am TGN induzieren. Das Applizieren der Tripeptide reduzierte die Menge des SGLT1-Proteins in der Plasmamembran um 40-50%, diese Reduktion korrelierte mit dem Rückgang des durch SGLT1 vermittelten Glukosetransports. Hinsichtlich der kurzfristigen Hemmung von SGLT1 durch die Tripeptide wurden für die effektiven intrazellulären Konzentration der Tripeptide  $IC_{50}$ -Werte von 2.0 nM (GlnCysPro, QCP) und 0.16 nM (GlnSerPro, QSP) ermittelt. Die beobachtete Hemmung von SGLT1 durch die Tripeptide QCP und QSP wurde, ähnlich wie beim hRS1-Protein, durch verschiedene intrazelluläre Monosaccharide, einschließlich Methyl- $\alpha$ -D-Glucopyranosid und 2-Deoxyglukose, verringert. Im Gegensatz dazu konnte die kurzfristige Hemmung von hOCT2 durch QCP nur nach Anhebung der intrazellulären Konzentration von AMG beobachtet werden. QCP und QSP werden durch den H<sup>+</sup>-Peptid-Kotransporter PEPT1 transportiert, der zusammen mit SGLT1 in den Enterozyten des Dünndarms kolokalisiert ist. Nach Einwärtstransport des Peptids wird dann im Anschluss der durch hSGLT1 vermittelte Glukosetransport gehemmt. Die Daten legen nahe, dass eine orale Applikation der Tripeptide QCP oder QSP dazu genutzt werden kann, die Absorption von D-Glukose im Dünndarm zu hemmen und somit als Therapeutika für Adipositas oder Diabetes mellitus genutzt werden könnte.

## 7. List of publications

**Vernaleken A.**, Veyhl M., Gorboulev V., Kottra G., Palm D., Burckhardt B.-C., Burckhardt G., Pipkorn R., Beier N., van Amsterdam C., Koepsell H. 2007. Tripeptides of RS1 (*RSC1A1*) block a monosaccharide-dependent exocytotic pathway of Na<sup>+</sup>-D-glucose cotransporter SGLT1. *J. Biol. Chem.* 2007 Aug 8; [Epub ahead of print]

Veyhl M., Keller T., Gorboulev V., **Vernaleken A.**, Koepsell H. 2006. RS1 (*RSC1A1*) regulates the exocytotic pathway of Na<sup>+</sup>-D-glucose cotransporter SGLT1. *Am. J. Physiol. Renal. Physiol.* 291:F1213-1223

Veyhl M.\*, **Vernaleken A.\***, Kipp H., Schwappach B., Koepsell H. (in preparation). Protein 14-3-3 modulates the function of the regulatory protein RS1 (*RSC1A1*).

(\* indicates authors with equal contribution)

## 8. References

- Aleu J., Blasi J., Solsona C., Marsal J. 2002. Calcium-dependent acetylcholine release from *Xenopus* oocytes: simultaneous ionic currents and acetylcholine release recordings. *Eur. J. Neurosci.* 16:1442-1448
- Arndt P., Volk C., Gorboulev V., Budiman T., Popp C., Izheimer-Teuber I., Akhoundova A., Koppatz S., Bamberg E., Nagel G., Koepsell H. 2001. Interaction of cations, anions, and weak base quinine with rat renal cation transporter rOCT2 compared with rOCT1. *Am. J. Physiol. Renal Physiol.* 281:F454-468
- Asano T., Ogihara T., Katagiri H., Sakoda H., Ono H., Fujishiro M., Anai M., Kurihara H., Uchijima Y. 2004. Glucose transporter and Na<sup>+</sup>-glucose cotransporter as molecular targets of anti-diabetic drugs. *Curr. Med. Chem.* 11:2717-2724
- Balamurugan K., Ortiz A., Said H.M. 2003. Biotin uptake by human intestinal and liver epithelial cells: role of the SMVT system. *Am. J. Physiol. Gastrointest. Liver Physiol.* 285:73-77
- Balla S., Thapar V., Verma S., Luong T.B., Faghri T., Huang C.-H., Rajasekaran S., delCampo J.J., Shinn J.H., Mohler W.A., Maciejewski M.W., Gryk M.R., Piccirillo B., Schiller S.R., Schiller M.R. 2006. Minimoto Miner: a tool for investigating protein function. *Nat. Meth.* 3:175-177
- Berry G.T., Mallee J.J., Kwon H.M., Rim J.S., Mulla W.R., Muenke M., Spinner N.B. 1995. The human osmoregulatory Na<sup>+</sup>-myo-inositol cotransporter gene (SLC5A3): molecular cloning and localization to chromosome 21. *Genomics.* 25:507-513
- Bishop N.E. 2003. Dynamics of endosomal sorting. *Int. Rev. Cytol.* 232:1-57
- Boles E., Hollenberg C.P. 1997. The molecular genetics of hexose transport in yeasts. *FEMS Microbiol. Rev.* 21(1):85-111
- Bollen M., Keppens S., Stalmans W. 1998. Specific features of glycogen metabolism in the liver. *Biochem. J.* 336:19-31
- Bradford M.M. 1976. A rapid and sensitive method for the quantitation of microgram quantities of protein utilizing the principle of protein-dye binding. *Analyt. Biochem.* 72:248-254



## 8. References

---

- Busch A.E., Quester S., Ulzheimer J. C. , Gorboulev V., Akhoundova A. Waldegger S., Lang F., Koepsell H. 1996. Monoamine neurotransmitter transport mediated by the polyspecific cation transporter rOCT1. *FEBS letters* 395:153-156
- Carriere V., Barbat A., Rousset M., Brot-Laroche E., Dussaulx E., Cambier D., De Waziers I. D., Beaune P., Zweibaum A. 1996. Regulation of sucrase-isomaltase and hexose transporters in Caco-2 cells: a role for cytochrome P-4501A1? *Am. J. Physiol. Gastrointest. Liver Physiol* 270:G976-986
- Casirola D.M., Ferraris R.P. 2006. alpha-Glucosidase inhibitors prevent diet-induced increases in intestinal sugar transport in diabetic mice. *Metabolism*. 55:832-841
- Chantret I., Barbat A., Dussaulx E., Brattain M.G., Zweibaum A. 1988. Epithelial polarity, villin expression, and enterocytic differentiation of cultured human colon carcinoma cells: a survey of twenty cell lines. *Cancer Res*. 48(7):1936-1942
- Chardin P., McCormick F. 1999. Brefeldin A: The Advantage of Being Uncompetitive. *Cell* 97(2):153-155
- Cheeseman C.I. 1997. Upregulation of SGLT-1 transport activity in rat jejunum induced by GLP-2 infusion in vivo. *Amer. J. Physiol*. 273:R1965-1971
- Conde C., Agasse A., Glissant D., Tavares R., Geros H., Delrot S. 2006. Pathways of Glucose Regulation of Monosaccharide Transport in Grape Cells. *Plant Physiol*. 141:1563-1577
- Daniel H., Kottra G. 2004. The proton oligopeptide cotransporter family SLC15 in physiology and pharmacology. *Pflügers Arch*. 447
- Davis R.J., Ganong B.R., Bell R.M., Czech M.P. 1985. sn-1,2-Dioctanoylglycerol. A cell-permeable diacylglycerol that mimics phorbol diester action on the epidermal growth factor receptor and mitogenesis. *J. Biol. Chem*. 260:1562-1566
- Deneka M., van der Sluijs P. 2002. 'Rab'ing up endosomal membrane transport. *Nat. Cell. Biol*. 4:33-35
- Diez-Sampedro A., Hirayama B.A., Osswald C., Gorboulev V., Baumgarten K., Volk C., Wright E.M., Koepsell H. 2003. A glucose sensor hiding in a family of transporters. *Proc. Natl. Acad. Sci. USA* 100:11753-11758

## 8. References

---

- Donaldson J.G., Finazzi D., Klausner R.D. 1992. Brefeldin A inhibits Golgi membrane-catalysed exchange of guanine nucleotide onto ARF protein. *Nature* 360:350-352
- Dower W.J., Miller J.F., Ragsdale C.W. 1988. High efficiency transformation of *E.coli* by high voltage electroporation. *Nucl. Acids Res.* 16:6127-6145
- Dudash J., Zhang X., Zeck R.E., Johnson S.G., Cox G.G., Conway B.R., Rybczynski P.J., Demarest K.T. 2004. Glycosylated dihydrochalcones as potent and selective sodium glucose co-transporter 2 (SGLT2) inhibitors. *Bioorg. Med. Chem. Lett.* 14:5121-5125
- Dyer J., Hosie K.B., Shirazi-Beechey S.P. 1997. Nutrient regulation of human intestinal sugar transporter (SGLT1) expression. *Gut* 41:56-59
- Ferraris R.P. 2001. Dietary and developmental regulation of intestinal sugar transport. *Biochem. J.* 360: 265-276
- Foufelle F., Girard J., Ferré P. 1996. Regulation of lipogenic enzyme expression by glucose in liver and adipose tissue: a review of the potential cellular and molecular mechanisms. *Adv. Enz. Regul.* 36:199-226
- Freeman S.L., Bohan D., Darcel N., Raybould H.E. 2006. Luminal glucose sensing in the rat intestine has characteristics of a sodium-glucose cotransporter. *Am. J. Physiol. Gastrointest. Liver Physiol.* 291:G439-445
- Fukumoto H., Kayano T., Buse J.B., Edwards Y., Pilch P.F., Bell G.I., Seino S. 1989. Cloning and characterization of the major insulin-responsive glucose transporter expressed in human skeletal muscle and other insulin-responsive tissues. *J. Biol. Chem.* 264:7776-7779
- Fukumoto H., Seino S., Imura H., Seino Y., Eddy R.L., Fukushima Y., Byers M.G., Shows T.B., Bell G.I. 1988. Sequence, tissue distribution, and chromosomal localization of mRNA encoding a human glucose transporter-like protein. *Proc. Natl. Acad. Sci. USA* 85:5434-5438
- Gáborik Z., Hunyady L. 2004. Intracellular trafficking of hormone receptors. *Trends in Endocrin. and Metab.* 15:286-293
- Ganapathy V., Brandsch M., Leibach F.H. 1994. Intestinal transport of amino acids and peptides. *Physiol. of the Gastrointest. Tract 3rd edn (Raven, New York, 1994)* pp. 1773-1794
- Gershoni J.M., George E.P. 1983. Protein blotting: Principles and applications. *Analyt. Biochem.* 131:1-15

## 8. References

---

- Groneberg D.A., Fischer A., Chung K.F., Daniel H. 2004. Molecular mechanisms of pulmonary peptidomimetic drug and peptide transport. *Am. J. Respir. Cell. Mol. Biol.* 30:215-260
- Groneberg D.A., Nickolaus M., Springer J., Döring F., Daniel H., Fischer A. 2001. Localization of the peptide transporter PEPT2 in the lung: implications for pulmonary oligopeptide uptake. *Am. J. Pathol.* 158:707-714
- Gruenberg J. 2001. The endocytic pathway: a mosaic of domains. *Nat Rev. Mol. Cell. Biol.* 2:721-730
- Gruenberg J., Kreis T.E. 1995. Membranes and sorting. *Curr. Opin. Cell. Biol.* 7:519-522
- Gründemann D., Koepsell H. 1994. Ethidium bromide staining during denaturation with glyoxal for sensitive detection of RNA in agarose gel electrophoresis. *Analyt. Biochem.* 216:459-461
- Harris R.C., Brenner B.M., Seifter J.L. 1986. Sodium-hydrogen exchange and glucose transport in renal microvillus membrane vesicles from rats with diabetes mellitus. *J. Clin. Invest.* 77:724-373
- Hediger M.A., Kanai Y., You G., Nussberger S. 1995. Mammalian ion-coupled solute transporters. *J. Physiol.* 482:7S-17
- Hediger M.A., Rhoads D.B. 1994. Molecular physiology of sodium-glucose cotransporters. *Physiol. Rev.* 74:993-1026
- Hediger M.A., Coady M.J., Ikeda T.S., Wright E.M. 1987. Expression cloning and cDNA sequencing of the Na<sup>+</sup>-glucose co-transporter. *Nature* 330(6146):379-81
- Helms J.B., Rothman J.E. 1992. Inhibition by brefeldin A of a Golgi membrane enzyme that catalyses exchange of guanine nucleotide bound to ARF. *Nature* 360:352-354
- Hirsch J.R., Loo D.D.F., Wright E.M. 1996. Regulation of Na<sup>+</sup>-glucose cotransporter expression by protein kinases in *Xenopus laevis* oocytes. *J. Biol. Chem.* 271:14740-14746
- Hirsh A.J., Cheeseman C.I. 1998. Cholecystokinin Decreases Intestinal Hexose Absorption by a Parallel Reduction in SGLT1 Abundance in the Brush-Border Membrane. *J. Biol. Chem.* 273:14545-14549
- Hurley J.H., Lee S., Prag G. 2006. Ubiquitin-binding domains. *Biochem. J.* 399:361-372

## 8. References

---

- Irie M., Terada T., Okuda M., Inui K. 2004. Efflux properties of basolateral peptide transporter in human intestinal cell line Caco-2. *Pflügers Arch.* 449:186-194
- Ishikawa Y., Eguchi T., Ishida H. 1997. Mechanism of beta-adrenergic agonist-induced transmural transport of glucose in rat small intestine. Regulation of phosphorylation of SGLT1 controls the function. *Biochim. Biophys. Acta* 1357:306-318
- Jiang W., Prokopenko O., Wong L., Inouye M., Mirochnitchenko O. 2005. IRIP, a new ischemia/reperfusion-inducible protein that participates in the regulation of transporter activity. *Mol. Cell. Biol.* 25:6496-6508
- Jungermann K., Stümpel F. 1999. Role of hepatic, intrahepatic and hepatoenteral nerves in the regulation of carbohydrate metabolism and hemodynamics of the liver and intestine. *Hepatogastroenterology.* 46:1414-1417
- Juris J. M., Michael A.N., Schmidt E.W., Gallwitz B. 2002. Gastric Inhibitory Polypeptide: the neglected incretin revisited. *Regul. Pept.* 107:1-13
- Kamsteed E.-J., Deen P.M.T. 2001. Detection of Aquaporin-2 in the Plasma Membranes of Oocytes: A Novel Isolation Method with Improved Yield and Purity. *Biochem. Biophys. Res. Commun.* 282:683-690
- Kanai Y., Lee W.S., You G., Brown D., Hediger M.A. 1994. The human kidney low affinity Na<sup>+</sup>-glucose cotransporter SGLT2. Delineation of the major renal reabsorptive mechanism for D-glucose. *J. Clin. Invest.* 93:397-404
- Karasov W.H., Diamod J.M. 1987. Adaptation of intestinal nutrient transport. In: Physiology of the gastrointestinal tract. L.R. Johnson, editor. pp. 1489-1497. Raven Press, New York
- Katsuno K., Fujimori Y., Takemura Y., Hiratochi M., Itoh F., Komatsu Y., Fujikura H., Isaji M. 2007. Sertgliflozin, a novel selective inhibitor of low-affinity sodium glucose cotransporter (SGLT2), validates the critical role of SGLT2 in renal glucose reabsorption and modulates plasma glucose level. *J. Pharmacol. Exp. Ther.* 320:323-330
- Kellett G.L. 2001. The facilitated component of intestinal glucose absorption. *J. Physiol.* 531:585-595
- Kellett G.L., Brot-Laroche E. 2005. Apical GLUT2. A major pathway of intestinal sugar absorption. *Diabetes.* 54:3056-3062

## 8. References

---

- Kipp H., Khoursandi S., Scharlau D., Kinne R.K. 2003. More than apical: Distribution of SGLT1 in Caco-2 cells. *Am. J. Physiol. Cell. Physiol.* 285(4):C737-749
- Kong C.T., Yet S.F., Lever J.E. 1993. Cloning and expression of a mammalian Na<sup>+</sup>/amino acid cotransporter with sequence similarity to Na<sup>+</sup>-glucose cotransporters. *J. Biol. Chem.* 268:1509-1512
- Korn T., Kühlkamp T., Track C., Schatz I., Baumgarten K., Gorboulev V., Koepsell H. 2001. The plasma membrane-associated protein RS1 decreases transcription of the transporter SGLT1 in confluent LLC-PK1 cells. *J. Biol. Chem.* 276:45330-45340
- Kroiss M., Leyerer M., Gorboulev V., Kuhlkamp T., Kipp H., Koepsell H. 2006. Transporter regulator RS1 (RSC1A1) coats the trans-Golgi network and migrates into the nucleus. *Am. J. Physiol. Renal Physiol.* 291:1201-1212
- Laemmli U.K., Beguin F., Gujer-Kellenberger G. 1970. A factor preventing the major head protein of bacteriophage T4 from random aggregation. *J. Mol. Biol.* 47:69-85
- Lambotte S., Veyhl M., Köhler M., Morrison-Shetlar A. I., Kinne R.K.H., Schmid M., Koepsell. H. 1996. The human gene of a protein that modifies Na<sup>+</sup>-D-glucose co-transport. *DNA Cell. Biol.* 15:769-777
- Liu M., Seino S., Kirchgessner A.L. 1999. Identification and characterization of glucoreponsive neurons in the enteric nervous system. *J. Neurosci.* 19:10305-10317
- Loflin P., Lever J.E. 2001. HuR binds a cyclic nucleotide-dependent, stabilizing domain in the 3'-untranslated region of Na<sup>+</sup>-glucose cotransporter (SGLT1) mRNA. *FEBS Letters* 509:267-271
- Loo D.D., Zeuthen T., Chandy G., Wright E.M. 1996. Cotransport of water by the Na<sup>+</sup>/glucose cotransporter. *Proc. Natl. Acad. Sci. USA* 93:13367-13370
- Mackenzie B., Panayotova-Heiermann M., Loo D.D., Lever J.E., Wright E.M. 1994. SAAT1 is a low affinity Na<sup>+</sup>-glucose cotransporter and not an amino acid transporter. A reinterpretation. *J. Biol. Chem.* 269:22488-22491
- Martín M.G., Wang J., Solorzano-Vargas R.S., Lam J.T., Turk E., Wright E.M. 2000. Regulation of the human Na<sup>+</sup>-glucose cotransporter gene, SGLT1, by HNF-1 and Sp1. *Am. J. Physiol. Gastrointest. Liver Physiol.* 278:591-603
- Meier J.J., Nauck M.A., Schmidt W.E., Gallwitz B. 2002. Gastric inhibitory polypeptide: the neglected incretin revisited. *Reg. Pept.* 107:1-13

## 8. References

---

- Miyamoto K, Hase K., Takagi T., Fujii T., Taketani Y., Minami H., Oka T., Nakabou Y. 1993. Differential responses of intestinal glucose transporter mRNA transcripts to levels of dietary sugars. *Biochem. J.* 295:211-215
- Moore B.W., Perez V.J. 1967 Specific acidic proteins of the nervous system. Specific acidic proteins of the nervous system. In FD Carlson, ed, Physiological and Biochemical Aspects of Nervous Integration. Prentice-Hall, Inc, The Marine Biological Laboratory, Woods Hole, MA, pp:343-359
- Mueckler M., Caruso C., Baldwin S.A., Panico M., Blench I., Morris H.R., Allard W.J., Lienhard G.E., Lodish H.F. 1985. Sequence and structure of a human glucose transporter. *Science.* 229:941-945
- Nichols B.J., Lippincott-Schwartz J. 2001. Endocytosis without clathrin coats. *Trends Cell. Biol.* 11:406-412
- O'Donovan D.G., Doran S., Feinle-Bisset C., Jones K.L., Meyer J.H., Wishart J.M., Morris H.A., Horowitz M. 2004. Effect of variations in small intestinal glucose delivery on plasma glucose, insulin, and incretin hormones in healthy subjects and type 2 diabetes. *J. Clin. Endocrinol. Metab.* 89:3431-3435
- Ogihara T., Isobe T., Ichimura T., Taoka M., Funaki M., Sakoda H., Onishi Y., Inukai K., Anai M., Fukushima Y., Kikuchi M., Yazaki Y., Oka Y., Asano T. 1997. 14-3-3 Protein binds to insulin receptor substrate-1, one of the binding sites of which is in the phosphotyrosine binding domain. *J. Biol. Chem.* 272(40):25267-25274
- Ohta T., Isselbacher K.J., Rhoads D.B. 1990. Regulation of glucose transporters in LLC-PK1 cells: effects of D-glucose and monosaccharides. *Mol. Cell. Biol.* 10:6491-6499
- Osswald C., Baumgarten K., Stümpel F., Gorboulev V., Akimjanova M., Knobloch K.-P., Horak I., Kluge R., Joost H.-G., Koepsell H. 2005. Mice without the regulator gene Rsc1A1 exhibit increased Na<sup>+</sup>-D-glucose cotransport in small intestine and develop obesity. *Mol. Cell. Biol.* 25:78-87
- Parent L., Supplisson S., Loo D.D., Wright E.M. 1992. Electrogenic properties of the cloned Na<sup>+</sup>-glucose cotransporter: I. Voltage-clamp studies. *J. Membr. Biol.* 125(1):49-62
- Peters K.W., Qi J., Watkins S.C., Frizzell R.A. 1999. Syntaxin 1A inhibits regulated CFTR trafficking in *Xenopus* oocytes. *Am. J. Physiol. Cell. Physiol.* 277:C174-180

## 8. References

---

- Pillay C.S., Elliott E., Dennison C. 2002. Endolysosomal proteolysis and its regulation. *Biochem. J.* 363:417-429
- Poppe R., Karbach U., Gambaryan S., Wiesinger H., Lutzenburg M., Kraemer M., Witte O.W., H., K. 1997. Expression of the Na<sup>+</sup>-D-glucose cotransporter SGLT1 in neurons. *J. Neurochem.* 69:84-94
- Rappoport J.Z., Simon S.M., Benmerah A. 2004. Understanding living clathrin-coated pits. *Traffic* 5:327-337
- Raybould H.E., Zittel T.T. 1995. Inhibition of gastric motility induced by intestinal glucose in awake rats: role of Na<sup>+</sup>-glucose co-transporter. *Neurogastroenterol. Motil.* 7:9-14
- Rayner C. K., Samsom M., Jones K.L., Horowitz M. 2001. Relationships of upper gastrointestinal motor and sensory function with glycemic control. *Diabetes Care.* 24:371-381
- Reinhardt J., Veyhl M., Wagner K., Gambaryan S., Dekel C., Akhoundova A., Korn T., Koepsell H. 1999. Cloning and characterization of the transport modifier RS1 from rabbit which was previously assumed to be specific for Na<sup>+</sup>-D-glucose cotransport. *Biochim. Biophys. Acta - Biomembranes.* 1417:131-143
- Rothman J.E., Orci L. 1992. Molecular dissection of the secretory pathway. *Nature* 355:409-415
- Sadee W., Anderle P. 2006. PEPT1. *UCSD-Nature Molecule Pages*
- Sambrock E., Fritsch E., Maniatis T. 1989. Molecular cloning, a laboratory manual. *Cold Spring Harbor Laboratory Press*
- Saumon G., Martet G., Loiseau P. 1996. Glucose transport and equilibrium across alveolar-airway barrier of rat. *Am. J. Physiol.* 270:183-190
- Saumon G., Seigné E., Clérici C. 1990. Evidence for a sodium-dependent sugar transport in rat tracheal epithelium. *Biochim. Biophys. Acta* 1023:313-318
- Scheepers A., Joost H.G., Schürmann A. 2004. The glucose transporter families SGLT and GLUT: molecular basis of normal and aberrant function. *J. Parenter. Enteral. Nutr.* 28:364-371
- Schiavo G.G., Benfenati F., Poulain B., Rossetto O., de Laureto P.P., B.R., D., Montecucco C. 1992. Tetanus and botulinum-B neurotoxins block neurotransmitter release by proteolytic cleavage of synaptobrevin. *Nature* 359:832-835

## 8. References

---

- Schmitt B.M., Koepsell H. 2002. An improved method for real-time monitoring of membrane capacitance in *Xenopus laevis* oocytes. *Biophys. J.* 82:1345-1357
- Shen H., Smith D.E., Yang T., Huang Y.G., Schnermann J.B., Brosius F.C. 1999. Localization of PEPT1 and PEPT2 proton-coupled oligopeptide transporter mRNA and protein in rat kidney. *Amer. J. Physiol.* 276:658-665
- Shioda T., Ohta T., Isselbacher K.J., Rhoads D.B. 1994. Differentiation-dependent expression of the Na<sup>+</sup>-glucose cotransporter (SGLT1) in LLC-PK1 cells: role of protein kinase C activation and ongoing transcription. *Proc. Natl. Acad. Sci. USA* 91:11919-11923
- Shirazi-Beechey S. P., Hirayama B.A., Wang Y., Scott D., Smith M.W., Wright E.M. 1991. Ontogenic development of lamb intestinal sodium-glucose cotransporter is regulated by diet. *J. Physiol.* 437:699-708
- Smanik P.A., Liu Q., Furminger T.L., Ryu K., Xing S., Mazzaferri E.L., Jhiang S.M. 1996. Cloning of the human sodium iodide symporter. *Biochem. Biophys. Res. Commun.* 226:339-345
- Sollner T., Whiteheart S.W., Brunner M., Erdjument-Bromage H., Geromanos S., Tempst P., Rothman J.E. 1993. SNAP receptors implicated in vesicle targeting and fusion. *Nature* 362:318-324
- Stevens F.J., Argon Y. 1999. Pathogenic light chains and the B-cell repertoire. *Immunol. Today* 20:451-457
- Stuart W.I., Trayhurn P. 2003. Glucose transporters (GLUT and SGLT): expanded families of sugar transport proteins. *Brit. J. Nutr.* 89:3-9
- Stümpel F., Kucera T., Gardemann A., Jungermann K. 1996. Acute increase by portal insulin in intestinal glucose absorption via hepatoenteral nerves in the rat. *Gastroenterology* 110:1863-1869
- Stümpel F., Scholtka B., Jungermann K. 1997. A new role for enteric glucagon-37: acute stimulation of glucose absorption in rat small intestine. *FEBS Letters* 410:515-519
- Sudhof T.C. 1995. The synaptic vesicle cycle: a cascade of protein-protein interactions. *Nature* 375:645-653
- Takahashi K., Nakamura N., Terada T., Okano T., Futami T., Saito H., Inui K.I. 1998. Interaction of beta-lactam antibiotics with H<sup>+</sup>-peptide cotransporters in rat renal brush-border membranes. *J. Pharmacol. Exp. Ther.* 286:1037-1042



## 8. References

---

- Thwaites D.T., Brown C.D., Hirst B.H., Simmons N.L. 1993. H<sup>+</sup>-coupled dipeptide (glycylsarcosine) transport across apical and basal borders of human intestinal Caco-2 cell monolayers display distinctive characteristics. *Biochim. Biophys. Acta* 1151(2):237-245
- Thwaites D.T., McEwan G.T., Hirst B.H., Simmons N.L. 1993. Transepithelial dipeptide (glycylsarcosine) transport across epithelial monolayers of human Caco-2 cells is rheogenic. *Pflügers Arch.* 425:178-180
- Tomoichiro A., Takehide O., Hideki K., Hideyuki S., Hiraku O., Midori F., Motonobu A., Hiroki K., Yasunobu U. 2004. Glucose transporter and Na<sup>+</sup>-glucose cotransporter as molecular targets of anti-diabetic drugs. *Curr. Med. Chem.* 11:2717-2724
- Turk E., Kerner C.J., Lostao M.P., Wright E.M. 1996. Membrane topology of the human Na<sup>+</sup>-glucose cotransporter SGLT1. *J. Biol. Chem.* 271:1925-1934
- Turk E., Zabel B., Mundlos S., Dyer J., Wright E.M. 1991. Glucose/galactose malabsorption caused by a defect in the Na<sup>+</sup>-glucose cotransporter. *Nature* 350:354-356
- Uldry M., Thorens B. 2004. The SLC2 family of facilitated hexose and polyol transporters. *Pflügers Arch.* 447:480-489
- Valentin M., Kuhlkamp T., Wagner K., Krohne G., Arndt P., Baumgarten K., Weber W., Segal A., Veyhl M., Koepsell H. 2000. The transport modifier RS1 is localized at the inner side of the plasma membrane and changes membrane capacitance. *Biochim. Biophys. Acta* 1468:367-380
- Van de Laar F.A., Lucassen P.L., Akkermans R.P., Van de Lisdonk E.H., De Grauw W.J. 2006. Alpha-glucosidase inhibitors for people with impaired glucose tolerance or impaired fasting blood glucose. *Cochrane Database Syst. Rev.* CD005061
- Van den Heuvel L.P., Assink K., Willemsen M., Monnens L. 2002. Autosomal recessive renal glucosuria attributable to a mutation in the sodium glucose cotransporter (SGLT2). *Hum. Genet.* 111:544-547
- Vayro S., Silverman M. 1999. PKC regulates turnover rate of rabbit intestinal Na<sup>+</sup>-glucose transporter expressed in COS-7 cells. *Am. J. Physiol.* 276:1053-1060
- Vayro S., Wood I.S., Dyer J., Shirazi-Beechey S.P. 2001. Transcriptional regulation of the ovine intestinal Na<sup>+</sup>-glucose cotransporter SGLT1 gene. Role of HNF-1 in glucose activation of promoter function. *Eur. J. Biochem.* 268:5460-5470

## 8. References

---

- Vernaleken A., Veyhl M., Gorboulev V., Kottra G., Palm D., Burckhardt B.-C., Burckhardt G., Pipkorn R., Beier N., van Amsterdam C., Koepsell H. 2007. Tripeptides of RS1 (*RSC1A1*) block a monosaccharide-dependent exocytotic pathway of Na<sup>+</sup>-D-glucose cotransporter SGLT1. *J. Biol. Chem.* 2007 Aug 8; [Epub ahead of print]
- Veyhl M., Keller T., Gorboulev V., Vernaleken A., Koepsell H. 2006. RS1 (*RSC1A1*) regulates the exocytotic pathway of Na<sup>+</sup>-D-glucose cotransporter SGLT1. *Am. J. Physiol. Renal. Physiol.* 291:F1213-1223
- Veyhl M., Spangenberg J., Puschel B., Poppe R., Dekel C., Fritzsich G., Haase W., H., K. 1993. Cloning of a membrane-associated protein which modifies activity and properties of the Na<sup>+</sup>-D-glucose cotransporter. *J. Biol. Chem.* 268:25041-25053
- Veyhl M., Wagner C.A., Gorboulev V., Schmitt B.M., Lang F., Koepsell H. 2003. Downregulation of the Na<sup>+</sup>-D-glucose cotransporter SGLT1 by protein RS1 (*RSC1A1*) is dependent on dynamin and protein kinase C. *J. Membr. Biol.* 196:71-81
- Wang Y., Aun R., Tse F.L.S. 1997 Absorption of G-glucose in the rat studies using *in situ* intestinal perfusion: a permeability-index approach. *Pharm. Res.* 14:1563-1567
- Wakisaka M., Kitazono T., Kato M., Nakamura U., Yoshioka M., Uchizono Y., Yoshinari M. 2001. Sodium-coupled glucose transporter as a functional glucose sensor of retinal microvascular circulation. *Circ. Res.* 88:1183-1188
- Wallace D.M. 1987. Large- and small-scale phenol extractions. *Meth. Enzymol., Academic Press, Orlando* 152:33-41
- Wei J., Hendershot L.M. 1996. Protein folding and assembly in the endoplasmic reticulum. *EXS.* 77:41-55
- Wideman R.D., Kieffer T.J. 2004. Glucose-dependent insulinotropic polypeptide as a regulator of beta cell function and fate. *Horm. Metab. Res.* 36:782-786
- Wright E.M. 1998. Genetic disorders of membrane transport. I. Glucose Galactose malabsorption. *Am. J. Physiol. Gastrointest. Liver Physiol.* 275:G879-882
- Wright E.M. 2001. Renal Na<sup>+</sup>-glucose cotransporters. *Am. J. Physiol. Renal. Physiol.* 280:10-18
- Wright E.M., Hirayama B.A., Loo D.F. 2007. Active sugar transport in health and disease. *J. Intern. Med.* 261:32-43

## 8. References

---

- Wright E.M., Loo D.D., Hirayama B.A., Turk E. 2004. Surprising versatility of Na<sup>+</sup>-glucose cotransporters: SLC5. *Physiology (Bethesda)*. 19:370-376
- Wright E.M., Loo D.D., Panayotova-Heiermann M., Lostao M.P., Hirayama B.H., Mackenzie B., Boorer K., Zampighi G. 1994. 'Active' sugar transport in eukaryotes. *J. Exp. Biol.* 196:197-212
- Wright E.M., Turk E. 2004. The sodium/glucose cotransport family SLC5. *Pflügers Arch.* 447:510-518
- Xie J., Guo Q. 2004. Par-4 Inhibits Choline Uptake by Interacting with CHT1 and Reducing Its Incorporation on the Plasma Membrane. *J. Biol. Chem.* 279:28266-28275
- Yaffe M., Rittinger K., Volinia S., Caron P.R., Aitken A., Leffers H., Gamblin S.J., Smerdon S.J., Cantley L.C. 1997. The structural basis for 14-3-3: phosphopeptide binding specificity. *Cell* 91(17):961-971
- Yaffe M. 2002. How do 14-3-3 proteins work? - Gatekeeper phosphorylation and the molecular anvil hypothesis. *FEBS Letters* 513:53-57
- Yasuda H., Kurokawa T., Fujii Y., Yamashita A., Ishibashi S. 1990. Decreased D-glucose transport across renal brush-border membrane vesicles from streptozotocin-induced diabetic rats. *Biochim. Biophys. Acta* 1021:114-118
- Zeuthen T., Zeuthen E., Klaerke D.A. 2002. Mobility of ions, sugar, and water in the cytoplasm of *Xenopus* oocytes expressing Na<sup>+</sup>-coupled sugar transporters (SGLT1). *J. Physiol.* 542:71-87
- Zhou L., Cryan E.V., D'Andrea M.R., Belkowski S., Conway B.R., Demarest K.T. 2003. Human cardiomyocytes express high level of Na<sup>+</sup>-glucose cotransporter 1 (SGLT1). *J. Cell. Biochem.* 90:339-346

## 9. Appendix

The present study characterised the regulatory effect of the hRS1 derived tripeptides QCP and QSP on the hSGLT1-mediated transport of AMG. However, since not only the middle region of hRS1, but also the N-terminal domain were shown to down-regulate hSGLT1-mediated transport of AMG, experiments aimed to characterise the N-terminal domain of hRS1 are still in progress. This appendix presents the results of the initial identification of the N-terminal inhibitory domain of hRS1.

### 9.1. N-terminal fragment of hRS1 down-regulates the hSGLT1 mediated uptake of AMG in *Xenopus* oocytes

As discussed in 4.1, the inhibition of the hSGLT1-mediated AMG uptake was also observed when various fragments of hRS1 were co-expressed together with hSGLT1. Thus, co-expression of the fragments encoding amino acids 1-251 and 251-617 with hSGLT1 resulted in the inhibition of AMG uptake by 40-50%, suggesting that both the N- and C-terminal domains of hRS1 are involved in the down-regulation of hSGLT1, and that effects of both domains are not additive. The fragment from the middle part of the protein (aa 251-535) exhibited the down-regulation of hSGLT1-mediated AMG uptake (4.1). Performance of additional truncations allowed attributing the inhibitory effect to a cRNA fragment coding for aa 407-415 (Fig. 4.1). Focussing on the investigation of the N-terminal part of the hRS1 protein, additional truncations were performed. Deletion of the aa 184-617 led to a decrease of the hSGLT1-mediated AMG uptake by about 70%. The observed inhibition of hSGLT1, mediated by this small fragment, was significantly stronger as by the hRS1wt protein (Fig. 9.1). Removal of the aa 1-50 caused a prevention of the down-regulatory effect. Therefore, next mutations were performed in the aa region 1-50. The fragment aa 20-40 did not

exhibit an inhibitory effect on hSGLT1, whereas the fragment aa 20-50 was able to down-regulate hSGLT1. This data suggested that the inhibitory effect of the N-terminal domain of hRS1 could be attributed to the fragment aa 40-50. The co-expression of hSGLT1 cRNA with cRNA coding for the fragment aa 40-50 of hRS1 revealed the down-regulation of hSGLT1-mediated AMG uptake by about 40% (Fig. 9.1). Interestingly, this inhibitory effect was not significantly different from the one mediated by hRS1wt, but significantly stronger than the effect of the fragment aa 1-183 (Fig. 9.1).

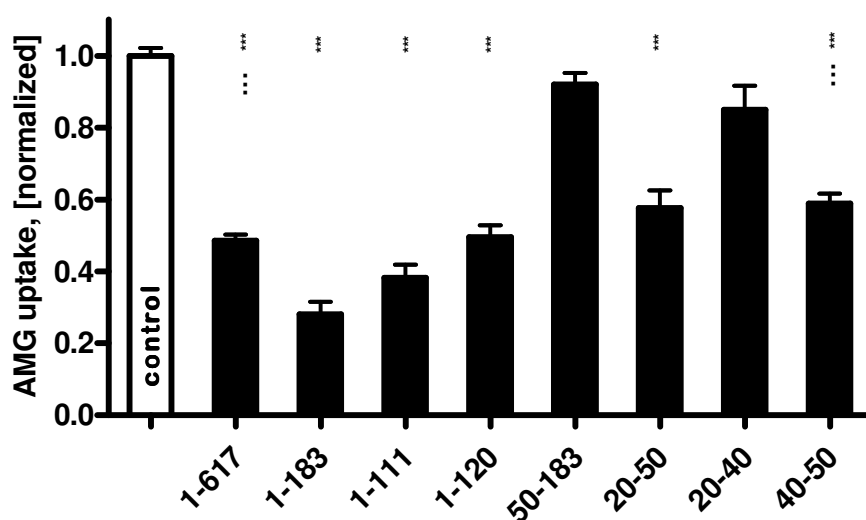


**Figure 9.1. Identification of the hRS1 fragments, that inhibit hSGLT1-mediated uptake of [<sup>14</sup>C]-AMG.** 2.5 ng of hSGLT1 cRNA were injected in *X. laevis* oocytes either alone (control) or together with 7.5 ng cRNA coding for hRS1wt (aa 1-617) or the indicated hRS1 fragments. Oocytes were incubated for three days and uptake of 50  $\mu$ M [<sup>14</sup>C]-AMG was measured. Uptake rates were normalized to parallel measurements in control oocytes from the same batch. Mean values  $\pm$  SE are indicated. The number of independent experiments is given in parentheses. \*\*,  $P < 0.01$  for difference to control; \*\*\*,  $P < 0.001$  for difference to co-expression of hSGLT1 and the small hRS1 fragment coding for aa 1-183, determined according to the ANOVA with post hoc Tukey's test.

## 9.2. Peptides derived from the N-terminus of hRS1 inhibit hSGLT1-mediated AMG uptake

Since the co-expression experiments described above do not differentiate between the post-transcriptional short-term effects of hRS1 on hSGLT1, and long-term effects that may involve endogenous oocyte proteins which participate

in the regulation of the hSGLT1, the experiments with co-injection of the synthetic peptides, derived from hRS1, into hSGLT1 expressing oocytes were performed. The acetylated synthetic peptides IKPSDSDRIEPac (comprises the eleven amino acid domain 40-50) and PEIRDSDSPKIac (reversal control peptide), were injected into the oocytes to a final concentration of 0.2 mM. Application of the peptide IKPSDSDRIEPac brought about the inhibition of hSGLT1-mediated AMG uptake by 50%, similar to the down-regulation observed in experiments described in 9.1. The reversal control peptide PEIRDSDSPKIac had no inhibitory effect on hSGLT1 (Fig. 9.2).

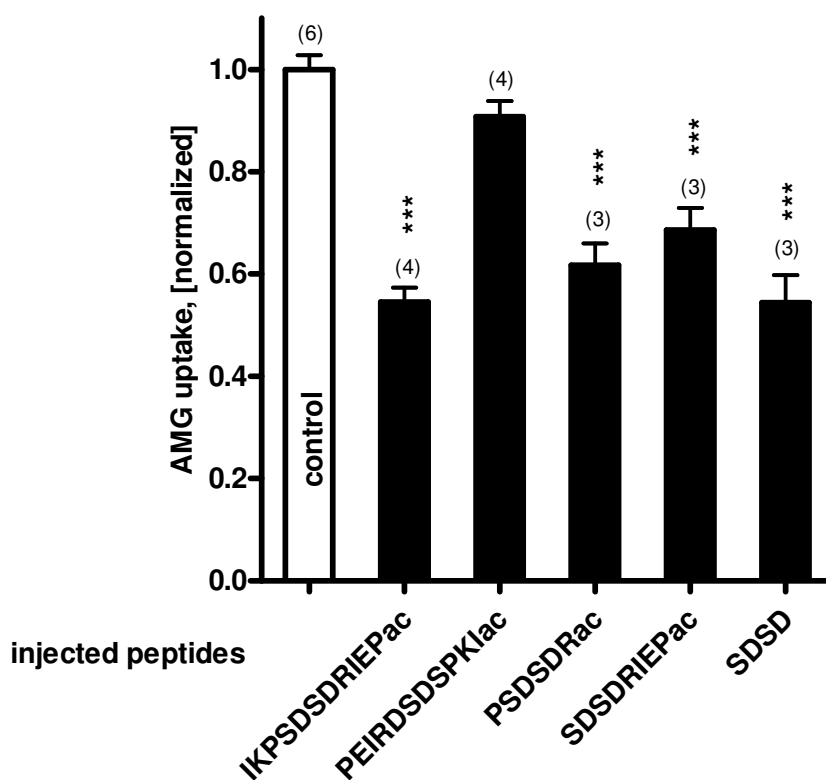


**Figure 9.2. Short-term effects of peptides derived from hRS1 on AMG uptake expressed by hRS1.** 2.5 ng of hSGLT1 cRNA were injected in *X. laevis* oocytes, the oocytes were incubated for three days, and 25 nl K-ORi buffer (control) or 25 nl K-ORi buffer containing 75 pmol of the indicated peptides were injected. Acetylated (ac) and nonacetylated peptides were injected. One hour later uptake of 50  $\mu$ M [ $^{14}$ C]-AMG was measured. Uptake measurements were normalized to parallel performed measurements in the control. Mean values  $\pm$  SE are indicated. The number of independent experiments is given in parentheses. \*\*\*,  $P < 0.001$  for difference to control, determined according to the ANOVA with post hoc Tukey's test.

To elucidate whether the whole eleven amino acids fragment is prerequisite for the down-regulation of hSGLT1 expressed in *Xenopus* oocytes, the effects of the peptides PSDSDRac, SDSDRIPeac, SDS, DSD, and SDS were investigated (Fig. 9.2, 9.3). The shortest peptide, which exhibited down-regulation of the hSGLT1-mediated AMG uptake, was SDS; the tripeptides DSD and SDS were not effective. The data suggests that the inhibitory effect of the N-terminal domain of hRS1 can be attributed to the peptide SDS comprising amino acids 43-46 of hRS1.

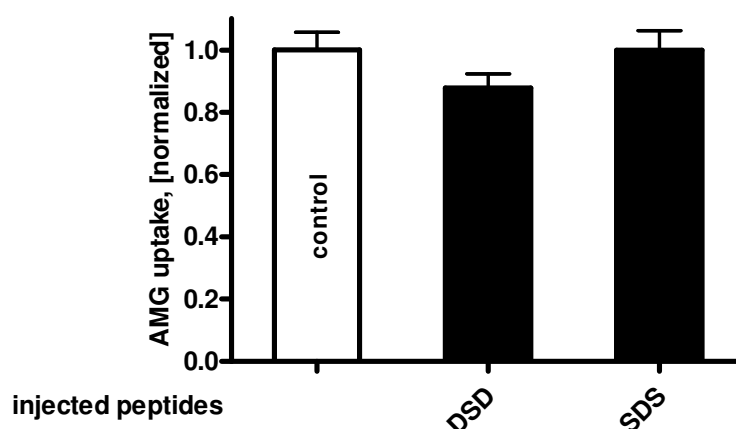


**Figure 9.3. Short-term effects of peptides derived from hRS1 on AMG uptake expressed by hRS1.** 2.5 ng of hSGLT1 cRNA were injected in *X. laevis* oocytes, the oocytes were incubated for three days, and 25 nl K-ORi buffer (control) or 25 nl K-ORi buffer containing 75 pmol of the indicated peptides were injected. One hour later uptake of 1.75  $\mu$ M [ $^{14}$ C]-AMG was measured. Uptake measurements were normalized to parallel performed measurements in the control. Mean values  $\pm$  SE are indicated.

Analysis of the hRS1 protein sequence performed with a novel tool for identifying motifs in protein, Minimotif Miner (Balla et al., 2006), revealed that hRS1 protein contains two consensus sequences for potential binding of 14-3-3 proteins. These predicted sequences are located in the N-terminal domain of hRS1, at the amino acid positions 30-36 and 80-85. Remarkably, the SDS peptide identified in the N-terminus of hRS1 as an inhibitor of hSGLT1 (9.3) is located between these two predicted 14-3-3 binding motifs and two QSP sequences, aa 19-21 and 90-93 (Fig. 9.4).

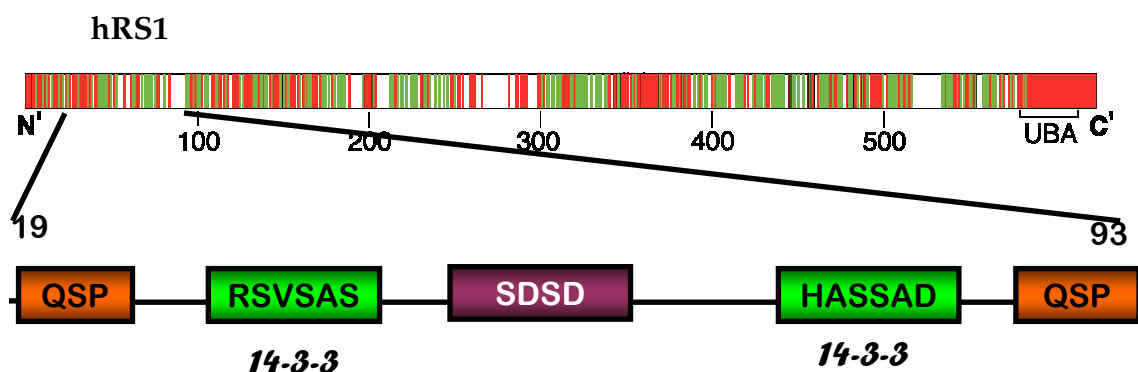


Figure 9.4. Localisation of the two QSP motifs, SDDS motif, and two 14-3-3 motifs for potential binding to 14-3-3 proteins in the sequence of hRS1.

14-3-3 proteins, identified by Moore and Perez in 1967, are the large family of ~30kDa acidic soluble proteins that exist primarily as homo- and heterodimers within all eukaryotic cells. Their unusual name refers to their elution position on DEAE-cellulose chromatography and gel electrophoresis during a systematic attempt at classifying bovine brain proteins (Moore and Perez, 1967). In humans, there are seven distinct 14-3-3 genes denoted  $\beta$ ,  $\gamma$ ,  $\epsilon$ ,  $\eta$ ,  $\sigma$ ,  $\tau$ , and  $\xi$ , while yeast and plants contain between 2 and 15 genes. Despite this genetic diversity, there is a surprisingly large amount of sequence identity and conservation between all the 14-3-3 isotypes. Different 14-3-3 molecules form distinct populations of dimers with unique recognition motifs for ligands. All 14-3-3 proteins bind to phosphoserine/phosphothreonine-containing peptide motifs RSXpSXP or RXXXpSXP (Yaffe et al., 1997). Many 14-3-3 binding proteins contain sequences that closely match these motifs, although a number of ligands bind to 14-3-3 in a phosphor-independent manner using alternative sequences that do not closely resemble these motifs. 14-3-3 proteins were found to interact with proteins such as various protein kinases (PKC, Raf, MAP), receptor proteins (GABA-receptor,  $\alpha$ 2-adrenergic receptor, glucocorticoid receptor, insulin-like growth factor I receptor), enzymes, structural and cytoskeletal proteins, small G-proteins and their regulators, proteins involved in control of apoptosis, cell cycle control, transcriptional control of gene expression, and scaffolding molecules (for review, see Yaffe, 2002). In the insulin signaling, 14-3-3 proteins were proposed



to function as a negative regulator that binds to the insulin receptors 1 and 2 in a phosphoserin-dependent manner irrespective to tyrosine phosphorylation states (Ogihara et al., 1997).

With respect to modulation of diverse group of cellular processes by 14-3-3s, regulation of SGLT1 by 14-3-3 and interaction of RS1 with 14-3-3 proteins remain obscure. For RS1, 14-3-3-mediated conformational changes might facilitate its interaction with other proteins or subcellular re-localisation (Veyhl et al., in preparation).

## 10. List of abbreviations

$\Omega$	Ohm
A	Amper
aa	Amino acid
ac	Acetylated
AMG	$\alpha$ -Methyl-glucopyranoside
AMP	Adenosine mono phosphate
ATP	Adenosine trisphosphate
CKII	Casein kinase II
$C_m$	Membrane capacitance
C-terminus	Carboxy-terminus
DNA	Deoxyribonucleic acid
DOG	Sn-1,2-dioctanoylglycerol
ESL	Enhanced chemiluminescence system
g	Gram
GLUT	Solute carrier family 2 (facilitated glucose transporter)
h	Hour
HB	Homogenisation buffer
Hz	Hertz
IgG	Immunoglobulin G
IRIP	Ischemia/reperfusion inducible protein
kb	Kilo base Pairs
kDa	Kilo Dalton
$K_m$	Michaelis-Menten constant
l	Litre
LB	Luria Bertani broth
M	Molar (mol per litre)
min	Minute
nm	Nanometer
N-terminus	Amino-terminus
$^{\circ}\text{C}$	Celsius
OCT	Organic cation transporter
ORi	Oocyte ringer solution
PAGE	Polyacrylamide gel electrophoresis
PCR	Polymerase chain reaction
PEPT	Solute carrier family 15 (oligopeptide transporter)

## 10. List of abbreviations

---

PI	Protease inhibitor
PKA	Protein kinase A
PMA	Phorbol-12-myristate-13-acetate
RNA	Ribonucleic acid
rpm	Revolutions per minute
SB	Sample buffer
SE	Standard error
sec	Second
SGLT	Solute carrier family 5 (sodium/glucose cotransporter)
SLC	Solute carriers
TEA	Tetraethylammonium
TGN	Trans-Golgi network
u	Unit
UBA	Ubiquitin associated domain
V	Volt
v/v	Volume/volume
W	Watt
w/v	weight/volume

### Amino acids:

A	Ala	Alanine
C	Cys	Cysteine
D	Asp	Aspartate
E	Glu	Glutamat
G	Gln	Glicine
H	His	Histidine
I	Ile	Isoleucine
K	Lys	Lysine
N	Ans	Aparagine
P	Pro	Proline
Q	Gln	Glutamine
R	Arg	Arginine
S	Ser	Serine
T	Thr	Threonine
V	Val	Valine

## Curriculum Vitae

### PERSONAL INFORMATION

**Family Name:** Vernaleken

**Birth Name:** Tsoukanova

**First Name:** Alexandra

**Date of Birth:** August 18, 1978

**Place of Birth:** Kaliningrad, Russian Federation

**Citizenship:** Russian Federation

### EDUCATION

September 1986- June 1995	Gymnasia # 293 of Krasnoselsky Region, Saint-Petersburg, Russian Federation	High school certificate
September 1995- July 1999	Faculty of Biology and Soil Sciences, Saint-Petersburg State University Saint-Petersburg, Russian Federation	Bachelor's degree in Biology
September 1999- December 2001	Faculty of Biology and Soil Sciences, Department of Biophysics Saint-Petersburg State University, Saint-Petersburg, Russian Federation	Master's degree in Biology, with distinction

### WORK EXPERIENCE

January 2002- December 2006	Bavarian Julius-Maximilians University of Wuerzburg Institute of Anatomy and Cell Biology I Wuerzburg, Germany	Scientific co-worker, PhD student
--------------------------------	--	--------------------------------------

## Acknowledgements

First of all, I would like to thank my supervisor Prof. Dr. Hermann Koepsell for giving me the opportunity to perform this work at his department and for sharing his scientific insight with me in the course of preparing this thesis. Furthermore, I would like to express my gratitude for the support from Prof. Dr. Roland Benz.

I would also like to thank all of my colleagues at the Institute of Anatomy and Cell Biology for their support and helpful discussions. A special thank-you goes to Alina Filatova for many hours of substantial scientific discussions.

I wish to thank Prof. Dr. G. Burckhardt and his team at the Institute of Physiology and Pathophysiology at the University of Göttingen for essential experimental support. Likewise, there was excellent help in preparing of synthetic peptides from Prof. Dr. D. Palm (University of Würzburg).

Moreover, I am very grateful to all my friends outside of the lab that made me feel less far from home and who contributed to the success of this work by sharing their biological and biochemical insight with me: Viacheslav Nikolayev, Olga Shevhuk, Olga Sokolova, and Julia Smolskaya.

Finally, I would like to thank my family, particularly my parents Prof. Dr. Mikhail Tsukanov and Dr. Liudmila Tsukanova, for their relentless support and encouragement of my education and my scientific career.

Furthermore, I would like to thank my husband Christoph Vernaleken for his great support, advice and incredible help in proofreading the manuscript and in preparing this work for print. There are not enough words to express all my gratitude and feelings.

### **Erklärungen zur Zulassung zum Promotionsverfahren.**

Hiermit erkläre ich ehrenwörtlich, dass ich diese Dissertation selbständig angefertigt habe und keine anderen als die von mir angegebenen Quellen und Hilfsmittel benutzt habe.

Weiterhin erkläre ich, dass ich diese Dissertation weder in gleicher noch in ähnlicher Form bereits in einem anderen Prüfungsverfahren vorgelegt habe.

Würzburg, 18.09.2007

Alexandra Vernaleken